Establishing redox buffers in chloroplasts through Flavo-diiron proteins in plants as strategy to enhance plant growth and stress tolerance

Dissertation
zur Erlangung des Doktorgrades
der Naturwissenschaften (Dr. rer. nat.)

der
Naturwissenschaftlichen Fakultät I
– Biowissenschaften –
der Martin Luther Universität
Halle-Wittenberg

vorgelegt
von Herrn **Suresh Tula**
geb. am 04.11.1987 in Jaggampeta

verteidigt am
10.09.2019

begutachtet von:

Prof. Dr. Nicolaus von Wirén (IPK, Gatersleben)

Prof. Dr. Klaus Humbeck (MLU, Halle)

Prof. Dr. Néstor Carrillo (IBR, Rosario)

HALLE (SAALE), GERMANY, 2019

Acknowledgments

The present research work was conducted in the laboratory of the Molecular Plant Nutrition group at the Leibniz Institute of Plant Genetics and Crop Plant Research (IPK). Financial support from the project ‘’Improvement of plant tolerance towards nutrient deficiency, abiotic and biotic stresses’’ funded by the BMBF was greatly acknowledged.

My sincere gratitude to my supervisor Dr. Mohammad-Reza Hajirezaei and Prof. Nicolaus von Wirén for giving me an opportunity to work in the project and for their constant support and guidance throughout my research.

I acknowledge Prof. Klaus Humbeck and Prof. Néstor Carrillo for their steadily support and the critical review of my thesis.

Special thanks to Prof. Néstor Carrillo for his time and helpful discussion, suggestions that improved the quality of my work during his stay in Germany.

My sincere thanks to:

Dr. Fahimeh Shahinnia, involved in the same project, for steady support and discussions.

Dr. Rodrigo Gomez for helping me with Photosynq instrument and guidance in taking photosynthesis measurements.

Dr. Michael Melzer, Dr. Twan Rutten, Sybille Freist, and Kirsten Hoffie for support and assistance at the TEM and confocal image analysis.

Dr. Yudelsy Antonia Tandron Moya for assistance in establishing the protocol for quantification of antioxidants as well as for measurements and analysis.

Nicole Schaefer for her technical assistance with the sugar measurements and other technicians for their kind help.

Special thanks to Enk Geyer and his colleagues for assistance during the growth experiments and taking care of my plants in the green house.

Dr. Britt Leps for her immense efforts in taking care of all the foreign students.

All Molecular Plant Nutrition and Metalloid Transport group members for their useful suggestions and lively discussion.

Finally, I thank my parents, and friends for their support.

Content

Abbreviations

AA-CET	Antimycin-cyclic electron transport chain
ADP	Adenosine diphosphate
ADP-Glc	Adenosine diphosphate glucose
AMG	Amyloglucosidase
AMP	Adenosine mono phosphate
APX	Ascorbate peroxidase
AQC	6-Aminoquinolyl-N-hydroxysuccinimidyl carbamate
CAT	Catalase
CBB	Calvin–Benson–Bassham
cDNA	Complementary deoxyribonucleic acid
CET	Cyclic electron transport
Chl	Chlorophyll
Col0	Columbia-0
Cyt b6f	Cytochrome B6f complex
DNA	Deoxyribonucleic acid
DNase	Deoxyribonuclease enzyme
EDTA	Ethylenediaminetetraacetic acid
ETC	Electron transport chain
FD	Ferredoxin
FDP (Flv)	Flavodiiron protein
Fm	Maximum chlorophyll fluorescence signal
FNR	Ferredoxin-$NADP^+$ oxidoreductase
Fv	Variable chlorophyll fluorescence signal
GFP	Green fluorescent protein
GR	Glutathione reductase
H_2O_2	Hydrogen peroxide
HPE1	High photosynthesis efficiency 1
HPLC	High performance liquid chromatography
IC-MS/MS	Ion chromatography – tandem mass spectrometry
LC-MS/MS	Liquid chromatography – tandem mass spectrometry
LET	Linear electron transport chain
LHC	Light harvesting complex

MAP	Mehlar Ascorbate Peroxidase
MES	2-(N-morpholino)-ethanesulfonic acid
ml	Milliliter
mM	Millimolar (concentration)
Mn-SOD	Manganese superoxide
MRM	Multiple reaction monitoring
MS	Murashige and Skoog medium
NADH	Nicotinamide adenine dinucleotide
NADP+	Nicotinamide adenine dinucleotide phosphate (oxidized form)
NADPH	Nicotinamide adenine dinucleotide phosphate
NDH	NAD(P)H dehydrogenase
nmol	Nanomole
NPQ	Non-photochemical quenching
O_2^-	Superoxide
ºC	Centigrade
P680	Primary electron donor in PSll
P700	Primary electron donor in PSI
PBCP	Photosystem ll Core Phosphate
PBS	Phycobilisomes
PC	Plastocyanin
PETC	Photosynthesis electron transport chain
PGR5	Proton gradient regulator 5
PGRL1	PGR5 like photosynthetic phenotype 1
PMF	Proton motive force
PQ	Plastoquinone
PSl	Photosystem l
PSll	Photosystem ll
PTOX	Plastid terminal oxidase
PsbS	PSll subunit S
Q_A	Primary quinone acceptor of PSII
Q_B	Secondary quinone acceptor of PSII
qE	Energy quenching
qL	Photosynthesis parameters based on pubble and lake

	model
qT	State transition
qRT-PCR	Quantitative real time-polymerase chain reaction
RNA	Ribonucleic acid
ROS	Reactive oxygen species
rpm	Revolutions per minute
RT-PCR	Reverse transcription - polymerase chain reaction
SP	Signal peptide
SE	Standard Error
SNN	Samsun
SOD	Superoxide dismutase
STN8	State transition
TLA	Truncated light chlorophyll antenna
UPLC	Ultra-performance liquid chromatography
ΔpH	Thylakoid delta pH
Δψ	Membrane potential
φNO	Radiation less energy decay
φNPQ	Light dependent NPQ
φPSII	Operating efficiency of PS II
µg	Microgram
µl	Microliter
µM	Micromolar
^{1}Chl*	Singlet Chlorophyll
$^{1}O_2$	Singlet oxygen
2PG	2-phosphoglycolate
^{3}Chl*	Triplet chlorophyll
3PGA	3-Phosphoglyceric acid

List of figures and Tables

1. Introduction

1.1 Photosynthetic light reaction

Photosynthetic organisms convert absorbed solar energy to chemical energy to support energy for growth and physiological processes (Ort et al., 1996). Among eukaryotic organisms, specifically plants perform photosynthesis in chloroplasts. Harvested solar energy by the light-harvesting pigments is mainly used for the synthesis of energy equivalents in the form of ATP and NADPH generated through the linear electron transport chain that bridge the two photosystems PSII and PSI. This way of energy capture is termed the light-dependent reaction. In stroma, ATP and NADPH generated through linear electron transport are used to power the Calvin-Benson-Bassham (CBB) cycle to fix inorganic carbon in sugars, which is termed the light-independent or dark reaction (Raines et al., 2003). In plants adjustment of light energy obsorbed to energy utilization influence the light reaction of photosynthesis that effect plant growth. Tuning of light reaction of photosynthesis in plants may improve plant growth.

1.1.1 Linear electron transport chain

In chloroplasts, the two light-harvesting pigments LHCII and LHCI absorb sunlight and transfer this physical energy to the reaction centers PSII and PSI, where the photochemical reaction takes place (Blankenship, 2013). The energy transferred to the reaction center PSII is used in two different chemical reactions, the oxidation of water at the waters-splitting complex or Mn_4CaO_5 cluster and the reduction of plastoquinone (PQ) (Govindjee and Coleman, 1990; Nugent, 2001). In PSII, the reaction center p680 is the primary electron donor that transfers electrons to primary plastoquinone (Q_A) and secondary plastoquinone (Q_B) via pheophytin (Pakrasi and Vermaas 1992, Vermaas 1993). The stable plastoquinone Q_B, which binds to the D1 protein, is a two-electron carrier. When Q_B is reduced fully, PQ accept electrons from Q_B and protons from the stroma form PQH_2, where protons translocate to lumen generates a proton gradient across the thylakoid membrane (Bowyer et al. 1991, Crofts and Wraight 1983) and the electrons flow to the cytochrome (Cyt) b6f complex.

The cytochrome b6f (cyt b6f) complex is the intermediate electron shuttle between the two photosystems and shuttles electrons from PQH_2 to the blue-copper protein plastocyanin (PC) (Baniulis et al., 2008). The Flow of electrons from PSII to PSI and protons from stroma to lumen is gated through the cyt b6f complex and is described as Q-cycle-type reaction mechanism (Mitchell et al., 1976). The PQH_2 binds to the Qo site of cyt b6f and

shuttles one electron to the Rieske iron-sulfur cluster through cyt f to plastocyanine and one electron to cyt b6 back to the PQ pool as the plastocyanine can accept only one electron. The physiological importance of the Q-cycle is that it pumps two protons per electron from the stroma to the lumen through the Cyt b6f complex (Mulkidjanian et al., 2010, Cramer et al., 2011, Cape et al., 2006). The oxidation of PQH_2 at the Qo site of the Cyt b6f complex may be the rate-limiting step in the photosynthetic electron transport chain (Tikhonov et al., 1981). At PSl, the photon energy absorbed by LHCl excites P700, the primary electron donor that shuttles one electron through several intermediate acceptors in PSl to reduce ferredoxin. Finally, the electrons are used up for reducing NADP+ (nicotinamide adenine dinucleotide phosphate) to NADPH through the reaction catalyzed by ferredoxin and ferredoxin:$NADP^+$ oxidoreductase (FNR). The transfer of electrons from water to NADPH through the electron transport chain is termed linear electron transport (Figure 1).

The protons generated in the water-splitting complex at PSll and also the protons translocated from stroma to lumen through the Cyt b6f complex generates proton gradient in the lumen (Sacksteder et al., 2000). This proton gradient across the thylakoid membrane is used for the synthesis of ATP through chloroplast ATP synthase. Finally, the energy equivalents ATP and NADPH produced in the linear electron transport chain are used for the dark reaction of photosynthesis.

The electron flux through the linear electron transport chain is coupled with import of protons from the stroma to the lumen and generates the proton motive force (pmf), which is comprised of two components: the pH difference in thylakoid (ΔpH) and the electric field (ΔΨ). Both pmf components equally contribute to ATP synthesis according to the chemiosmotic hypothesis (Mitchell et al., 1966). The ΔpH component of pmf contributes to the acidification of lumen and induces dissipation of excess light energy as heat by regulatory mechanisms like the non-photochemical quenching (Li et al. 2009).The ΔΨ regulates the charge recombination process at PSll (formation of radical pairs: Chl P680+ Phe− • → 3[P680+ Phe−] • → 3P680) where triplet (3P680) interacts with triplet oxygen to form singlet oxygen ($^1O_2$) (Davis et al., 2016). Right after illumination, the pmf is primarily stored as ΔΨ by proton buffering groups (Lys and carboxyl groups of thylakoid membrane proteins) that activates ATP synthase. The movement of the counter ions K^+ and Mg^{2+} as well as anions like Cl^- to the lumen stabilize the ΔΨ, which is required to maintain ΔpH (Kramer et al., 2003; Shikanai &Yamamoto, 2017). The counter ions play an important role in regulating the functioning of the two pmf components ΔpH and ΔΨ to avoid down-regulation of photosynthesis (Spetea et al., 2017).

Recent evidence shows that chloroplast envelope and thylakoid membrane ion channels and transporters play a major role in the regulation of the pmf (Spetea et al., 2017). Among several channels, few of them have been reported to affect the pmf or pmf components. For example, TPK3 which is K^+ efflux channel in the thylakoid membrane regulates ΔΨ (Carraretto et al., 2016).

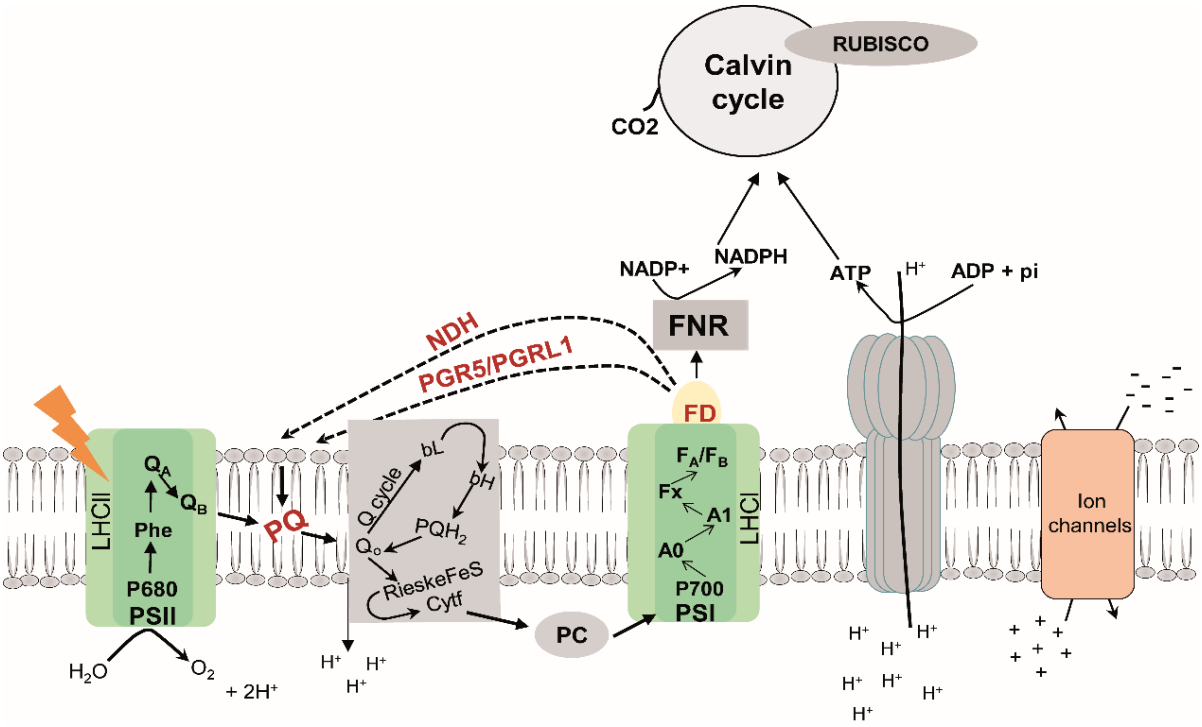

Figure 1. Schematic representation of the photosynthetic electron transport chain in chloroplasts. Electrons from PSII (Photosystem II) shuttle to PSI (Photosystem I) through the linear electron transport chain (LET) and finally reduce NADP+, (electron flow is marked in continuous black arrows). The cycling electron transport (CET) pathway PGR5/PGRL1 and NDH cycle electrons around PSI, which keeps PSI in a more oxidized state (marked in dotted lines). The protons generated at PSII and transported through the Cyt b6f complex (Cytochrome b6f) from the stroma to the lumen are used for ATP synthesis in the ATP synthase complex. Ion channels counter-balance the pH in the lumen through import or export of ions (marked in orange). The energy equivalents ATP and NADPH are used for CO_2 fixation in the Calvin cycle. P680, reaction center of photosystem II; Phe, Pheophytin; Q_A, primary plastoquinone site; Q_B, secondary plastoquinone site; LHC, light harvesting complex; PQ, Plastoquinone; Cyt b6f, Cytochrome b6f complex; PC, Plastocyanin; P700, reaction center of PSI; A0, chlorophyll a molecule; A1, Vitamin K; Fx, FA,FB, iron sulfur centers; FD, Ferredoxin; FNR, ferredoxin-NADP reductase; NADP+ and NADPH, nicotinamide adenine dinucleotide phosphate. ADP, adenosine diphosphate; ATP, adenosine triphosphate. PGR5, proton gradient regulator 5; PGRL1, PGR5 like photosynthetic phenotype 1; NDH, NAD(P)H dehydrogenase.

1.1.2 Cyclic electron transport chain

The cyclic electron transport pathways in photosynthetic organisms operate around PSl, are involved in ATP synthesis and secure effective photosynthesis through regulation of luminal pH. For assimilation of one CO_2 molecule 2 molecules of NADPH and 3 molecules of ATP are required, but the energy equivalents generated through linear electron flow (LEF) are inefficient to drive CO_2 assimilation is compensated by CET pathways (Allen et al., 2002).

The light energy absorbed by the light harvesting complex in PSll and PSI is used for splitting of two water molecules at the water-spliting complex, which liberates four photons and molecular O_2 released into the thylakoid lumen. The resulting four electrons are transferred through PSll intermediates into the PQ pool through LEF to reduce 2NADP+ and translocate eight protons from the stroma to the lumen at the Cytb6f complex (Sacksteder et al., 2000). The CFo sub-complex of ATP synthase has 14 subunits and requires 14 protons for one turn producing 3 ATP molecules. Altogether, 12 protons that are resulting from LEF can bind to the CFo subunit of ATP synthase and produce only 2.57 ATP molecules (Vollmar et al., 2009). To generate 3 ATP molecules, one electron needs to be cycled through PSl to the Cyt b6f complex. During electron cycling process, protons translocate from stroma into the lumen establish ΔpH for additional ATP synthesis without NADPH production through cylic electron transport (CET) pathway (Allen, 2002; Munekage et al., 2004). However, to maintain the required ratio of ATP:NADPH for metabolic reaction in the chloroplasts both LEF and CET pathways need to be adjusted frequently.

In higher plants, two partial electron routes around PSl are present: the NADP(H) dehydrogenase-dependent pathway (Peng et al., 2008; Yamamoto et al., 2011) and the antimycin-A sensitive pathway (AA-CET) (Bendall and Manasse, 1995). Recent data have shown that both pathways accept electrons from ferredoxin (personal communication T. Shikanai) by two proteins, referred to as PGR5 and NDH (Fig. 1). The two thylakoid proteins, proton gradient regulator 5 (PGR5) and PGR5 like - 1 (PGRL1) are proposed to be involved in AA-CET (DalCorso et al., 2008; Munekage et al., 2002). The PGRL1 protein forms homo- or heterodimers that interact functionally with PGR5 and accept electrons from ferredoxin to reduce the PQ pool. This model predicts that PGRL1 and PGR5 interact with PSl and Cytb6f (Hertle et al., 2013). The in vivo interaction of PGR5 with PGRL1 and the regulation of the AA-sensitive CET pathway was proposed by DalCorso et al. (2008). The function of PGR5 is difficult to predict but later it was proposed that PGR5 is involved in the

regulation of LEF via Cyt b6f to protect PSl from photo-damage under fluctuating light condition (Suorsa et al., 2012).

In higher plants as well as in cyanobacteria there are two different types of NADP(H) PQ oxidoreductases: type l-NADH dehydrogenase and type ll-NADH dehydrogenase. The NDH-l is a multi-subunit, which is similar to mitochondrial complex 1 while the NDH-ll is a simple flavoenzyme. The chloroplast-specific NDH is localized to stroma thylakoid, cycle's electrons around PSl and pumps protons into the lumen. Here, FD is the final electron donor for NDH to reduce PQ referring to as ferredoxin-plastoquinone reductase (Munekage et al., 2004; Yamamoto et al., 2011; Peltier et al., 2016). NDH interacts with the low abundant light-harvesting complexes LHCA5 and LHCA6 and form a super-comlex with PSl (Peng et al., 2008; Yadav et al., 2017). Chloroplast NDH is structurally similar to cyanobaterial NDH-1, which has different subunits necessary for the chloroplasts environment (Peltier et al., 2016). The cyanobacterial NDH-1 is involved in several functions like respiration, CO_2 assimilation and in the CET pathway (Ogawa, 1991). The NDH-CET pathway is not essential for photosynthesis under normal conditions (Munekage et al., 2004), but plays an important role under stress conditions to prevent over-reduction of the chloroplast stroma (Shikanai, 2007). NDH-l is absent in unicellular green algae, where plastidial NDH-ll replaces NDH-I electron transport activity. The cyanobacterial NDH-ll is not involved in chlororespiration but acts as PQ redox sensor (Peltier et al., 2016). Moreover, in angiosperms NDH-ll is associated with plastoglobulins involved in prenylquinone synthesis.

In C3 and C4 plants, CET pathways play very important roles in plant growth and development. In C3 plants, CET pathways balance the ATP/NADPH ratio and regulate photosynthesis by activating photoprotective mechanisms. In C4 photosynthesis, CO_2 is fixed by phosphoenolpyruvate carboxylase (PEPC) to oxaloacetate that in turn is reduced to malate using NADPH in mesophyll cells. Malate is then shuttled to bundle sheath cell, where NADP- malic enzyme decarboxylate malate to release CO_2 and NADPH. To fix released CO_2, extra ATP molecules are required is supplemented through the CET pathways (Figure. 1). In addition, the CET pathway plays very important role during early induction of photosynthesis to adjust the light reaction of photosynthesis until dark reaction of photosynthesis is active. Introducing CET like pathways, Flv proteins in plants which act as electron sinks adjust the energy equivalents may support plant growth.

1.2 Terminal O_2 electron sinks that sustain photosynthesis in plants

Under changing environmental conditions, increased electron pressure in the PETC (Photosynthesis electron transport chain) must be dissipated to avoid photo-damage of the photosystems and production of oxygen radicals (Asada et al., 1999). The CET pathways in chloroplasts cannot act as true electron sinks but are associated with the adjustment of the energy equivalents in metabolic pathways and photosynthesis regulation. Oxygenic photosynthetic organisms evolved several electron sinks for fine-tuning and sustaining of photosynthesis. Terminal O_2 sinks in photosynthetic organism- cyanobacteria, algae and plants are Mehler reaction (Water water cycle), plastid terminal oxidase (PTOX) and flavodiiron proteins. In higher plants photorespiration acts as a large electron sink that sustains photosynthesis (Figure 2).

1.2.1 Photorespiration

In 1920, Otto Warburg proposed that O_2 inhibits photosynthesis and this phenomenon is termed as ‘’Warburg effect’’, but later changed to photorespiration which release fixed CO_2. The oxygenation reaction of rubisco fixes O_2 and produces phosphoglycolate, which is metabolized in the glycolate pathway in three different organelles: chloroplasts, mitochondria and peroxisomes. Photorespiration generates one molecule of fixed CO_2 and one of 3-phosphoglycerate (3PGA) (Bauwe *et al.*, 2010). In total, about 25% of carbon that is fixed during photosynthetic carbon assimilation is lost during photorespiration (Ludwig and Canvin, 1971). Initially, it was thought that reducing the photorespiration rate in plants could enhance plant growth and yield, but contrary to this idea photorespiratory Arabidopsis mutants like those defective in mitochondrial serine transhydroxymethylase or *D-GLYCERATE 3-KINASE* (*GLYK*) can not survive under ambient air (~0.04% CO_2) and grow only under high CO_2 levels (>1% CO_2), when the oxygenation reaction is suppressed (Somerville and Ogren, 1982, Boldt et al. 2005). Bypassing photorespiration in plants by introducing the glycolate catabolic pathway from E. coli into chloroplasts enhanced plant growth (Maier et al., 2012). Regarding its impact on the electron balance, photorespiration which works in competition with carboxylation reaction during light reaction of photosynthesis adjust the stromal redox pressure by consuming excess energy equivalents keeping electron transport chain in more oxidized state and also enhances photosynthesis efficiency under low CO_2 conditions (Ort & Baker, 2002; Peltier & Cournac, 2002).

1.2.2 Mehler reaction (Water-water-cycle)

Photoreduction of O_2 at the PSI acceptor side is a process called Mehler reaction (Mehler et al., 1951). The process of reducing oxygen generates superoxide radicals ($O_2^{\bullet-}$), which are then converted to H_2O_2 (Hydrogen peroxide) by superoxide dismutase (CuZn-SOD) that in turn binds on the stromal side of the thylakoid membrane. H_2O_2 is then scavenged by peroxidase specifically by ascorbate-peroxidase (APX) that reduces H_2O_2 to H_2O (Figure 2). This entire process of scavenging oxygen radicals is called Mehler-peroxidase reaction or water-water-cycle (WWC). The monodehydroascorbate radicals (MDA) generated in the ascorbate peroxidase reaction are highly reactive (Miyake & Asada, 1992). These MDA radicals are reduced by MDA reductase using NADPH or by glutathione/NADPH system as electron donor (Asada, 1999). In the Mehler-peroxidase reaction, the superoxide radical production ($O_2^{\bullet-}$) and the regeneration of ascorbate require electrons from NADPH and protons in the stroma that contribute to higher ΔpH than the Mehler reaction alone (Schreiber and Neubauer, 1990) and protect the photosystem from photo damage under low CO_2 and high light conditions (Asada, 1999). The WWC acts as a short term safety valve in the early induction of photosynthesis to activate non-photochemical quenching (NPQ) and to dissipate absorbed light energy as heat at PSII. However, at the other end of the electron transport chain at PSI, the production of oxygen radicals can damage the cells (Ort & Baker, 2002).

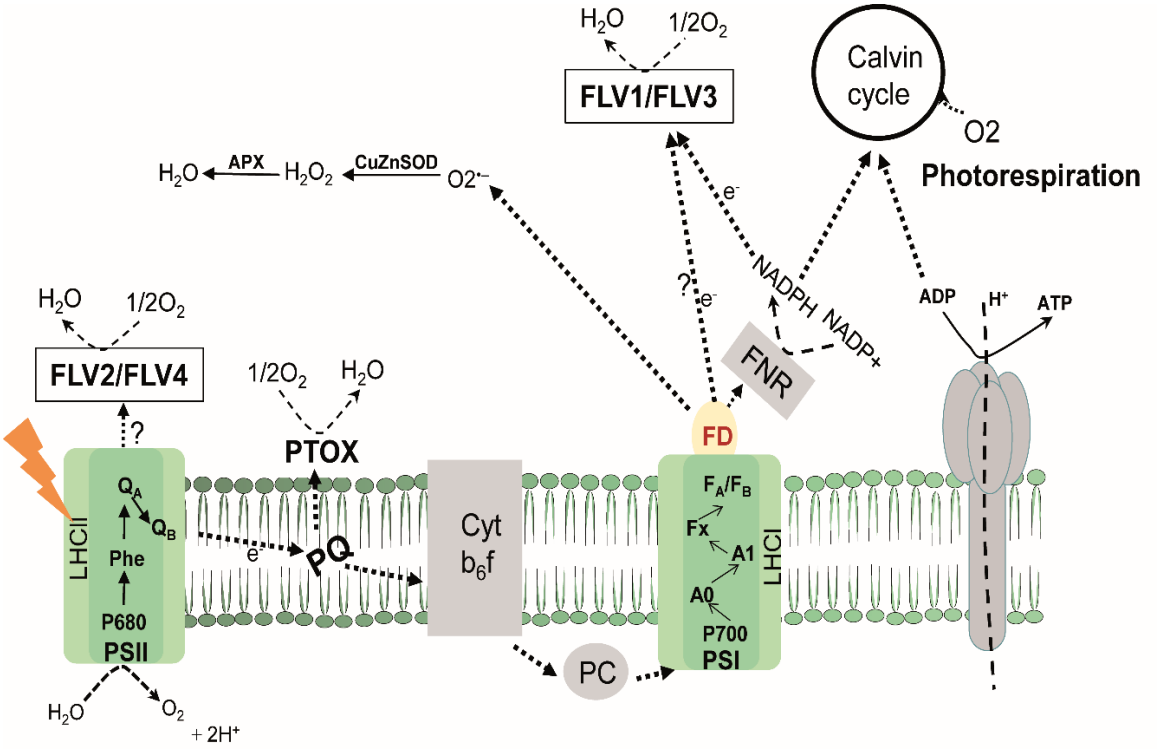

Figure 2. Schematic representation of electron-consuming pathways in photosynthetic organisms. CO_2 fixation and photorespiration act as largest electron sinks that consume nearly more than half of the electrons generated in PSII. Auxiliary pathways like the Mehler reaction at PSI consume electrons that generate (ΔpH) for ATP synthesis. In the plastid terminal oxidase (PTOX) pathway molecular oxygen is reduced to water and keeps plastoquinone (PQ) in a more oxidized state during chloroplast development and assembly of photosystems. The flavodiiron proteins (Flv) Flv1/Flv3 accept electrons from PSI and Flv2/Flv4 accept electrons from PSII to reduce molecular oxygen to water. P680, reaction center of photosystem II; Phe, Pheophytin; Q_A, primary plastoquinone site; Q_B, secondary plastoquinone site; LHC, light harvesting complex; PQ, plastoquinone; Cyt b6f, cytochrome b6f complex; PC, plastocyanin; P700, reaction center of PSI; A0, chlorophyll a molecule; A1, Vitamin K; Fx, FA,FB, iron sulfur centers; FD, ferredoxin; FNR, ferredoxin-NADP reductase; NADP+ and NADPH, nicotinamide adenine dinucleotide phosphate. ADP, adenosine diphosphate; ATP, adenosine triphosphate; APX, ascorbate peroxidase; CuZn-SOD, copper zinc superoxide dismutase.

1.2.3 Plastid terminal oxidase (PTOX)

The PTOX is a non-heme diiron quinol oxidase that transfers electrons from plastoquinol (PQH2) to molecular oxygen and generates H_2O and oxidized plastoquinone (PQ) (Carol et al., 1999; Wu et al., 1999). The PTOX is required for chloroplast biogenesis and the functioning of mature thylakoids (Foudree et al., 2012; Putarjunan et al., 2013). Specifically, during chloroplast development when electron transport chain components are not fully assembled, PTOX is the only component to oxidize the PQ pool (Nawrocki et al., 2015) and is involved in carotenoid biosynthesis. Plants grown under non-stress conditions

have low levels of PTOX (Lennon et al., 2003) but higher levels under stress, especially when plants are exposed to high light or abiotic stress (Quiles et al., 2006, Stepien and Johnson, 2009). PTOX is proposed to act as a safety valve in oxidizing the PQ pool under stress conditions to avoid formation of triplet chlorophyll (^{3}Chl*) and singlet oxygen. However, overexpression of Arabidopsis PTOX couldn't protect plants under high light (Rosso et al., 2006) but instead tobacco plants expressing *C. reinhardtii PTOX (*Ahmad et al., 2012) or Arabidopsis PTOX (Heyno et al., 2009) showed enhanced photo damage. Finally, the redox state of the PQ pool is directly affected by PTOX that influences the PQ pool (Figure 2).

1.3 Regulatory mechanism that control photo damage

During evolution plants and other photosynthetic organisms developed long-term and short-term responses to high light and other disturbances in the reaction centers. Long-term responses are characterized by acclimation or adaptation responses in plants (Anderson et al., 1988). The long term stress conditions cause severe damage to the photosystems as light induced damage to the reaction centers takes place within minutes (Tyystjärvi and Aro, 1996). Under long-term responses, oxygenic organisms adapt different strategies to overcome photo damage to the photosystems by adjustment the stoichiometry of PSII and PSI (Pfannschmidt et al., 2009) and also reducing the antenna size and increase in xanthophyll cycle pigments (Demmig-Adams and Adams, 1992; Demmig-Adams, 1998; Matsubara et al., 2008). The short-term response, which is induced quickly to counteract fluctuating light conditions like activation of CET pathways that increase in luminal acidification of thylakoid memebrane, that dissipate excess energy through NPQ. The other short-term response is exerted by cytochrome b6f, which is an important step in regulataing the ETC. state transition mechanism which is a short-term response that adjust the light distribution between the photosystems prevent photo damage to the reaction centers (Rochaix, 2013).

1.3.1 Non-photochemical quenching

In photosynthetic organisms, light harvesting is a vital process, as excess energy absorbed by the light-harvesting complexes is dissipated harmlessly as heat. This photoprotective mechanism is defined as non-photochemical quenching (NPQ). NPQ takes place in the photosynthetic membranes of cyanobacteria, algae and plants and is measured indirectly by quenching of chlorophyll florescence (Demmig-Adams et al., 2014). NPQ, the

thermal dissipation of light energy is composed of three components (qE, qT, qI). qE (Energy quenching) is the major and most important component contributing to NPQ, a ∆pH-dependent process (Niyogi et al. 2005). The qT, state transition is involved in the shuttling of phosphorylated LHCII between PSII and PSI to balance excitation energy (Minagawa, 2011), and the other component contributing to NPQ is qI (Photosynthesis parameter based on pubble and lake model), photoinhibition of photosystem.

As mentioned above, qE is the major component of NPQ induced under increased ∆pH upon increasing photosynthesis and induces protonation of the light-harvesting components or activation of the xanthophyll cycle (Ruban et al., 2012). The carotenoid violaxanthin and zeaxanthin act as powerful acceptors of ^{1}Chl* excitation energy (Müller et al., 2001). Zeaxanthin itself acts as an antioxidant, scavenging singlet oxygen and preventing thylakoid membranes from photo oxidation. Xanthophylls are also involved in decreasing the fluidity of the membrane (Tardy and Havaux, 1997).

In higher plants, the light-harvesting complex (LHC) protein family consists of LHCII and LHCI antenna proteins. All LHCII bind to chlorophyll and xanthophyll pigments, which mediate the collection of light energy and dissipation of excitation energy as heat. In Arabidopsis, the LHC family protein PsbS (PSII subunit S) is responsible for the induction of qE (Li et al., 2002). PsbS proteins are induced under low pH in the thylakoid lumen and perform faster induction of NPQ (Niyogi & Truong, 2013). The LHC proteins are conserved across phototrophis organisms, are essential for the survival and are valuable under varying environment conditions.

1.3.2 Cytochrome b6f complex

In the past it has been proposed that photosynthesis regulates the two photosystems via reduction kinetics of p700+ and the ∆pH generated by thylakoid lumenal acidification under fluctuating illumination (Rumberg & Siggel 1969). This proposition was later confirmed by (Tikhonov et al., 1981). Recently, it was shown that Cytb6f mechanism is important for seedling growth under fluctuating light conditions (Colombo et al., 2016).

The key aspect in the regulation of cytb6f is a pH-sensitive reaction between PQH2 and the Rieske iron-sulfur protein in cytb6f complex (Nishio & Whitmarsh, 1993). The oxidation of PQH2 involves the formation of a hydrogen bond between the hydroxyl group of PQH2 and with the specific residues of the Qo site of the Rieske iron-sulfur protein (Crofts et al., 1999). Under low pH in the thylakoid lumen, the H+ acceptor protonates in the Qo site rendering it unable to accept electrons from PQH2. This pH-sensitive reaction triggered by

ΔpH protects PSI from photoinhibition under fluctuating light by reduction of Cytb6f and electron flow. Further, Cytb6f may be the switch between the cyclic and linear electron transport pathways under varying environmental conditions.

1.3.3 State transitions

In photosynthetic organisms, the light-harvesting complexes (LHCs) absorb and transfer light energy to the reaction centers for splitting of H_2O. The PSII peripheral antenna consists of six different complexes that bind to several pigments like chlorophyll a and b, and xanthophylls (Jansson, 1999). In higher plants three types of major LHCII antenna proteins, LHCB1, LHCB2 and LHCB3, exist in heterotrimers that bind to the PSII by other three minor LHCII monomers CP24, CP26 and CP29 (Dekker and Boekema, 2005). The PSI antenna proteins, LHCI in Arabidopsis has six antenna proteins (LHCA1-6). Among all the LHCA5 and LHCA6 levels are low which together form a half ring on the sides of PSL core (Rochaix, 2011).

The PSII and PSI light-harvesting complexes (LHCII and LHCI) absorb light at two different wavelengths of solar spectrum. The PSII (LHC) absorbs blue and red wavelengths of the light spectrum, while PSI absorbs far-red, which drives the photosynthesis. These different light absorption properties create a disproportion of excitation between PSII and PSI under continuous light conditions. Under such conditions, obtaining optimal photosynthesis electron transport rates, sharing of absorbed light energy or adjustment of light absorption is required. For balancing the excitation, plants and algae developed a state transition mechanism, by which the distribution of excitation energy between the LHCs of the two photosystems PSII and PSI is adjusted (Murata 1969; Wollman, 2001). In cyanobacteria, state transition depends on the redistribution of energy between phycobilisomes (PBS) and chlorophyll (chl).

State transition mechanisms were first observed in red algae and green algae by the movement of LHCII that binds to PSI-LHCs (Wollman, 2001). Although in plants the light-harvesting complexes are different from other photosynthetic organisms, the concept of state transition is similar. The phosphatases and kinases are central components of state transitions that are regulated by the redox status of the PQ pool. Under illumination, PSII becomes overexcited and reduces the PQ pool. The reduction and oxidation of PQH2 and the cytb6f complex activates STL1 and STT7 protein kinases in *C. reinhardtii* (Bonardi et al., 2005), while in higher plants like *A. thaliana,* STN8 (State transition) and STN7 kinases are the orthologues involved in state transitions. In cyanobacteria, no orthologues similar to

plants are found but the rpaC gene is responsible for state transitions (Emlyn-Jones *et al.*, 1999). The redox activation and deactivation of protein kinases phosphorylate a pool of LHCII and lead to distribution of LHCIIs between the two photosystems PSII and PSI to form a PSI-LHCI-LHCII complex, called state 2. Under over-excitation of PSI, LHCII undergoes dephosphorylation that leads to detachment of LHCII from PSI and involves transfer of energy to PSII, called state 1. In Arabidopsis, PHOTOSYSTEM II CORE PHOSPHATASE (PBCP) acts as the antagonist of STN8 responsible for dephosphorylation of the PSII subunit (Samol et al., 2012), whereas another PPH1/TAP38 dephosphorylates LHCb subunits and acts as antagonist to STN7 (Pribil et al., 2010; Shapiguzov et al., 2010). In other organisms, the dephosphorylation mechanisms are not well studied.

In *C. reinhardtii,* regulatory mechanism of state transition is responsible for photo protection under high light (Finazzi *et al.*, 2001), but in plants state transition had no role in photo protection (Lunde *et al.*, 2003). In cyanobacteria, state transition was shown to be important under low light conditions, which helps in the distribution of excitation energy between the two photosystems (Mullineaux et al., 2004). In *C. reinhardtii* the state transition regulatory mechanism acts as a switch between linear and cyclic electron transport pathways (Wollman, 2001). Other factors like nutrient deprivation (sulfur), ATP deficiency and anoxia can also induce state transitions.

1.4 Strategies for improving photosynthesis

Photosynthesis is a crucial chemical reaction on earth (Deatsman, 2006) through which plants, green algae and cyanobacteria convert solar energy to chemical energy through the splitting of water into electrons, protons and O_2. Therefore, photosynthesis, the green engine of life on earth, not only maintains O_2 levels but also supplies energy in the form of carbon compounds (Blankenship, 2013). Thus, understanding the mechanism of photosynthesis has gained outstanding agronomic importance. By 2050, the global demand for food is expected to double (Tilman, 2011). However, due to environmental constraints present crop yield trends are likely to fail meeting this demand (Ray, 2013 & 2012). To address this issue, one possible attractive tool is to engineer crops with improved or fine-tuned photosynthesis and enhanced tolerance to environmental stresses (Zhu, 2010 and Ort, 2015).

Plants are inefficient in utilizing the incident light energy due to their protective mechanisms. The theoretical maximum efficiency of C_3 and C_4 photosynthesis is 4.6 % and 6%, respectively, estimated for the conversion of solar energy into biomassunder exposure to

the complete solar spectrum (Zhu 2010). About 75% of incident light energy is lost during the initial stages of light harvesting in plants due to various reasons, like inefficient utilization of the complete solar spectrum, the reflectance of a part of the light or its transmission and energy release in the form of heat (cotton, 2015) (Figure 3).

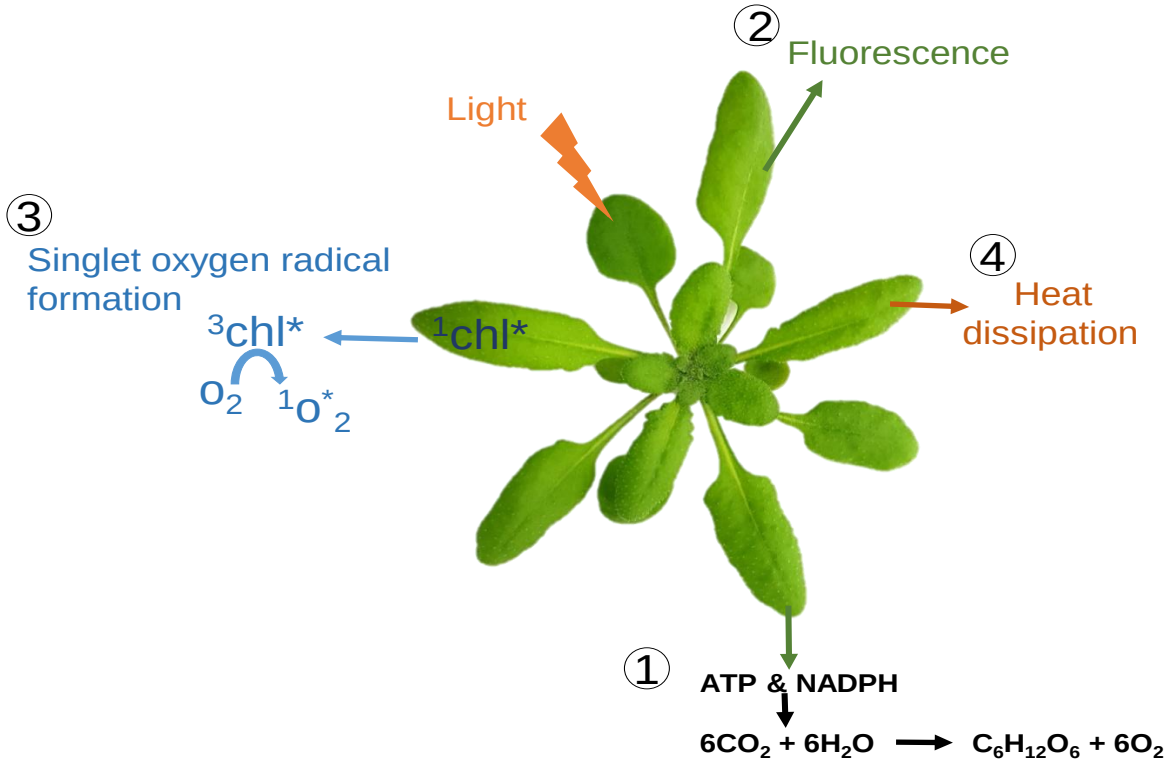

Figure 3. The fate of light energy during leaf illumination. 1. The amount of light energy utilized for synthesis of ATP and NADPH used for co_2 fixation. 2. Part of the light energy is re-emitted in the form of fluorescence. 3. Formation of triplet chlorophyll due to charge recombination at psll produces singlet oxygen that damages photosystems. 4. Excess energy released as heat through non-photochemical quenching mechanism (npq). ^{1}chl*, singlet chlorophyll; ^{3}chl*, triplet chlorophyll; h_2o_2, hydrogen peroxide; $^1o_2$, singlet oxygen.

The photosynthetic active radiation ranges from 400–700 nm, the photon energy above or below these wavelengths is not used at all for photochemistry. At this point only 48.7% of incident light is used for photochemistry while the remaining energy gets lost (Zhu 2010). In part, the energy lost is due to the optical properties of chlorophyll pigment. The photon energy absorbed in the far red drives the photochemistry. In fact, the loss of energy in PSII is an adaptive photo-protective mechanism, whereas fine tuning of the light reaction and manipulation of photo-protective mechanisms could result in a significant increase in

crop yields. Several approaches have been proposed that include: 1. Fine tuning of light harvesting and photochemistry; 2. Identification of metabolites that block photosynthesis; 3. Manipulation of photo-protective mechanisms; 4. Introducing new electron sinks that sustain photosynthesis (Figure 4).

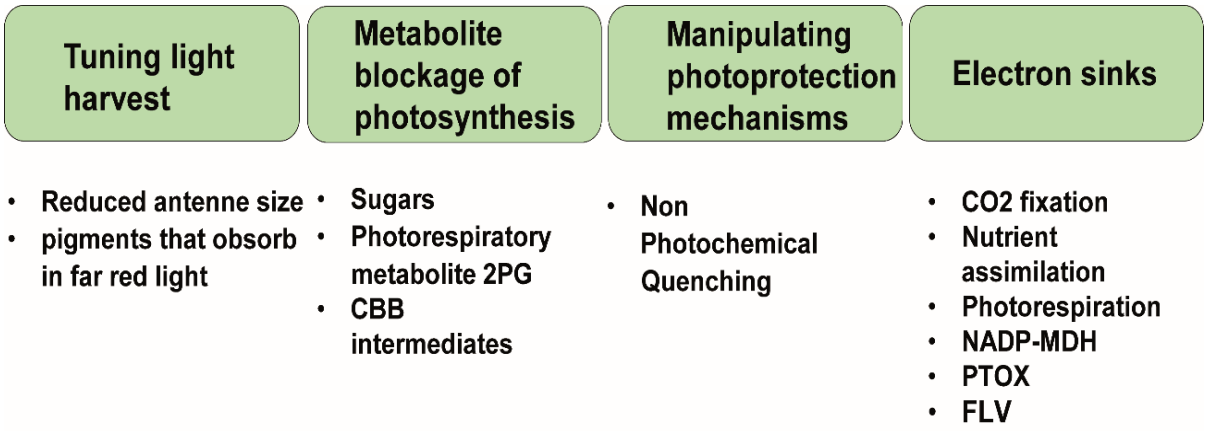

Figure 4. Potential targets for enhancing photosynthesis to increase plant growth and yield potential.

Optimizing or fine tuning of light-harvesting pigments in plants has the potential to enhance photosynthesis and yield. The concept of truncated light chlorophyll antenna (TLA) which represents the antenna size of photosystem that are smaller than the WT has profound application. By this way, using TLA concept high densities of microalgae and cyanobacteria were achieved in in-vitro cultivation (Nakajima and Ueda 1997, 1999; Melis et al. 1999; Polle et al. 2003; Nakajima et al. 2001; Mussgnug et al. 2007) (Kirst et al. 2014). Recently, application of the TLA concept in higher plants revealed promising results. For example, a tobacco mutant with an altered antenna size showed a 25% increase of leaf and stem biomass compared with the WT (Kirst et al., 2017). Despite reduced chlorophyll contents it showed an increase in photosynthesis rate, consequently faster growth rates with similar yield as the WT (Gu et al, 2017). The high photosynthetic efficiency 1 (HPE1) Arabidopsis mutant with reduced chlorophyll synthesis showed improved photosynthesis efficiency and 50 % increase in carbohydrate accumulation as well as 10% increase in dry weight in mature plants (Jin et al 2016). Another approach, introducing cyanobacterial solar pigments to plants that adsorb light beyond the photosynthetic active radiation (PAR) of 400–700 nm can improve light energy use. Extending the useable photosynthetic light in higher plants by introducing cyanobacterial enzymes for the synthesis of chlorophyll d or chlorophyll f that are active from 700–750 nm resulted in a 19% increase of capture photons (Chen et al., 2011).

Another interesting approach is to identify and alleviate the metabolite blockage of photosynthesis to enhance plant growth. Photosynthesis in plants is regulated by two ways: i) the light regulation of the expression of photosynthesis genes and the activity of the corresponding gene products; ii) the rate of end products used down-stream of the Calvin cycle is largely depending on the environmental conditions and the plant nutritional status affecting photosynthesis (Matthew et al, 2003). Sugar concentrations are known to affect the gene expression of photosynthesis components in a way that the depletion of sugars elevates the photosynthesis rate. Accumulation of sugars that exceed the sugar drain by metabolism or export, sugars repress the photosynthesis genes and the photosynthesis rate (Stitt, 1991; Krapp *et al*., 1993; Van Oosten and Besford, 1994). For instance, the photorespiratory metabolite 2-phosphoglycolate (2PG) inhibits the Calvin cycle intermediates triose phosphate isomerase and SBPase, and alleviated levels of 2PG stimulate carbon flux through the Calvin cycle and increase plant growth (Franziska et al., 2017).

Carbon fixation through the Calvin cycle in chloroplasts is the primary pathway for the synthesis of carbon compounds in C3 plants (Sharkey 1985). The triose phosphates generated in the Calvin cycle are used for the synthesis of starch and sucrose (Woodrow and Berry 1988, Geiger and Servaites 1994, Quick and Neuhaus 1997). The balance between triose phosphate utilization and regeneration avoids depletion of these intermediates and is thus critical for the functioning of the Calvin cycle in chloroplasts. The balance of intermediates is achieved through the catalytic activity of certain enzymes in the Calvin cycle. Sedoheptulose-1,7- bisphosphatase (SBPase) and fructose-1, 6-bisphosphatase (FBPase) are two enzymes that are redox-regulated through thioredoxins. Genetic engineering of these enzymes potentially increases plant biomass and yield. Identifying such metabolic constraints may pave the ways for future enhancement of yield potentials.

In plants, when the absorbed light energy exceeds the demand for CO_2 fixation, excess energy is safely dissipated as heat through (NPQ) of chlorophyll fluorescence to avoid photo-oxidative processes (Müller et al., 2001). The induction of NPQ is very fast but the relaxation is slow and takes minutes to several hours until CO_2 fixation is suppressed. It has been estimated by simulation models that the relaxation processes causes a loss of 7.5 – 30% CO_2 by a crop canopy during a diurnal course (Long et al., 1994, Werner et al., 2004, Zhu et al., 2004). Manipulation of relaxation time frame of NPQ may avoid such substantial losses of CO_2 fixation and enhance plant growth and yield. Experimental evidence shows

that overexpression of two enzymes, violaxanthin de-epoxidase and zeaxanthin epoxidase together with PsbS subunit in WT tobacco plants recovered faster from energy dissipation and boosted a 20% increase in dry weight biomass (Kromdijk et al., 2016).

Atmospheric CO_2 fixation in plants through the carboxylation reaction of Rubisco is the primary pathway that consumes nearly 50% of electrons originated from PSII. Reduced CO_2 fixation due to internal or external factors affects PSII activity and causes over-reduction of the electron transport chain that potentially inhibits the photosystems. Nitrogen assimilation is the second most important pathway that consumes excess electrons. Increasing CO_2 fixation and nitrogen assimilation in plants may improve the ratio of energy absorption to energy utilization to enhance PSII activity and finally yield.

Oxygenic photosynthetic organisms have alternative electron sinks besides CO_2 fixation, which consume excess photon energy, thereby alleviating over-reduction of the electron transport chain under rapidly varying environmental conditions. Flavodirion proteins (Flv) and photorespiration are two major electron sinks in photosynthetic organisms, which sustain photosynthesis rate. In higher plants, Flv proteins are absent, whereas photorespiration acts as major electron sink that functions at the expense of CO_2. Expression of Flv proteins in crop plants can generate additional electron sinks (Yamamoto et al., 2016). Plastid terminal oxidase (PTOX), a thylakoid membrane protein, serves as safety valve preventing over-reduction of the plastoquinone (PQ) pool and potentially contributing to the proton motive force (Aluru et al. 2006, Ivanov et al., 2012, Laureau et al., 2013). Another chloroplastic envelope membrane protein, NADP dependent malate dehydrogenase (NADP-MDH), maintains the redox state of the stroma by export of reductants from the chloroplast through exchange with other metabolites via the malate valve (Gietl 1992; Taniguchi and Miyake 2012; Heyno et al. 2014) and that avoid electron exceptor limitation at PSI (Chaux et al., 2015). Electron consuming pathways adjust the photosynthesis rate and avoid photodamage in oxygenic organisms.

1.4.1 Function of flavodiiron proteins in the light reaction

Flavodiiron (FDPs) proteins, also called flavoproteins (Flvs), are a class of soluble and modular proteins functioning in the reduction of nitric oxide (NO) to nitrous oxide (N_2O) and O_2 to H_2O (Saraiva et al., 2004; Vicente et al, 2008a-b). FDPs are widespread among prokaryotes (Wasserfallen et al., 1998) and also in few eukaryotes including anaerobic protozoa, green algae and lower plants (Zhang et al., 2009; Peltier et al., 2010; Allahverdiyeva et al., 2015b). These proteins alleviate nitrosative stress in the cells

(Rodrigues et al., 2006) and avoid toxic effects of O_2 in anaerobic organisms (Hillman et al., 2009). In oxygenic photosynthetic organisms, Flv proteins protect photo systems from photo inhibition under fluctuating light conditions.

Among most FDPs, two core domains are conserved, which are comprising of the N-terminus metallo-β-lactamase-like-domain having a non-heam diiron active site (FeFe) and a flavodoxin-like (FMN) domain at the C-terminus belonging to class A (Vicente et al., 2002; 2008a; Allahverdiyeva et al., 2015b). The O_2 or NO are reduced in the non-heme diiron active site of the metallo-β-lactamase-like-domain (Silaghi-Dumitrescu et al., 2005). The C-terminal flavodoxin-like domain FMN acts as cofactor and transfers electrons to the Fe-Fe (non-heme diiron centre). The monomers of FDPs are separated from each other and are not able to transfer electrons among themselves (Vicente et al., 2008a). However, FDPs form oligomeric structures (homodimers or homotetramers) in a head-to-tail fashion, bringing the redox-active centers together and allowing faster transfer of electrons. FDPs are classified into four different classes based on the C-terminal fusion domains. The class-A FDPs are terminal oxidases in the electron transport components; class-B FDPs have a rubredoxin-like domain at the C-terminus, called flavorubredoxin, but are restricted to enterobacteria; class-C FDPs have a NADPH-flavin reductase domain and are present in oxygenic photosynthetic organisms (cyanobacteria, algae and lower plants); class-D FDPs have NADH:FIRd fused to class-B FDPs and are present in anaerobic protozoae.

The oxygenic photosynthetic FDPs of class-C have 3 typical protein domains required to transfer electrons within the protein from NADPH to O_2 (Figure 5). Among all the class-C FDPs, Flv1 and Flv3 are conserved in all photosynthetic organisms including cyanobacteria, algae, lower plants and gymnosperms, but Flv2 and Flv4 are restricted to β-cyanobacterial species. During the course of evolutionary adaption, FDPs have become lost in diatoms and angiosperms (Ilík et al., 2017; Peltier et al., 2010). Phylogenetic analysis of class-C FDPs group them into two clusters, A and B (Zhang et al., 2009). The primary structural features of FDPs (specifically Flv1) are that cluster A has no canonical ligands in the Fe-Fe active site but has many other residues (Gonçalves et al., 2011). These structural features suggest that the formation of heterodimers between the two clusters (Zhang et al., 2012)

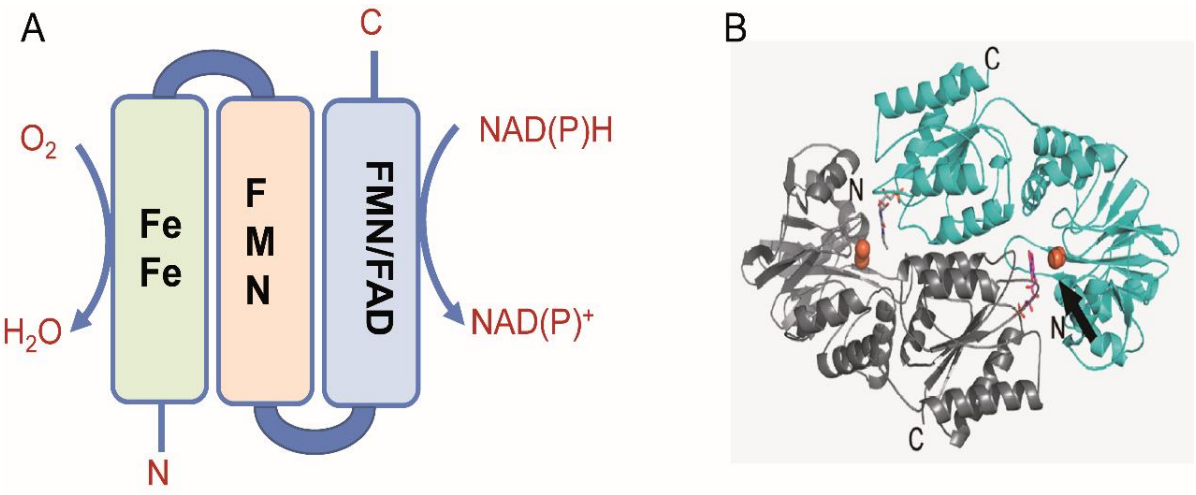

Figure 5. Modular protein structure and function of Flv proteins. (A) Flv proteins reduce molecular oxygen to water, which involves three functional domains (Metallo-β-lactamase-like-domain, flavodoxin-like (FMN) domain and non-heme diiron centre). (B) Heterodimer formation of Flv proteins Flv2 and Flv4. The arrow points to the di-iron reaction site in Flv4 (cyan) and flavin mononucleotide from Flv2 (gray). Modified from Zhang et al. 2012 and Allahverdiyeva et al. 2015b.

The class-C FDPs in the oxygenic phototrophs, specifically in the β-cyanobacterial species *Synechocystis* sp. PCC 6803 (hereafter *Synechocystis*), are non-N_2-fixing cyanobacteria that express four different FDP's (Flv1, Flv2, Flv3, Flv4). Genomic organization of FDPs in cyanobacteria differs, as Flv1 and Flv3 are classified as Flv3 - Flv1 operon or separated by 1-5 ORFs, whereas Flv2 and Flv4 are organized as Flv4-ORF- Flv2 operon. Most studies on FDPs are focused on the regulation of photosynthesis and cell metabolism. The Flv1 and Flv3 function in light-dependent O_2 reduction down-stream of PSI and prevent ROS (Reactive oxygen species) production (Helman et al., 2003). The Flv1 and Flv3 proteins protect PSI, which is prone to photoinhibition under fluctuating light conditions (Allahverdiyeva et al., 2013; Allahverdiyeva et al., 2015a). In addition, Flv1 and Flv3 form homodimers under stress conditions, which is distinct from light-dependent O_2 reduction where Flv3 except electrons directly from FD to reduce O_2 to H_2O (Mustila et al., 2016). As reported, Flv3 interacts with FD9 in *Synechocystis* (Cassier-Chauvat and Chauvat 2014).

The other two FDPs, Flv2 and Flv4 are encoded by the operon *flv4-sll0218-flv2* and regulated by CO_2 and light (Bersanini et al., 2013). FDPs also function in O_2 photoreduction by accepting electrons directly from PSII but the final electron acceptor is unknown (Helman et al., 2003; Allahverdiyeva et al., 2015b; Shimakawa et al., 2015). Recently, overexpression of GST- Flv4 in E.coli mediated NADH-dependent O_2 reduction showing that Flv2 and Flv4 can reduce O_2 to H_2O (Shimakawa et al., 2015). In an N_2-fixing cyanobacterial

strain, *Anabaena* sp. PCC 7120, which is a filamentous heterocystous encoding six different FDPs in the genome. The Flv1A and Flv3A function specifically in vegetative cells and are predicted to function like Flv2 and Flv4 heterodimers in *Synechocystis*. In lower plants, Flv proteins are reducing O_2 at the onset of light and generating an electron sink at downstream of PSI in *Physcomitrella patens* (Gerotto et al., 2016) and liverworth *Marchantia polymorpha* (Shimakawa et al., 2017).

The Flv proteins mediate Mehler like reaction or compensate CET pathways, as observed in the *Chlamydomonas reinhardtii* pgrl1 mutant (Dang et al., 2014) and in *Physcomitrella patens,* in which Flv-deficient mutants showed a higher accumulation of the PGR5 protein under fluctuating light (Gerotto et al., 2016). This phenomenon has been recently also observed in Arabidopsis by heterologous expression of *Physcomitrella patens* Flv1/Flv3 that was transformed in the background of *pgr5* deficient mutant. The authors demonstrated that Flv1/Flv3 heterodimers partially compensated the CET pathway in the *pgrl5* mutant (Yamamoto et al., 2016), indicating that Flv proteins are functional in higher plants. Furthermore, Shimakawa et al. (2017*)* illustrated that the Flv1 protein contributes to P700 oxidation during early induction of photosynthesis, protecting PSI from photoinhibition in *Marchantia polymorpha.* Recently*,* Gomez et al. (2017) indicated that introduction of cyanobacterial Flv1/Flv3 into tobacco chloroplasts resulted in an enhanced proton motive force of dark-adapted leaves and exhibited similar photosynthetic performance under steady-state illumination, but displayed faster recovery of various photosynthetic parameters, including electron transport and non-photochemical quenching during dark/light transitions. Based on these results, they emphasized that flavodiiron proteins obviously act as electron sinks during light transitions and contribute to the protection of photosynthesis and its efficiency under changing environmental conditions. Further studies revealed that the overexpression of *Physcomitrella* Flv1/Flv3 in *pgrl5* and *ndh* (NADH dehydrogenase) rice mutant background restored the biomass to the WT level (Wada et al., 2017). In addition, Hasunuma et al. (2014) demonstrated that increased ATP synthesis mediated by the overexpression of cyanobacterial Flv3 gene resulted in the accumulation of glycogen that in turn promotes cell dry weight. Thus, ectopic expression of Flv genes from lower plants in higher plants appear as a promising strategy to rescue mutant phenotype of alternative pathways and enhance plant growth.

1.4.2 Flv proteins act as electron sinks and may enhance plant growth under stress conditions

Any external factor that limits plant growth and development is considered as stress. Being sessile, plants frequently encounter various stress factors. Plant survival under stress depends on the impact of the stress, i.e. its duration and intensity. When plants are exposed to moderate stress conditions, they survive by adaptation or acclimation strategies and also by repair mechanisms, whereas mild or chronic stress conditions cause severe damage to plants leading finally to death. Further, stress is broadly classified in two factors, abiotic and biotic. Abiotic stress factors include drought or unbalanced soil water regimes, salinity, light, cold or heat, whereas biotic factors are caused by pathogens, herbivores or insects (Figure 6).

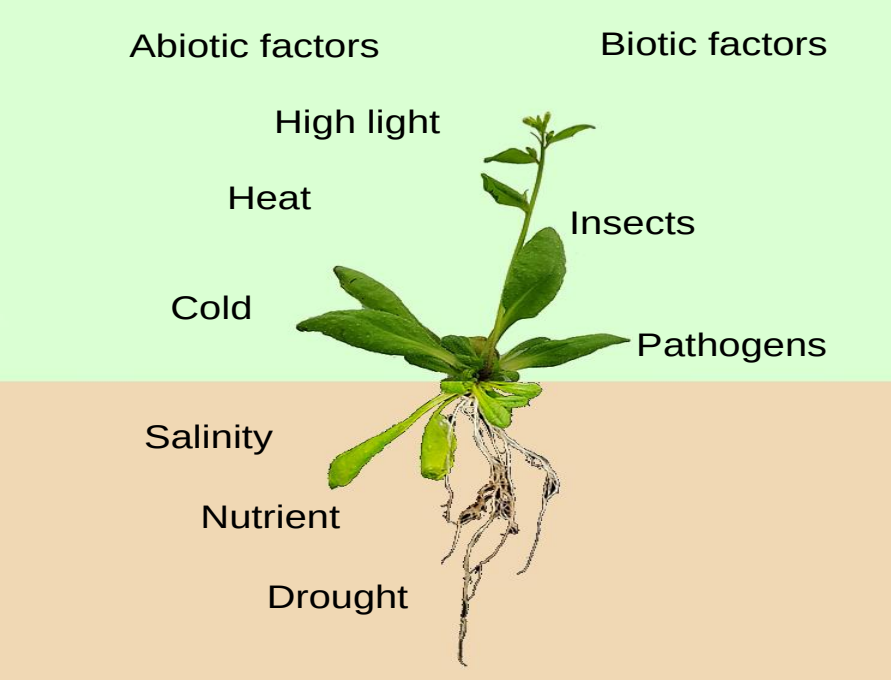

Figure 6. Diverse stress factors are classified into biotic and abiotic stresses. These stresses generate secondary stress like osmotic and oxidative stress that limits plant growth and development.

Worldwide drought is the major stress factor affecting the agricultural productivity i.e. crop yield and quality (Wang et al., 2011). Drought stress aggravates the impact of other stress factors to which plants are exposed. For example cold, heat or salt stress result in water loss. In response to drought stress, plants close the stomata to prevent water losses, which influences the dark reaction of photosynthesis and leads to reduced growth and yield loss. To cope with drought stress, plants exhibit drought escape or develop resistance

mechanisms that are further classified into drought avoidance and drought tolerance (Levitt, 1980; Price et al., 2002).

The chloroplast plays an important role in adaptation of plants to stress (Fernandez et al., 2008), as it is the centre of central metabolic processes and acts as environmental sensor to perceive stress. Inhibition of photosynthesis in drought-stressed plants due to limitation of internal CO_2 affects the Calvin cycle (Flexas *et al*., 2004; Pinheiro & Chaves, 2011). Starch, the transitory storage carbon is considered a crucial molecule in plants exposed to abiotic stresses (Thalmann et al., 2017). The degradation of starch during photosynthesis-limiting conditions provides carbon and energy to sustain plant survival. The released soluble sugars act as osmoprotectants that stabilize the cell turgor and the integrity of cell membranes (Peshev & Van den Ende 2013). In drought-stressed plants, nitrogen metabolism is reduced (Garg et al., 2001; Xu and Zhou, 2005), while the levels of certain amino acids are enhanced, since these can be beneficial for stress acclimation. For instance, proline acts as osmolyte involved in ROS scavenging (Szabados and Savoure, 2010) or GABA acts a non-proteinogenic amino acid that is also involved in ROS scavenging (Rhodes *et al.*, 1986).

The physiological and molecular responses of plants under stress conditions are associated with the energy status of the cells (Saglio et al., 1980). In the chloroplast, the energy carriers ATP and NADPH are used to drive several metabolic reactions, transport pathways and repair mechanisms like PSll D1 protein turnover. Low CO_2 conditions induce the formation of ROS in the chloroplast, which damages the ATP synthase in the chloroplast (Lawlor and Tezara, 2009). Under such conditions, the mitochondrial ATP synthase supports the ATP requirement for the metabolic reactions in the chloroplast and also for photosynthesis repair mechanism (Flexas *et al.* (2005, 2006) ; Atkin and Macherel (2009).

In plants, limitation of the terminal electron acceptor under stress conditions induces over-reduction of the electron transport chain (Lawlor, 2002; Flexas *et al.*, 2004). Under such conditions, electrons leak from the electron transport chain and reduce O_2 to form ROS, which have deleterious effects on the photosystem. Plants evolved several mechanisms to protect photosystems from damage and for saveguarding photosynthesis during stress. Under short-term stress conditions, chloroplasts activate photo-protective mechanisms like NPQ, alternative electron transport pathways, photorespiration and ROS scavenging enzymes. Under long-term stress conditions, the ratio of photosystem PSll and PSl, the size of the antenna and chlorophyll pigments are reduced.

Under long-term drought stress, plants show a decrease in most of the photosystem proteins, specifically Lhcb5, Lhcb6 and PsbQ (Chen et al., 2016). This adaptation leads to a change in the PSII/PSI ratio and reduces the ability of the light-harvesting complex to prevent an excess of absorbed light energy. Another plant adaptation to drought stress is to reduce the content of photosynthesis pigments. The chlorophyll pigments a and b decrease under drought stress (Farooq et al., 2009), and this affects the binding of light-harvesting proteins to PSII (Sayed, 2003). Carotenoids act as light harvesting pigments, apart they function like antioxidant that protect the photosystem from photodamage under drought stress conditions by scavenging ROS (Jaleel et al., 2009).

Under short-term drought stress, the imbalance between light energy absorption and utilization activates photo-protective mechanisms. Under such conditions, plants are able to dissipate excess light energy absorbed in the light-harvesting complex of PSII by releasing it in the form of heat through NPQ. Lumenal pH (∆pH) is the trigger for the activation of NPQ in photosynthetic organisms. The proton gradient regulator 5 (PGR5) and proton gradient regulator-like 1 (PGRL1) around PSI generate the ∆pH across the thylakoid membrane through the Cyt b6f complex to activate NPQ (Munekage et al. 2002, 2004; Nandha et al. 2007; Takahashi et al. 2009). The genes pgr5 and pgrl1a and pgrl1b are upregulated under drought stress (Lehtimaki et al., 2010) and protect ETC from overreduction. As shown in Arabidopsis plants expressing pgr5 enhance drought stress tolerance (Long et al., 2008). Another AEF pathway is provided by NADP-dependent malate dehydrogenase (NADP-MDH), a nuclear-encoded chloroplast protein that exports energy from the stroma to the cytosol through the malate-oxalate shuttle. This shuttle acts as a short-term adjustment of stromal redox homeostasis under varying environmental conditions (Scheibe et al., 2005). Moreover, also the mitochondrial AOX pathway is induced under certain stress conditions (Vanlerberghe et al., 1997) to avoid over-reduction of the electron transport chain. Also ROS-scavenging enzymes are highly expressed under stress conditions, as they detoxify ROS and prevent oxidative damage. Chloroplasts developed different layers of antioxidants to detoxify ROS, including superoxide dismutase (SOD), catalase (CAT), ascorbate peroxidase (APX), glutathione reductase (GR) and low molecular-weight reductants like ascorbate, glutathione, carotenoids, α-tocopherol and flavonoids. Considering the importance of these antioxidative mechanisms, overexpression of APX (Badawi et al., 2004), CAT (Roychoudhury and Ghosh, 2013) or Mn-SOD (Wang et al., 2004) conferred enhanced tolerance to several oxidative stresses.

The AEF pathways that act as electron sinks in chloroplasts protect the photosystem by conferring tolerance to low-temperature stress (Leonardos et al., 2003; Strand et al., 2003). In plants, three true electron-consuming pathways exist, the Mehler peroxidase pathways, PTOX and photorespiration. The Mehler ascorbate peroxidase (MAP) pathway plays a major role under stress conditions, as long as NADPH is available. The plastid terminal oxidase (PTOX) keeps PSII in a more oxidized state by accepting electrons from plastoquinol to reduce O_2 to H_2O under stress conditions (Sun and Wen, 2011). The photorespiratory pathway is the largest electron sink under low CO_2 conditions, including drought stress (Cruz de Carvalho 2008). In addition, the photorespiratory pathway is important for the degradation of photoinhibitors that reduce Calvin cycle efficiency in plants. Like photorespiration, an additional electron sink exists in photosynthetic organisms and lower plants driven by Flv proteins that reduce O_2 to H_2O and prevent ROS production. The expression of Flv proteins Flv2, Flv3, Flv4 in cyanobacteria *Synechocystis* sp. PCC 6803 is strongly affected under environmental clues. In cyanobacteria, Flv proteins are specifically expressed under low CO_2, Fe deficiency and fluctuating light conditions preventing over-reduction of electron transport chain and ROS production (Allahverdiyeva et al., 2015). Analyses of Flv mutants in *Physcomitrella patens* (Gerotto et al., 2016) and liverwort (Shimakawa et al., 2017) showed that Flv proteins are involved in alternative electron pathways, protecting PSI from photoinhibition. Heterologous expression of *P. patens* Flv proteins in Arabidopsis and rice protected PSI from photoinhibition under fluctuating light, indicating that Flv proteins are also functional in angiosperms. This raises the question why Flv proteins have become lost in angiosperms and whether their re-establishment may improve photosynthetic efficiency especially under stress conditions.

1.5 Occurrence of Flv proteins in the plant kingdom

In the electron transport chain of photosynthetic organisms, excess electrons may leak, where they interact with molecular O_2 and generate ROS that inhibit photosystem I and II. Photosynthetic organisms have evolved two alternative electron flow pathways that consume excess electrons generated in the PSII complex, flavodiiron proteins and photorespiration (Figure 7). In aquatic environments, the exchange of gases is 10^4 times slower than that on land (Shimakawa et al., 2017). The photosynthetic organisms that survive in wet and drought environments like cyanobacteria, algae and also lower plants, frequently encounter energy imbalance and suffer from over-reduction of the ETC. In cyanobacteria, Flv proteins act as major AEF pathways that consume excess electrons and

prevent photoinhibition of photosystems while photorespiratory activity is low or completely absent. During the course of evolution nearly 100 billion years ago, Flv proteins became lost and replaced by photorespiration as electron-consuming pathway of highest capacity (Hanawa et al., 2017**).**

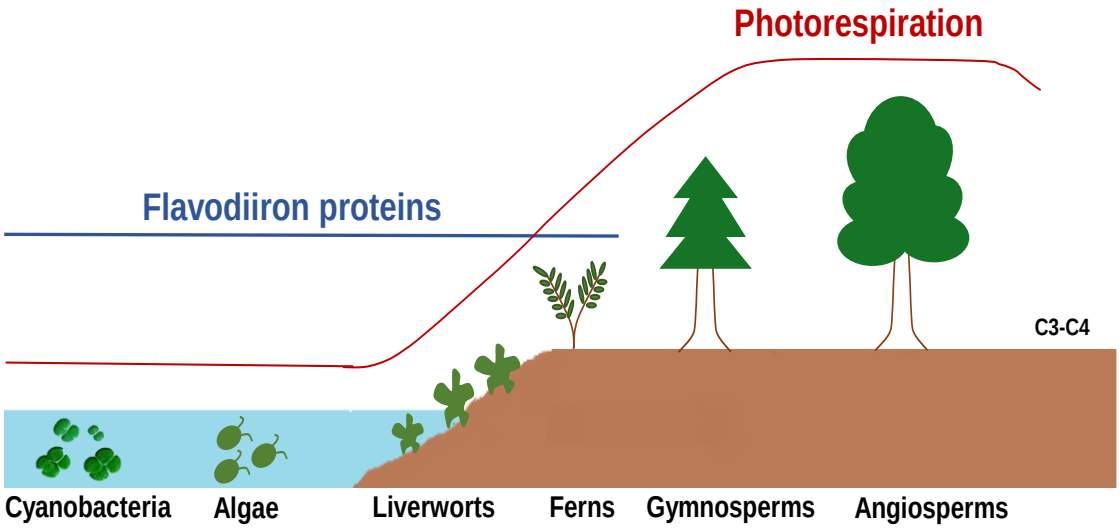

Figure 7. Flavodiiron proteins have been lost in higher plants during evolutionary adaptation. Flavodiiron proteins act as electron sinks in photosynthetic organisms and lower plants that survive in aquatic environment and dry lands, where in land plants photorespiration exists as major electron sink. Modified from Hanawa et al. (2017).

Altogether, the above-mentioned studies emphasize a possible improvement of plant growth under ambient and stress conditions using Flv proteins, whose overexpression in chloroplasts might function like mehler reaction and generate an electron sink. This in turn stimulates the formation of pmf for ATP synthesis and prevents over-reduction of the ETC leading to protection of the photosystem from photoinhibition under ambient and stress conditions. To test this hypothesis, cyanobacterial Flv proteins from *Synechocystis* were expressed in Arabidopsis plants to generate homodimers consisting of Flv1, Flv3, Flv2, Flv4 proteins and, alternatively, Flv1 and Flv3 or Flv2 and Flv4 were co-expressed to generate heterodimers with the goal to evaluate their impact on growth parameters under different light intensities and drought stress conditions. In particular, we aimed at investigating firstly whether Flv's can mediate electron transfer from the PETC to oxygen when expressed in plants as it was the case for their *Physcomitrella* counterparts, and secondly, whether this process improves plant growth under different conditions. Hereby, chl a fluorescence was used to study the influence of Flv's on photosynthetic activity and quantitative metabolic and

sugar profiling. The results presented in this thesis provide strong evidences that flavodiiron proteins enhance the photosynthetic efficiency and thus balance the energy production, which in turn is associated with enhanced carbohydrate accumulation. The maintenance of electron flow and the increased carbohydrate production resulted in enhanced growth of Arabidopsis plants.

1.6 Aims and approaches

The tuning of light reaction of photosynthesis and energy flexibility adjustments for the metabolic demand are the major limiting steps in improving photosynthesis. In plants the energy adjustments in chloroplasts are regulated by switching the electron flow between LEF and CET pathways to maintain the energy demand required for the chloroplast metabolism that improve light reaction of photosynthesis. Like mehler reaction, the cyanobacterial Flv proteins in plants may dissipate electrons that support higher ATP synthesis. Further, Flv proteins are lost in higher plants, firstly introduced Flv proteins in plants are functional is assayed in transgenic lines using fluorescence measurements and the energy adjustments that support plant growth was test under light intensities.

Initially, to determine the effect of Flv genes on plant growth under ambient conditions, the overexpression lines of all Flv genes were tested for growth traits under constant illumination but different light intensities under short-day conditions (8 h/16 h day/dark) in soil or in hydroponic cultures (chapter 1, subchapter 3.2.1 – 3.2.2). Next, the overexpression lines were grown in long-day conditions with constant illumination (16 h/8 h day/dark regime) to study biomass and yield formation (chapter 1, subchapter 3.2.3). The impact of Flv proteins in overexpression lines was also tested under application of drought stress (chapter 2, subchapter 5.3).

To investigate the impact of Flv protein on the photosynthesis electron transport chain, chlorophyll a fluorescence measurements were carried out during the early induction of photosynthesis in ambient and stress conditions (chapter 1, subchapter 3.3.1 – 3.3.3, chapter 2, subchapter 5.1, 5.2). Further, to study the impact of Flv proteins as AEF pathway that establishes a pmf for ATP synthesis, adenine nucleotide measurements were carried out in rosette leaves of all independent Flv overexpression lines (chapter 1, subchapter 3.4, chapter 2, and subchapter 5.5). In addition, a detailed metabolic profiling was carried out to elucidate the impact of Flv proteins on the pathways involved in primary metabolism (chapter 1, subchapter 3.5.1 – 3.5.4, 3.6, chapter 2, subchapter 5.4). Finally, the impact of the dioxygen scavenging reaction of Flv proteins on the redox status was investigated (chapter 1, subchapter 3.6 and 3.7, chapter 2, subchapter 5.6). Taken together, these experiments were envisaged to elucidate whether Flv proteins can enhance the metabolic activity and/or compensate for a loss of photosynthetic efficiency and thus enhance overall plant growth under ambient and stress conditions.

2. Material & Methods

2.1 Binary vector construction, transformation of Flv genes and localization studies

2.1.1 Binary vector construction

The Flv1, Flv3, Flv2, Flv4 genes were amplified from *Synechocystis* genomic DNA (Deoxyribonucleic acid) and cloned in TA cloning vector were confirmed by sequencing. Signal peptide (SP) of pea ferredoxin-$NADP^+$ reductase gene (FNR) fused to Flv genes at 5' region and cloned in the pCHF3 binary vector using Gibson cloning approach. Flv genes were driven by a CaMV-35S promoter and terminated by the pea *rbcS*-E9 gene. For Flv1/Flv3 and Flv2/Flv4 binary vector constructs, individual Flv genes together with promoter and terminator were cloned in the pCHF3 binary vector using Gibson cloning approach. All the constructs were sequenced and verified prior to plant transformation. The binary vector containing Flv genes were transfered to agrobacterium strain using heat shock protocol (Holsters et al., 1978; Weigel and Glazebrook, 2006b).

2.1.2 Plant transformation

The Agrobacterium strain EHA105 harbouring binary vectors containing Flv genes TPFlv1, TPFlv3, TPFlv2, TPFlv4 single or combinations TPFlv1/Flv3, TPFlv2/Flv4 were introduced to Arabidopsis (Col0) using the floral dip method (Clough et al., 1998). The WT (Col0) plants, in the phase of bolting or early flowering, were used for transformation. Prior to transformation, 10 ml of overnight culture of the transformed Agrobacterium strain in YEB media carrying the constructs were freshly inoculated in 400 ml YEB medium with respective antibiotics 20 mg l-1 Rifampicin, 100 mg l-1 Ampicillin and 50 mg l-1 Kanamycin and incubated at 28°C in a rotary shaker at 180 rpm (Revolutions per minute) overnight. Next day, when the OD600 of the Agrobacterium culture reached 0.8, the culture was pelleted down and dissolved in the infection medium (10 mM $MgCl_2$, 0.3% Silwet L-77 and 5% sucrose). The aerial parts of the plants were dipped in the infection medium for 5 minutes. The infected plants were placed in a tray and covered with a plastic hood to maintain humidity. On the following day, the hood was removed and the plants were well watered. Finally, the seeds were harvested and screened on selection plates containing ½ MS and 50 mg l-1 kanamycin. The Flv gene integration were confirmed by PCR using gene-specific oligos (Appendix table 1) and transferred to soil for further growth.

The Flv tobacco transformants were generated through the somatic embryogenesis method as described previously (Pathi et al., 2013). The leaf of in-vitro grown tobacco (*Nicotiana tabacum*, Samsun, SNN) plants was cut to small pieces (explants) and was used for transformation. 1 ml of overnight Agrobacterium culture carrying the constructs was freshly inoculated in 100 ml YEB medium containing antibiotics 20 mg l-1 Rifampicin, 100 mg l-1 Ampicillin and 50 mg l-1 Kanamycin and kept at 28°C in a rotary shaker at 180 rpm overnight. After 3-4 hrs of incubation at 28°C in a rotary shaker, when the OD600 reached 0.4, the culture was pelleted down and dissolved in infection medium (1/2 MS and 200 µM acetosyringone). The bacterial culture was kept at 28°C on a rotary shaker (180 rpm) for 1 h before transformation. The explants were placed in bacterial culture and incubated for 25-30 minutes on a shaker. The infected explants were transferred to co-cultivation media (MS media, 0.8% agar, 200 µM acetosyringone, 2% (w/v) sucrose) and kept in dark for 3 days. The explants were cultured in preselection media (MS media, 20 g/l sucrose, 0.2 mg l-1 IAA, 2 mg l-1 BAP, 50 mg l-1 Kanamycin and 250 mg l-1 cefotaxime). The individual plantlets were separated and cultured in rooting media (1/2 MS). The positive transformants were confirmed by PCR using gene specific oligos (Appendix table 1) and transferred to soil. Out of five independent homozygous lines per construct, three independent lines were selected based on expression data and used for further experiments.

2.1.3 Flv proteins localization studies

The fusion of transit peptide (TP) of pea FNR gene and Flv's genes with C-terminal GFP (Green fluorescent protein) tag in pGWB5 gateway vector driven by CaMV-35S promoter were transiently expressed in N. benthamiana leaves using agro-infiltration to determine the chloroplast localization of Flv proteins (Appendix Figure 1). The agrobacterium strain EHA105 harboring the gene of interest was kept overnight culture at 28°C in YEB medium containing (50 mg l-1) kanamycin, (100 mg l-1) ampicillin, and (30 mg l-1) rifampicin. The OD of the culture was checked in the following day. 1 ml of culture was inoculated in fresh YEB medium. The pre-culture was incubated at 28°C for 4-5 h and once the absorbance reached 1 at 600 nm, the culture was pelleted down by centrifugation at 3500 rpm. The pellet was dissolved in buffer containing 0.5 M $MgCl_2$, 0.5 M MES (2-(N-morpholino)-ethanesulfonic acid) (pH 5.6) and 0.1 M acetosyringone. Three to four young leaves were infiltrated on the adaxial side of the leaf using needleless syringe without damaging the leaf. After 48h, infiltrated leaf sections were photographed.

2.1.4 Confocal imaging of GFP

The infiltrated leaves were excised from the plant and hand cut to small leaf sections that were first degassed to remove air and placed on the glass slides covered with cover slips. Leaf sections were analyzed for GFP signal using a laser scanning microscope (LSM780, Carl Zeiss, and Germany). GFP signal was probed using a 488 nm laser and fluorescence signal was detected between 491–535 nm.

2.2 Growth conditions, phenotype under different light intensities and sampling

2.2.1 Growth conditions

The homozygous seeds of all Flv overexpression lines and wild type (Col0) were surfaced sterilized using 70% EtOH and 0.05 % tween20 and were rinsed for 15 minutes followed by 30 sec 96% EtOH wash. The dried seeds were kept at 4°C for 48 hrs and spread on agar plates containing half-strength MS (Murashige and Skoog) media placed vertically in growth chambers. Two weeks old seedlings were transferred to soil mixture (70l substrate 1, 23l vermiculite and 372g plantacote depot 4m) and placed in environmental controlled growth cabinets at 22°C with 80% relative humidity of air and 8 h photoperiod at 135 µmol photons m^{-2} s^{-1} light intensity. The ambient CO_2 levels were maintained in growth chambers (390 ppm) and plants were irrigated once every three days.

2.2.2 Phenotype under varying light intensity

Two week old seedlings were illuminated under four different light intensities using fluorescent lights (Philips, Master HPI-T Plus 250 W): low light (LL 50-60 µmol photons m^{-2} s^{-1}), moderate light (ML 135-150 µmol photons m^{-2} s^{-1}), moderately high light (270-300 µmol photons m^{-2} s^{-1}) and high light conditions (HL 600-650 µmol photons m^{-2} s^{-1}). The plants were covered with a hood. Other conditions were kept constant and the light intensity and heat were monitored regularly in the environmentally controlled growth chambers. The aerial parts of six weeks old plants were harvested for the measurement of shoot dry weight.

2.2.3 Sampling

Rosettes of six weeks old individual plants grown under moderate light intensity 135-150 µmol photons m^{-2} s^{-1} in growth chambers were harvested at different time points (0, 4, 8, 16, 20 and 24 h) and immediately placed in liquid nitrogen. The plant material was ground to fine powder and used for biochemical analysis.

2.3 Determination of carbohydrates, amino acids and metabolites

2.3.1 Carbohydrate analysis

The frozen plant material of (50mg) fine powder was weighed and extracted with 700 µl of 80% EtOH. The samples were incubated at 80°C for 1 h on heating block and cooled down to room temperature followed by centrifugation at 14000xg for 10 minutes. The supernatant was transferred to new tubes and the pellet was stored at 4°C for starch analysis. The samples were subjected to vacuum evaporation at 40°C and finally dissolved in 200 µl deionized water. Thereafter, samples were used for determination of sugars (glucose, fructose and sucrose). The sugar levels in the samples were measured using the enzymatic method of Ahkami *et al.* (2013). 10 µl of sample was dissolved in 290 µl of buffer (100 mM Imidazol-HCl, 5 mM $MgCl_2$, 2 mM NAD and 1 mM ATP) and 1 µl of G6PDH (1:1 dilution) incubated for 2-3 minutes in microtiter plate to determine the base line using Elisa reader (synergy ht biotek). Glucose, fructose and sucrose were determined by adding 1 µl of hexokinase enzyme (1:2 dilution), 1 µl of phosphoglucoisomerase (PGI) (1:3 dilution) and 1 µl of ß-fructosidase (10 mg/100 ml buffer without NAD and ATP) incubated in microtiter plate and read the absorption values of NADH (Nicotinamide adenine dinucleotide) formed in each reaction.

Starch was estimated as glucose that is released from the hydrolysis of starch. The left over pellet was washed twice with 80% ethanol and dried at 80°C for 1 hr in heating block. The pellet was suspended in 200 µl of 0.2 N KOH and placed at 4°C overnight. Additional 200 µl of 0.2 N KOH was added to the samples and incubated at 80°C for 1 hr. Samples were cooled down to room temperature and the pH was adjusted to 6.5-7.5 with 1N acetic acid. The samples were centrifuged at maximum speed for 10 min and 50 µl of the supernatant were incubated with buffer containing 7u/mg of Amyloglucosidase (AMG) in 50 mM NaAc, PH 5.2 at 37°C overnight to release glucose that was measured by enzymatic method as described above for sugars.

2.3.2 Amino acids analysis

Analysis of soluble amino acids was carried out essentially according to Mayta et al. (2018). Soluble amino acids profiling was carried out by derivatization with 6-aminoquinolyl-N-hydroxysuccinimidyl carbamate (AQC, self-made at IPK). UPLC (Ultra-performance liquid chromatography) was performed for separation of amino acids using AcQuity H-Class (Waters GmbH, Germany) and amino acid derivatives were detected using fluorescence detection with emission wavelength of 473 nm and excitation wavelength at 266 nm (PDA eλ Detector, Waters Germany). For amino acid measurements, 10 µl of 80% ethanol extract dissolved in water was added to 80 µl of 0.2 M boric acid (pH 8.8) and the reaction was initiated by addition of 10 µl AQC and incubation at 55°C for 10 min. One µl of derivatized sample was injected into the C18 column (Omega C18, 1.6 µm, 100x2.1 mm, Phenomenex, Germany) with a flow rate of 0.6 ml min^{-1} and duration of 11 min at 40°C. The eluent A and eluent B solutions (Waters GmbH, Germany) were used for generating a gradient for separation of amino acids. All amino acid standards were purchased commercially from Sigma-Aldrich, Germany.

2.3.3 Primary metabolites

Primary metabolites were prepared and measured as described in Ghaffari et al. (2016) with minor modifications. Approximately 100 mg of fine powdered leaf material was weighted and extracted in 1 ml of equal volumes of chloroform and methanol extraction solution and kept at 4°C for rigorous mixing for 20 min. Subsequently, 300 µl water was added to each sample and mixed thoroughly for 1 min. The samples were centrifuged at 14 000 rpm for 10 min at 4°C and the supernatant was transferred to new Eppendorf tubes. Samples were vacuum-dried in speed vac (Alpha 2-4 LD plus) at 40°C and finally 200 µl of water added to each tube (HPLC -High performance liquid chromatography grade water) followed by the analysis using ion chromatography coupled to mass spectrometry (IC-MS/MS).

Primary metabolites were separated on ICS 5000 (Dionex) ion chromatography through ion exchange column AS11-HC (250×2 mm) connected to a 10×2 mm AG11-HC guard column and an ATC-1 anion trap column (Thermofisher, Dionex, Germany). The columns were equilibrated with 96 % water (HPLC grade) and 4 % KOH at a flow rate of 0.38 ml min^{-1} and column temperature was maintained at 37°C. Simultaneously, the samples were analyzed by MS (Agilent 6490 Triple Quadrupole MS system), which was operated in negative ion electrospray at unit resolution in a multiple reaction monitoring (MRM) mode. The MRM acquired data for each compound was processed using Agilent MassHunter Workstation

and Mass Hunter Quantitative Analysis software (version B.07.01). For normalization of the data ^{13}C-pyruvate was used as internal standard.

2.3.4 Adenine nucleotide analysis

Nucleotides were detected employing a highly sensitive fluorescence UPLC method established in our group based on Haink and Deussen (2003) with some modifications. Prior to UPLC separation, an aliquot of the samples (20 µl) used for metabolites (Ghaffari et al. 2016) or standards (mixture of ATP, ADP, AMP and ADPGlc) was derivatized with 10% (v/v) chloracetaldehyde (45 µl) and a buffer containing 62 mM sodium citrate and 76 mM potassium di-hydroxide phosphate, pH 5.2 adjusted with KOH (435 µl). The mixture was incubated for 40 min at 80°C, cooled immediately on ice, centrifuged at 20,000 *g* for 1 min and used for UPLC analysis. Separation was carried out with a reversed phase UPLC system (Agilent Infinity 1200). The gradient was accomplished with a buffer (TBAS/KH_2PO_4) containing 5.7 mM tetrabutylammonium bisulfate and 30.5 mM potassium di-hydroxide phosphate, pH 5.8 (Eluent A) and an eluent containing pure acetonitrile and TBAS/KH_2PO_4 in a ratio of 2:1 (Eluent B) (Roti C Solv HPLC, Roth, Karlsruhe, Germany). The column used was Eclipse plus C18 (1.8 µm, 2.1x50 mm, Agilent, Germany). The gradient was accomplished as follow: The column was equilibrated with eluent A (90 %) and eluent B (10 %) for at least 30 minutes and changed at 0 min to 90% A and 10 % B, kept for 1.0 min, at 2.0 min to 40% A and 60% B, kept for 2 min, at 4.3 min to 10% A and 90% B and at 5.4 min to 90% A and 10% B and kept for 1.6 min. Flow rate was 0.6 ml/min and column temperature was 37°C. The excitation wavelength was set at 280 nm and the emission wavelength at 410 nm. In all cases chromatograms were integrated using the software MassHunter, release B.04.00 (Agilent Germany).

2.3.5 Non-enzymatic antioxidant measurements

A new rapid procedure was established to determine the concentrations of the antioxidants. The extraction of leaf material was performed as described by Tausz et al., (1996) with slight modifications. Approximately 100 mg of fresh leaf material was ground to fine powder using tissue lyzer and homogenized with 1 mM EDTA (Ethylenediaminetetraacetic acid) and 0.1% formic acid at 4°C under green safelight and centrifuged at maximum speed (15.000 rpm) for 10 min. The measurement of oxidized and reduced glutathione was immediately carried out in freshly prepared extracts. The separation and analysis of desired compounds was carried out on a C18 column (Acquity

UPLC HSS T3, 1.8 µm, 2.1x150 mm, Waters Germany) and a UPLC/MS-MS (Infinity ll, 6490 Triple Quadrupole LC/MS, Agilent Germany), respectively. 2 µl of extracts and the corresponding standards were injected in the mobile phase consisting of purest water plus 0.1 % formic acid and pure methanol plus 0.1 % formic acid. The temperature of auto sampler and the column was maintained at 8°C and 37°C, respectively. Separated compounds were eluted at a flow rate of 0.5 ml/min. The evaluation and quantification of the compounds were performed using the software MassHunter, release B.04.00 (Agilent Germany).

2.4 Chlorophyll a fluorescence measurements

Chlorophyll a fluorescence measurements were analyzed using multispec v1.0 device using the photosynQ software (Kuhlgert et al., 2016). Fully expanded leaves of six weeks old plants adapted for 4h dark period were used for the measurements. The minimal fluorescence (F_0) was measured in the dark adapted leaves before applying saturating pulse of light (sp, 500 ms, 3000 µmol photon m^{-2} s^{-1}) using red led light (emission at 650 nm) and to determine the maximal fluorescence (F_m). The (F_m') and (F_s) steady state fluorescence was determined during actinic light illumination (150 µmol photon m^{-2} s^{-1}). Chlorophyll transient induction measurements on dark adapted leaves were carried out during first one minute after light illumination as described (Gomez et al., 2017). The PSll photosynthesis parameters were calculated respectively according to Baker (2008; $Fv/F_m = (F_m - F_o)/F_m$; $NPQ = (F_m - F_m')/F_m'$). Fv (Variable chlorophyll fluorescence) indicates the difference between minimal fluorescence (F_0) and maximal fluorescence (F_m). Other parameters Φ_{PSII} (operating efficiency of PSll), Φ_{NPQ} (Light dependent NPQ), Φ_{No} (Radiation less energy decay) and ql were calculated according to Kramer et al., (2004).

2.5 Transmission electron microscopy

TEM analysis was performed according to Mayta et al., (2018). Cuttings of 2 mm^2 from the central part of Arabidopsis leaves from three different wild type and transgenic Flv plants were used for sample preparation. Conventional and microwave-assisted fixation substitution, resin embedding, sectioning, and microscopic analysis were performed as described (Kraner et al., 2017).

2.6 RNA isolation, cDNA synthesis and expression analysis

Total RNA (Ribonucleic acid) extract from young leaves was carried out according to Logemann *et al.,* (1987). Total RNA was subjected to DNase treatment (Thermo). The single strand cDNA (complementary DNA) synthesis was performed using Revert Aid first strand cDNA synthesis kit (Thermo) with 1 µg total RNA and oligo (dt) primer at 42°C for 60 min. The cDNA was used for the analysis of gene expression using the gene specific oligos (Appendix table 1).

2.7 Chlorophyll and protein measurements

The extraction of chlorophyll (Chls) pigments was carried out using 80% acetone from leaf tissues stored at 4°C. The quantification of chlorophyll content using spectrophotometric method as described (Porra *et al.*, 1989). The total protein concentration in leaf tissue was determined using the microplate method as described (Dreher *et al*., 2005).

2.8 Application of drought stress

All Arabidopsis plants including Columbia (Col0) and three independent lines of each gene (Flv1, Flv3, Flv1/Flv3 and Flv2, Flv4, Flv2/Flv4) were used for drought tolerance experiment. The seeds were surfaced sterilized and kept at 4°C for 48 h for stratification. 10 days old seedlings grown on ½ MS (Murashige and Skoog) media were transferred to pots with equal amount of soil. After four weeks, water withholding was performed to have natural drought treatment and the field capacity was regularly monitored using moisture meter (Delta-T, SM150 kit). All pots were maintained at 5% field capacity, adjusting the moisture content by addition of required water every alternative days by both weighing the pots and measuring the field capacity. Chlorophyll a fluorescence measurements were taken and rosettes of individual plants were harvested for biochemical analysis.

2.9 Statistical analysis

Data analysis was carried out using Sigma plot, version 12.3. Expression of Flv genes in the transgenics were different and the data obtained cannot be compared between the genes. So, statistical differences between WT and transgenic lines were analyzed using Student's T-test.

3. Results

3.1 Expression and localization of cyanobacterial flavodiiron proteins in Arabidopsis

3.1.1 Generation of homozygous plants, expression analysis and localization of Flv proteins

To investigate the impact of additional AEF pathways in chloroplasts on photosynthesis and plant growth, transgenic Arabidopsis (Col0) lines constitutively expressing individual Flv1, Flv2, Flv3, Flv4 genes or a combination of Flv1/Flv3 or Flv2/Flv4. Individual Flv gene constructs, driven by the cauliflower mosaic virus (CaMV) 35S promoter and carrying a pea FNR signal peptide (SP) fused to the 5'-end of the gene in the pCHF3 binary vector, were used for Arabidopsis transformation (Figure 8A). For each construct, five independent transformants were selected upon screening on selection medium. The integration of Flv genes in the genome was confirmed by PCR analysis. Three lines of each construct were selected for further experiments based on transcript levels obtained by RT-PCR (Reverse transcription-ploymerase chain reaction) (Figure 8B). Real time qPCR (Quantitative polymerase chain reaction) was not performed on the Flv-expressing lines for not having internal controls to compare the expression of Flv genes. Further, to see Flv protein levels in expressing lines, we requested for antibodies to perform western blot from a group working on Flv proteins in Finland, they don't have enough aliquot of antibodies to share with us. Homozygous seeds were generated for all selected independent lines that showed different expression levels in all three lines of Flv1, Flv3, Flv1/Flv3 and Flv2, Flv4, Flv2/Flv4. Ubiquitin used as an internal marker was similar in the wild type and all investigated transgenic lines (Figure 8B).

Chloroplast localization of the fusion proteins TPFlv1, TPFlv2, TPFlv3, and TPFlv4 was validated by fusing GFP to C-terminus of Flv genes in PGWB5 gateway binary vector

driven by 35S promoter (Appendix Figure 1). The construct was expressed in tobacco leaves using the agro-infiltration method (see materials and methods, subchapter 2.1.3). GFP signal detection by confocal scanning electron microscopy revealed that the fusion proteins TPFlv1, TPFlv2, TPFlv3, and TPFlv4 were all localized to the chloroplasts (Figure 8C).

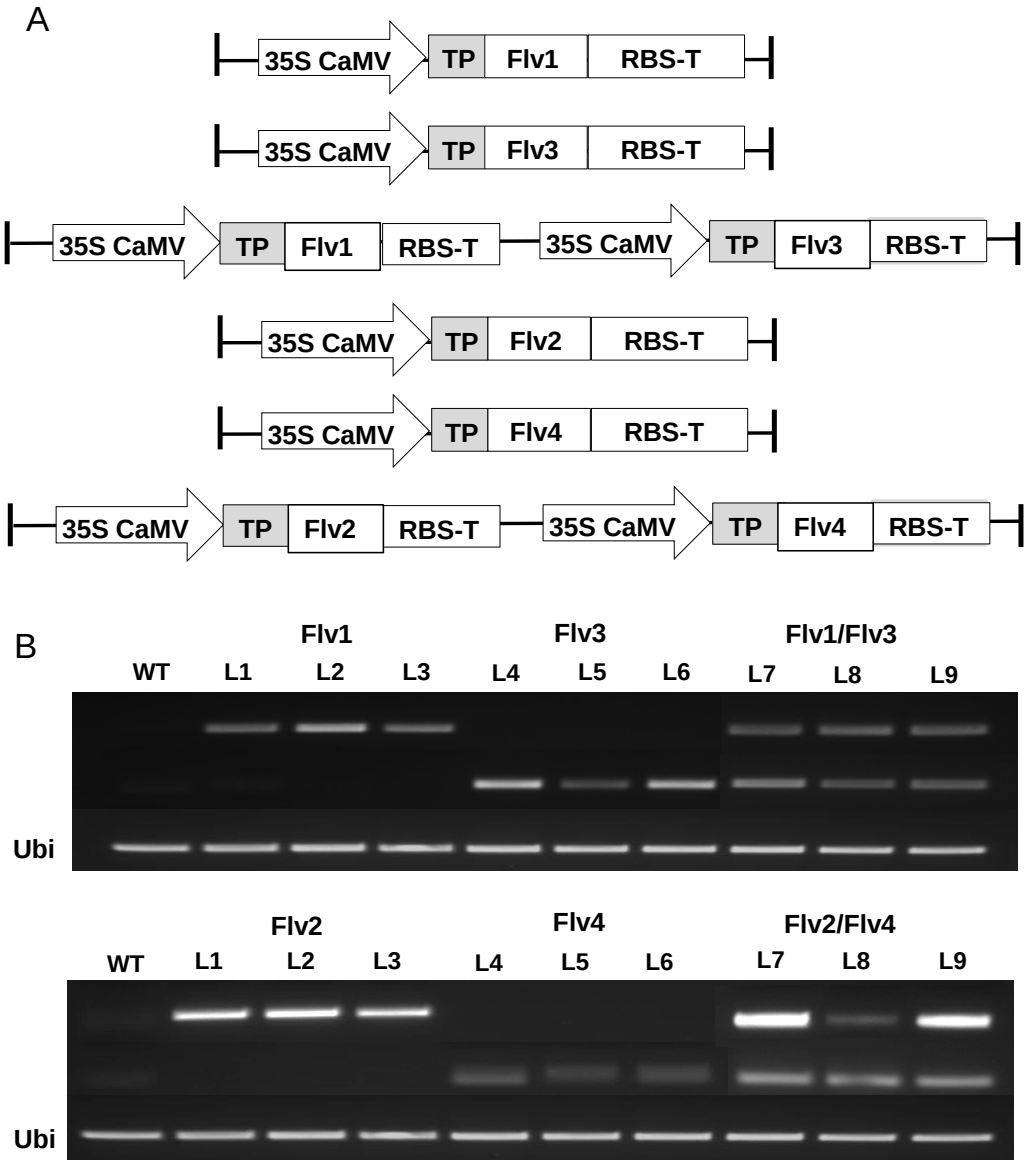

Figure 8 . (Left and Right) Construction of binary vectors, expression and localization of Flv1, Flv2, Flv3, and Flv4 proteins in chloroplasts of Arabidopsis. (A) Constructs for expression of Flv1, Flv2, Flv3, Flv4 genes and combination of Flv1/Flv3, Flv2/Flv4 genes. The DNA sequence for the pea FNR transit peptide (TP) was fused to 5'-end of the Flv proteins for chloroplast localization (gray box). Promoter (35s CaMV) and terminator (RBS-t) sequences are indicated. (B) Expression analysis of Flv genes in Arabidopsis transformants. Ubiquitin was used as an internal control, lower line. For each transformant, three independent lines are shown (L1 to L9). (C) Localization of Flv1-, Flv2-, Flv3-, or Flv4-GFP fusion proteins in chloroplasts of *N. benthamiana* after Agro-infiltration.

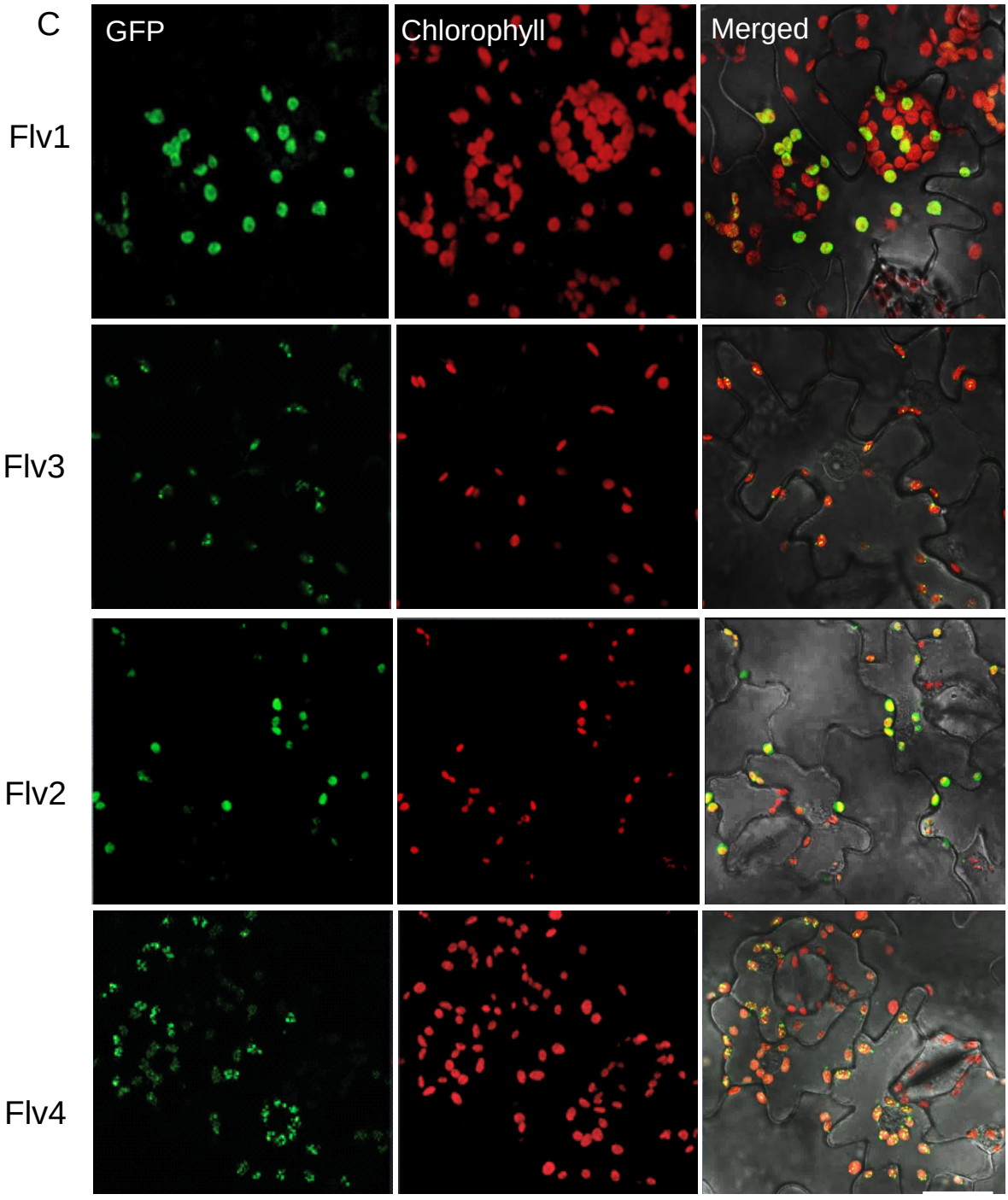
C
GFP
Chlorophyll
Merged
Flv1
Flv3
Flv2
Flv4

3.2 Characterization of the growth of Flv-expressing Arabidopsis plants

3.2.1 Growth responses to different light conditions in soil culture

To evaluate the impact of introduced Flv proteins on plant development, WT and transgenic plants were grown at different light intensities and analyzed for biomass formation (Figure 9A, B, Figure 10A, B). At low light intensity (50 µmol photons m^{-2} s^{-1}) the Flv-expressing lines and WT plants showed no visual differences (Figure 9A-a, 10A-a) and also biomass (Figure 9B-a, 10B-a). However, Flv-expressing lines showed a visual difference in plant growth at light intensities of 150 µmol photons m^{-2} s^{-1} or 300 µmol photons m^{-2} s^{-1} (Figure 9A-b, 10A-b). The increase in biomass was confirmed by determination of shoot dry weights six weeks after germination, which significantly increased by up to 1.3 times in all three investigated transgenic lines expressing Flv1, Flv3, Flv1/Flv3, except for L7, L8 (Figure 9B-b) at 150 µmol photons m^{-2} s^{-1} light intensity, whereas in Flv2, Flv4, Flv2/Flv4 the three investigated transgenic lines showed a significant increase up to 1.2 times (Figure 10B-b) compared to WT plants, except for L2, L5, L8. Under 300 µmol photons m^{-2} s^{-1} light intensity, the Flv1-, Flv3-, Flv1/Flv3-expressing lines showed 20% higher shoot biomass, except for L3 (Flv1) (Figure 9B-c), whereas in Flv2-expressing lines showed increase up to 1.3 times and also L6 (Flv4), L7, L9 (Flv2/Flv4) lines except L4, L5 (Flv4), L8 (Flv2/Flv4) compared to wild type (Figure 10B-c). At highest light intensity (600 µmol photons m^{-2} s^{-1}), observed higher biomass in L8, L9 (Flv1/Flv3) and L4 (Flv4) Flv-expressing lines compared to wild type (Figure 9B-d, Figure 10B-d). The targeting Flv proteins to chloroplasts improve plant growth was clearly observed under high illumination conditions. In all subsequent experiments, growth conditions were set to 150 µmol photons m^{-2} s^{-1} to investigate the biochemical mechanism underlying biomass increase at this light intensity.

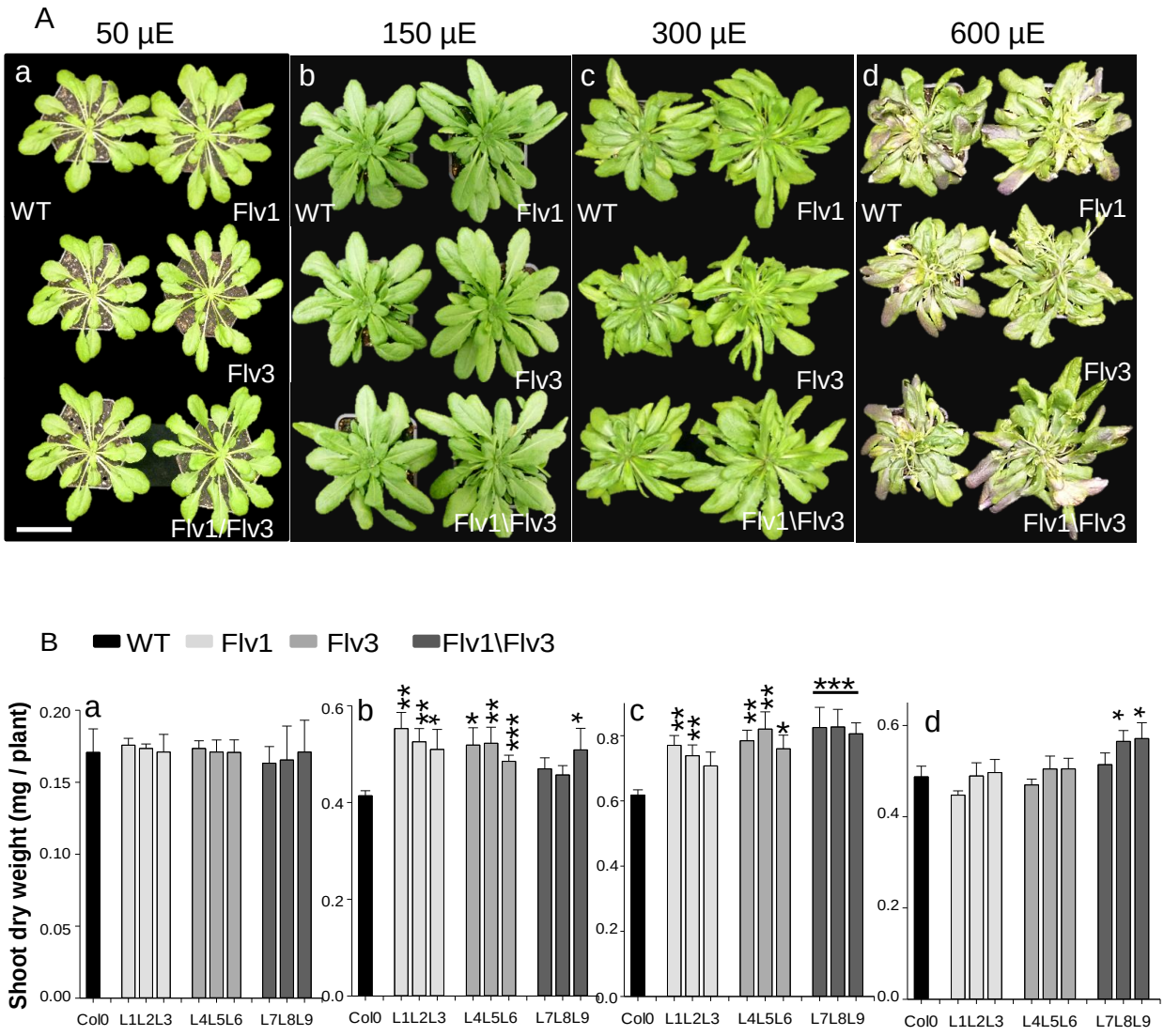

Figure 9. Growth of Arabidopsis plants expressing cyanobacterial Flv genes (Flv1, Flv3, Flv1/Flv3) under different light intensities. (A) Visual appearance of Arabidopsis plants grown under short day conditions (8h/16h – light/dark regime) at four different light intensities: 50, 150, 300 and 600 µmol photons m^{-2} s^{-1}. (B) Shoot dry weight of three independent transgenic lines per construct. Bars represent means of 5 biological replicates ±SE. Significant differences between WT and transgenic lines are indicated by asterisks according to Student's t test (* $p \leq 0.05$, ** $p \leq 0.01$ and ***$p \leq 0.001$). Bar = 3 cm. Photographs and shoot dry weight were determined six weeks after germination.

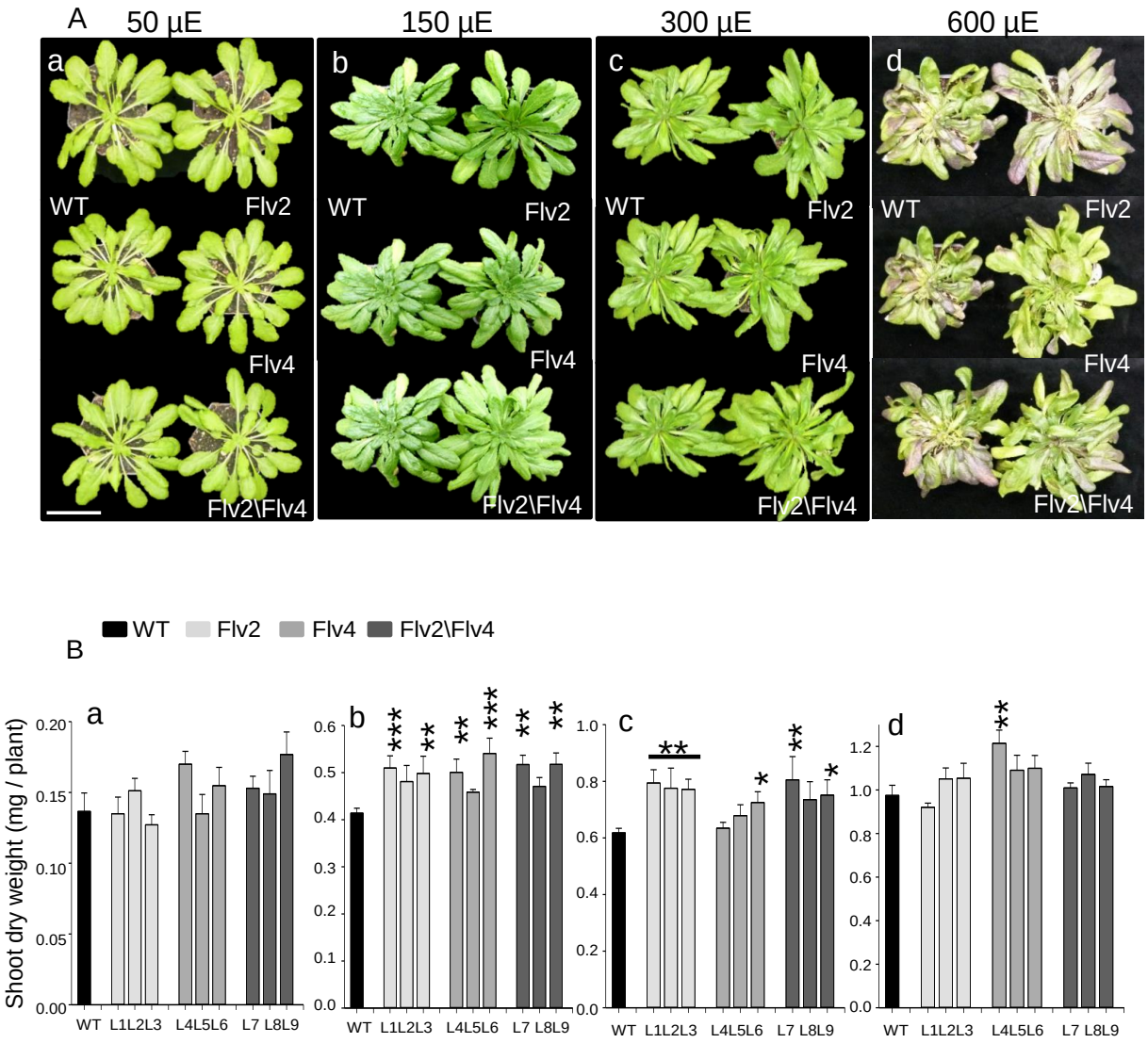

Figure 10. Growth of Arabidopsis plants expressing cyanobacterial Flv genes (Flv2, Flv4, Flv2/Flv4) under different light intensities. (A) Visual appreance of Arabidopsis plants grown under short day conditions (8hr/16hrs – light/dark regime) at four different light intensities: 50, 150, 300, and 600 µmol photons m^{-2} s^{-1}. (B) Shoot dry weight of three independent transgenic lines per construct. Bars represent means of 5 biological replicates ±SE. Significant differences between WT and transgenic lines are indicated by asterisks according to Student's t test (*p≤0.05, **p≤0.01 and ***p≤0.001). Bar=3cm. Photographs and shoot dry weight were determined six weeks after germination.

3.2.2 Growth of Arabidopsis lines expressing Flv genes in hydroponic culture

The effect of Flv gene expression on plant growth was assayed in hydroponic culture at a light intensity of 150 µmol photons m^{-2} s^{-1} and in a 8h/16h-light/dark regime. Flv-expression lines showed better growth than the wild type (Figure 11A, Figure 12A). The Flv-expressing lines Flv1, Flv3, or Flv1/Flv3 showed significant increases of shoot dry weight up to 1.7 times (Figure 11B) and root dry weight up to 1.4 times in all investigated lines except for L5, L9 (Figure 11C), whereas in Flv2-, Flv4-, and Flv2/Flv4-expressing lines the shoot dry was up to 1.6 times higher (Figure 12B), while root dry weight was up to 1.9 times higher than the wild type, except for L6 (Figure 12C). The above results demonstrate that Flv proteins enhance the total dry weight of the plant.

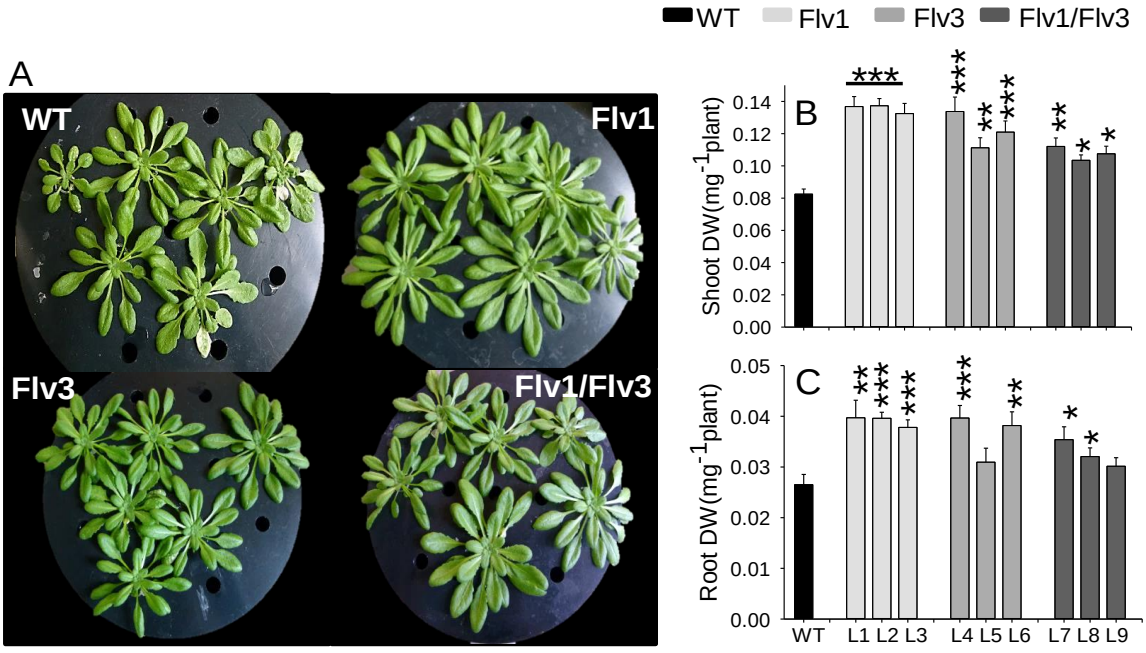

Figure 11. Hydroponic cultivation of Arabidopsis (WT) plants expressing cyanobacterial Flv genes (Flv1, Flv3, or Flv1/Flv3) in full nutrient solution. (A) Visual appearance of Arabidopsis plants grown under 150 µmol m^{-2} s^{-1} light intensity in phyto-chambers under short day conditions (8h/16h – light/dark regime). (B) Shoot dry weight and (C) Root dry weight of three independent transgenic lines per construct. Bars represent means of 5 biological replicates ±SE. Significant differences between WT and transgenic lines are indicated by asterisks according to Student's t test (*p≤0.05, **p≤0.01 and ***p≤0.001). Photographs and dry weight were determined six weeks after germination.

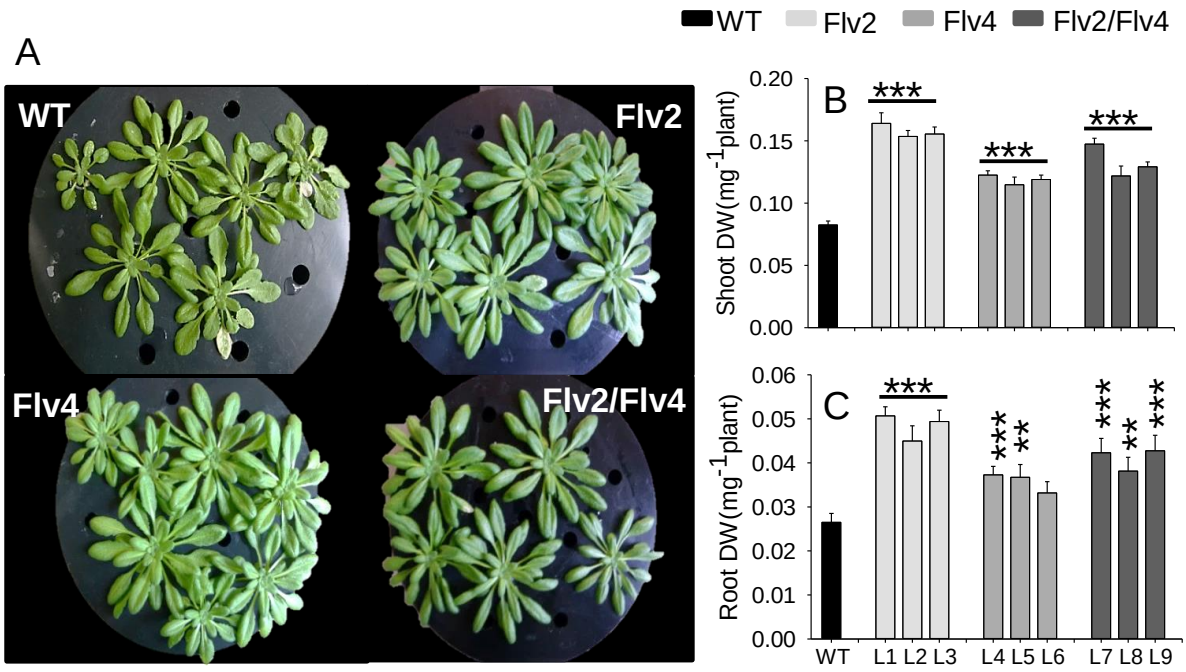

Figure 12. Hydroponic cultivation of Arabidopsis (WT) plants expressing cyanobacterial Flv genes (Flv2, Flv4, or Flv2/Flv4) in full nutrient solution. (A) Visual appearance of Arabidopsis plants grown under 150 µmol m^{-2} s^{-1} light intensity in phyto-chambers under short day conditions (8h/16h – light/dark regime). (B) Shoot dry weight and (C) Root dry weight of three independent transgenic lines per construct. Bars represent means of 5 biological replicates ±SE. Significant differences between WT and transgenic lines are indicated by asterisks according to Student's t test (*p≤0.05, **p≤0.01 and ***p≤0.001). Photographs and dry weight were determined six weeks after germination.

3.2.3 Effect of Flv genes on final yield in Arabidopsis and tobacco expressing lines

To assess the impact of Flv gene expression on yield traits in mature plants, total shoot dry weight and seed yield were determined in Arabidopsis plants grown under a long-day regime to promote transition to the reproductive stage. Transgenic plants showed early flowering (data not shown) and a bushy phenotype with increased inflorescences compared to WT siblings (Figure 13). Shoot dry weight was up to 1.7 times higher in all investigated lines of Flv1, Flv3, and Flv1/Flv3 except for L2 (Flv1), L9 (Flv1/Flv3) (Figure 13B) and up to 1.6 times higher in Flv2-, Flv4-, and Flv2/Flv4-expressing lines except for L9 (Flv2/Flv4) (Figure 13E). Seed size was not affected by Flv genes (data not shown), but seed weight was significantly increased and between 1.1 and 1.8-times higher in Flv-expressing lines Flv1, Flv3, or Flv1/Flv3, except for L4, L5 (Flv3) (Figure 13C). In parallel, seed weight increased by up to 1.4 times in the lines L3 (Flv2) and L1 (Flv4) and up to 1.6 times in all Flv2/Flv4-expressing lines (Figure 13F) relative to the wild type. These results indicate that

cyanobacterial Flv genes can enhance the final seed and biomass yield of Arabidopsis plants.

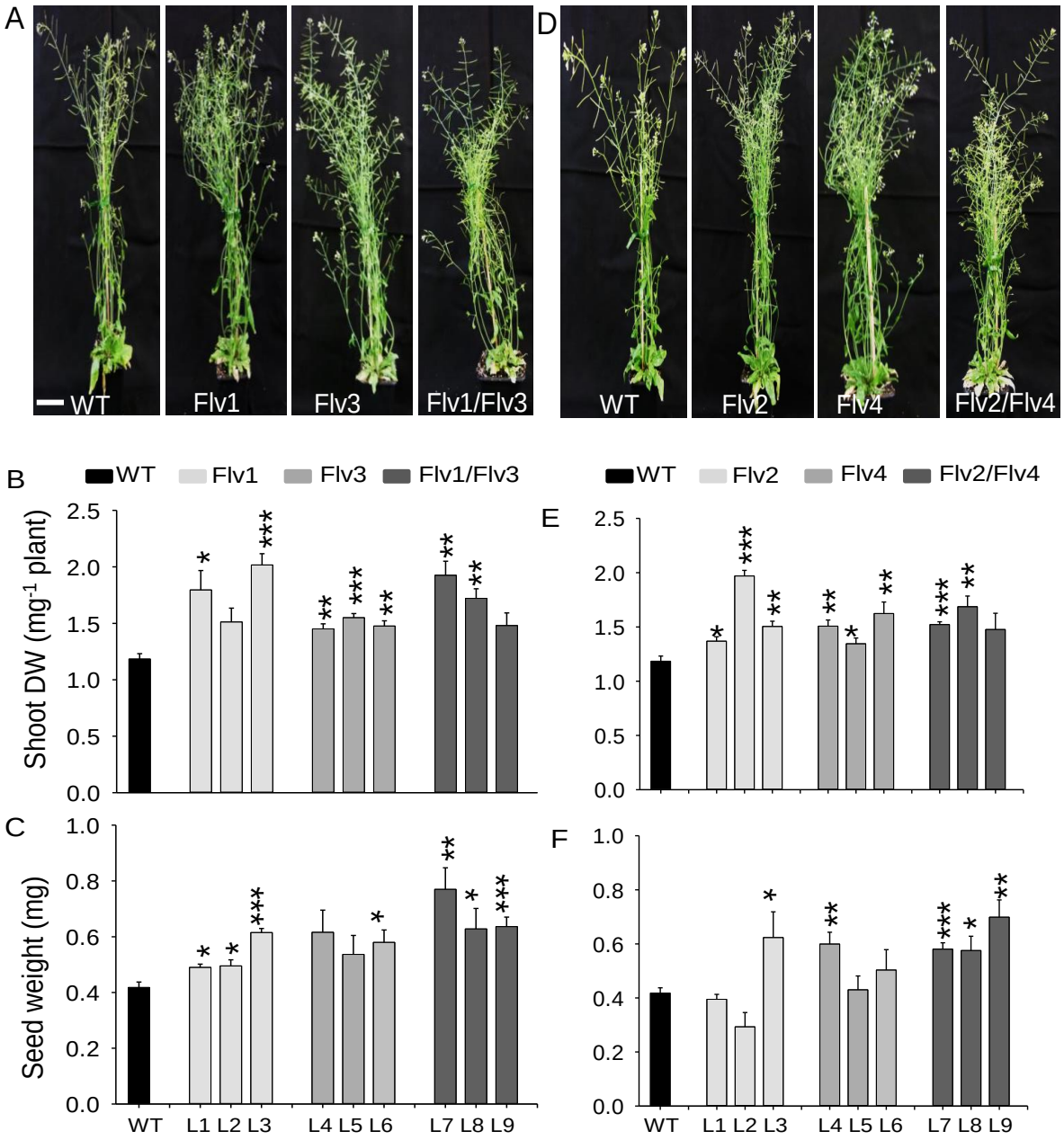

Figure 13. Yield analysis of Flv-expressing and WT (Col0) Arabidopsis plants grown until maturity. (A and D) Visual appearance of Flv-expressing Arabidopsis plants under long-day conditions in a growth chamber (16h/8h-light/dark regime and 150 µmol m^{-2} s^{-1}). (B and E) Shoot dry weight and (C and F) seed weight of plants at maturity. Bars represent means ±SE of 5 biological replicates. Significant differences between WT and transgenic lines are indicated by asterisks according to Student's t test (*p≤0.05, **p≤0.01 and ***p≤0.001). Bar = 5cm.

To verify the impact of Flv gene expression on growth traits as examined in Arabidopsis, Flv genes were expressed also in another plant species, which is tobacco. RT-PCR analysis was carried out to study the expression of Flv genes in Tobacco plants (Appendix figure S2). When tobacco plants were grown under long days at 250 µmol photons m^{-2} s^{-1} and in a 16h/8h-light/dark regime until maturity, shoot dry weight and seed weight were significantly higher than of WT plants (Figure 14 and 15). The expression of Flv genes accelerated plant growth as characterized by faster development of secondary leaves compared to wild type. The shoot dry weight was higher in the line L2 (Flv1), lines L5 and L6 (Flv3) (Figure 14B), whereas shoot dry weight was higher than in the wild type in the lines L2 (Flv2), L5 and L6 (Flv4), and L8 (Flv2/Flv4) (Figure 15B). The final yield was higher in L2 expressing Flv1, in L4 and L6 expressing Flv3, and in L7 and L9 expressing Flv1/Flv3 (Figure 14C), whereas yield was higher in L1 and L3 (Flv2), all lines (Flv4) and L7 and L8 (Flv2/Flv4) (Figure 15C) compared to wild type plants. These results indicate that similar to Arabidopsis Flv gene expression enhances shoot biomass and grain yield also in tobacco plants.

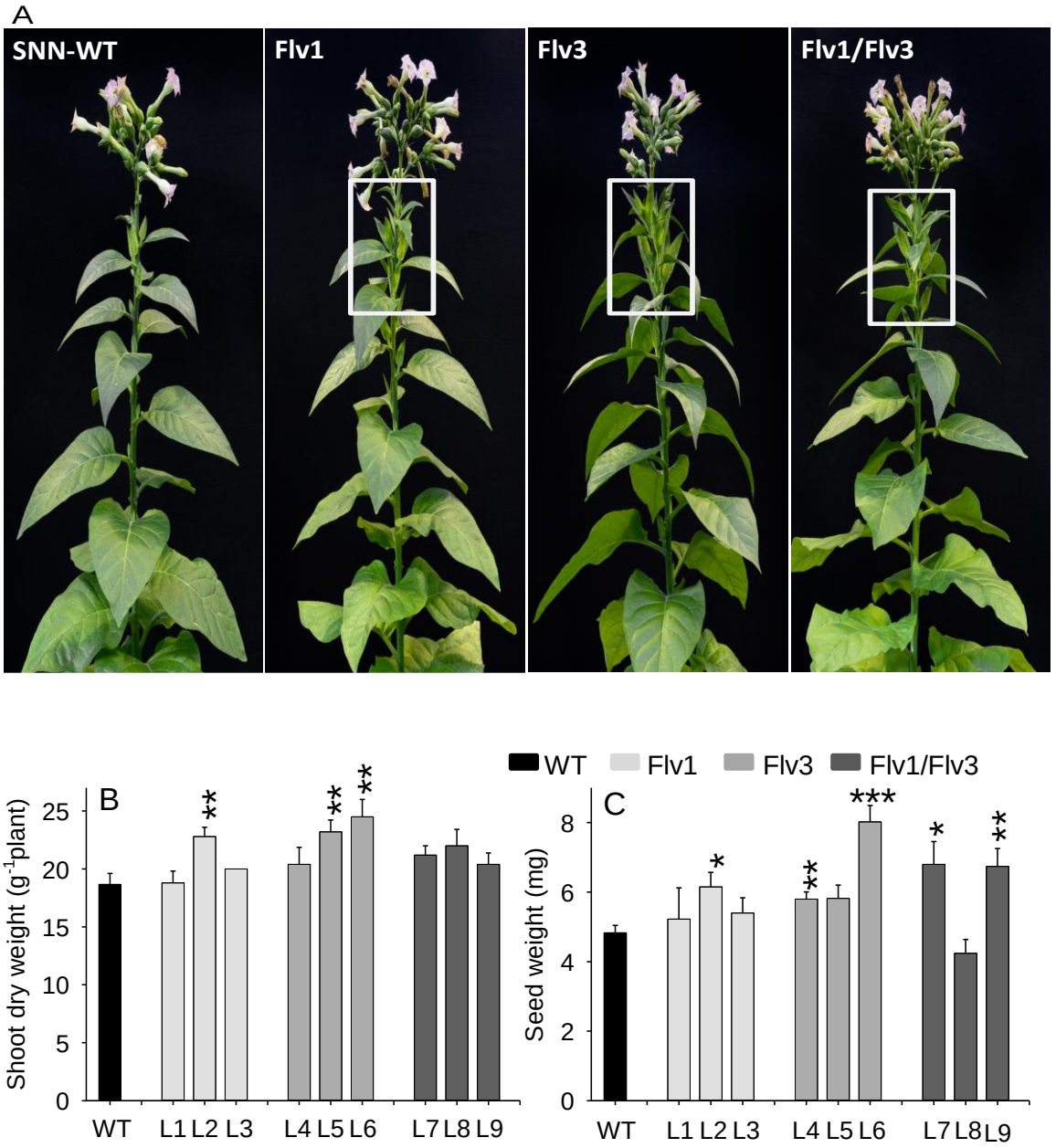

Figure 14. The phenotype of Flv expression (Flv1, Flv3, Flv1/Flv3) and WT tobacco plants. (A) Visual appreance of Flv expressing tobacco plants grown in the greenhouse (16 h/8h-light/dark regime at 250 µmol $m^{-2}s^{-1}$). (B) Shoot dry weight and (C) Seed weight of three independent transgenic lines per construct. Bars represent means of 5 biological replicates ±SE. Significant differences between WT and transgenic lines are indicated by asterisks according to Student's t test (*p≤0.05, **p≤0.01 and ***p≤0.001). Total shoot dry weight and seed weight were determined at the final developmental stage (ripening).

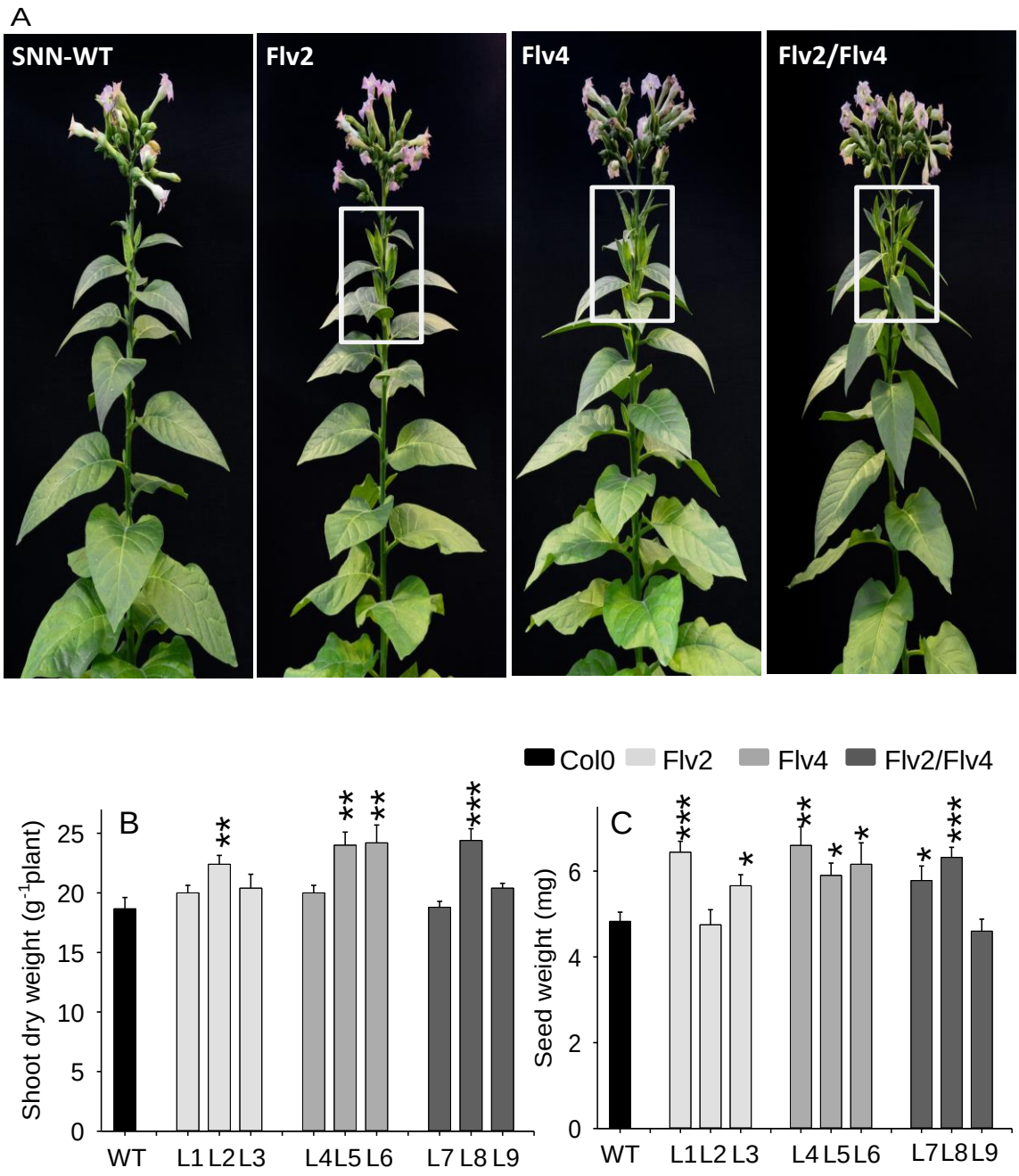

Figure 15. The phenotype of Flv expression (Flv2, Flv4, Flv2/Flv4) and WT tobacco plants. (A) Visual appreance of Flv expressing tobacco plants grown in the greenhouse (16 h/8h-light/dark regime at 250 µmol $m^{-2}s^{-1}$). (B) Shoot dry weight and (C) Seed weight of three independent transgenic lines per construct. Bars represent means of 5 biological replicates ±SE. Significant differences between WT and transgenic lines are indicated by asterisks according to Student's t test (*p≤0.05, **p≤0.01 and ***p≤0.001). Total shoot dry weight and seed weight were determined at the final developmental stage (ripening).

3.3 Influence of Flv proteins on photosynthetic performance

3.3.1 Flv proteins affect photosynthetic efficiency in Flv-expressing lines

To study the impact of Flv protein function on photosynthetic performance, the maximum quantum efficiency of photosystem II (Fv/Fm), the quantum yield of PSII (φII) and the fraction of open reaction centers (qL) (Baker, 2008) were determined in fully expanded leaves of dark-adapted six weeks-old plants expressing Flv genes.

Determination of Fv/Fm values in dark-adapted leaves showed a moderate but significant increase of this parameter in lines expressing Flv3, Flv1/Flv3, or Flv4 compared to WT, while transgenic lines expressing Flv1, Flv2, or Flv2/Flv4 showed no differences (Figure 16A, Figure 17A). These results indicate that the transgenic plants carrying Flv3*,* Flv1/Flv3*,* or Flv4 genes showed higher photosynthetic performance.

During the early induction of photosynthesis, φ_{PSII} values in Flv1-expressing lines illuminated with 150 µmol photons m^{-2} s^{-1} did not differ from those of WT counterparts, while in Flv3-*,* Flv1/Flv3-expressing lines (Figure 16B) and Flv2-, Flv4-, Flv2/Flv4-expressing lines (Figure 17B) were higher. The qL parameter also showed an increase in Flv3-*,* Flv1/Flv3- (Figure 16C) and Flv2-, Flv4-, Flv2/Flv4-expressing lines (Figure 17C) compared to wild type but not in Flv1-expressing lines. The above chlorophyll a fluorescence measurements predict that Flv proteins are functional in higher plants that accept electrons at both photosystems.

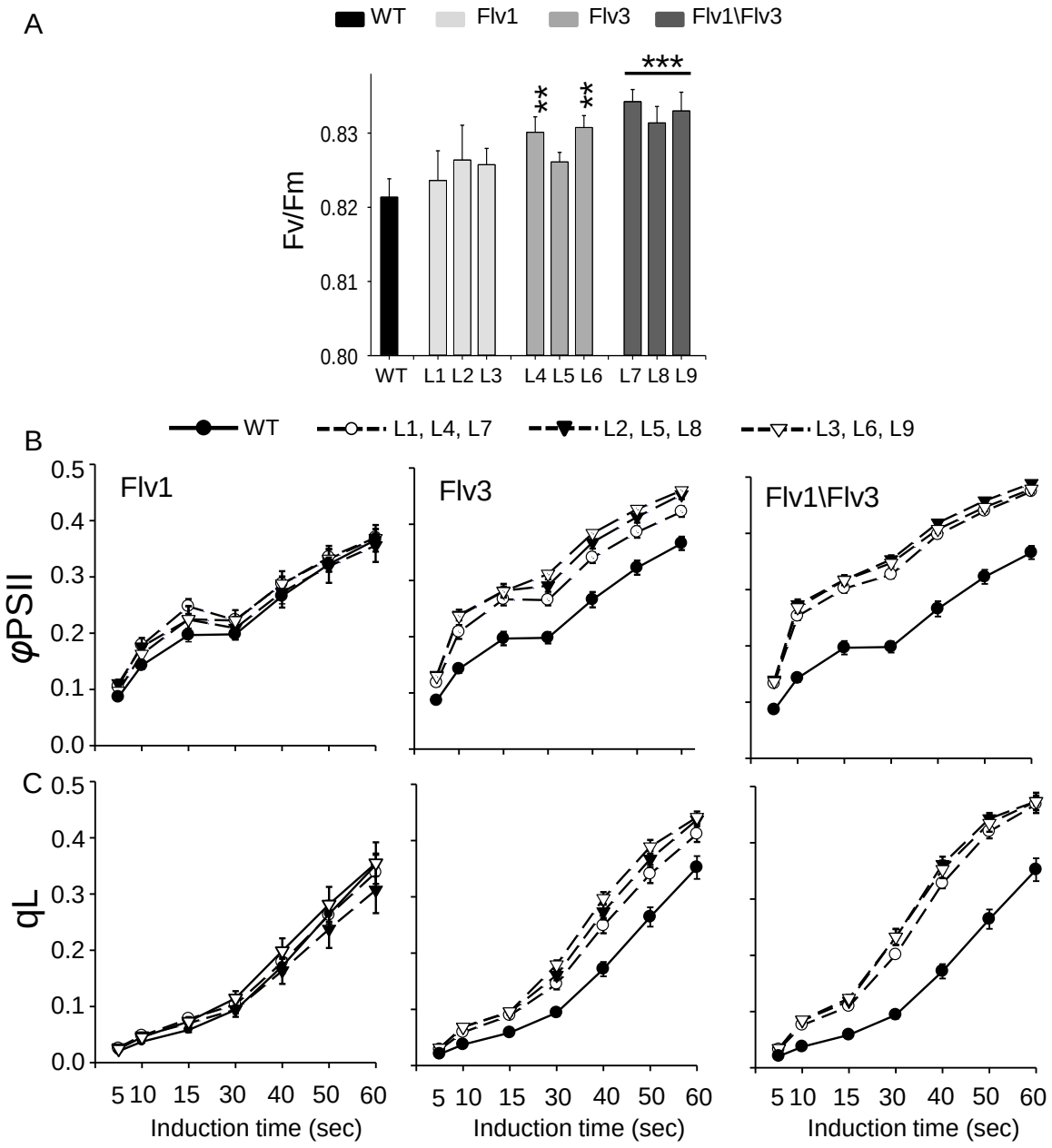

Figure 16. Effect of Flv gene expression on photosynthetic efficiency of PSII and oxidation state of the electron transport chain during early induction of photosynthesis (first 60 sec) in Flv1, Flv3, or Flv1/Flv3-expressing plants. (A) The maximum quantum yield of PSII (Fv/Fm). (B) φPSII, quantum yield of PSII and (C) qL, fraction of open PSII reaction centers. Values were determined at 150 μmol photons m^{-2} s^{-1} of actinic illumination on dark-adapted leaves of WT (black bar and circles) and three independent transgenic lines of Flv1-, Flv3- and Flv1/Flv3-expressing plants: open circles (L1, L4, L7), black triangles (L2, L5, L8) and open triangles (L3, L6, L9). Bars and data points represent mean of 8 biological replicates ±SE. Significant differences are indicated by asterisks according to Student's t test (**p≤0.01, ***p≤0.001).

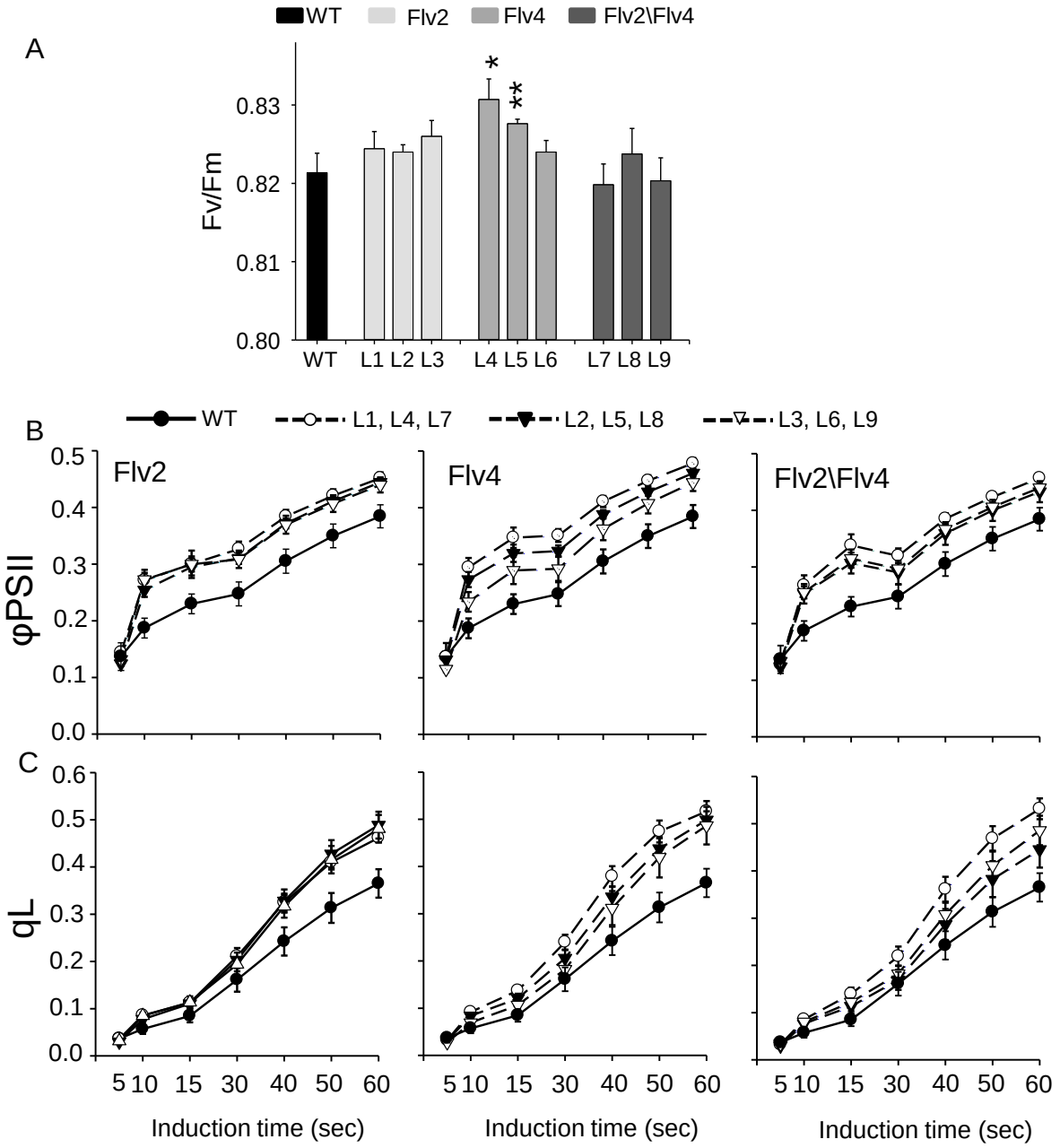

Figure 17. Effect of Flv gene expression on photosynthesis efficiency of PSII and oxidation state of the electron transport chain during early induction of photosynthesis (first 60 sec) in Flv1-, Flv3-, Flv1/Flv3-expressing plants. (A) The maximum quantum yield of PSII (Fv/Fm). (B) φPSII, quantum yield of PSII and (C) qL, fraction of open PSII reaction centers. Values were determined at 150 μmol photons m^{-2} s^{-1} of actinic illumination on dark-adapted leaves of WT (black bar and circles) and three independent transgenic lines of Flv1-, Flv3- and Flv1/Flv3-expressing plants: open circles (L1, L4, L7), black triangles (L2, L5, L8) and open triangles (L3, L6, L9). Bars and data points represents mean of 8 biological replicates ±SE. Significant differences are indicated by asterisks according to Student's t test (**p≤0.01, ***p≤0.001).

3.3.2 Early induction of NPQ parameters in Flv expression lines

The quantum yield of quenching due to light-induced processes φIINPQ was significantly higher throughout the whole measurement in Flv1-expressing lines and to a lesser extent also in Flv3- and Flv1/Flv3-expressing lines (Figure 18A), whereas in Flv2-, Flv4-, Flv2/Flv4-expressing lines, the φNPQ was lower compared to the wild type (Figure 19A). In contrast to φNPQ, φNO, the quantum yield of non-light-induced quenching processes was lower in all Flv-expressing lines (Figure 18B, Figure 19B).

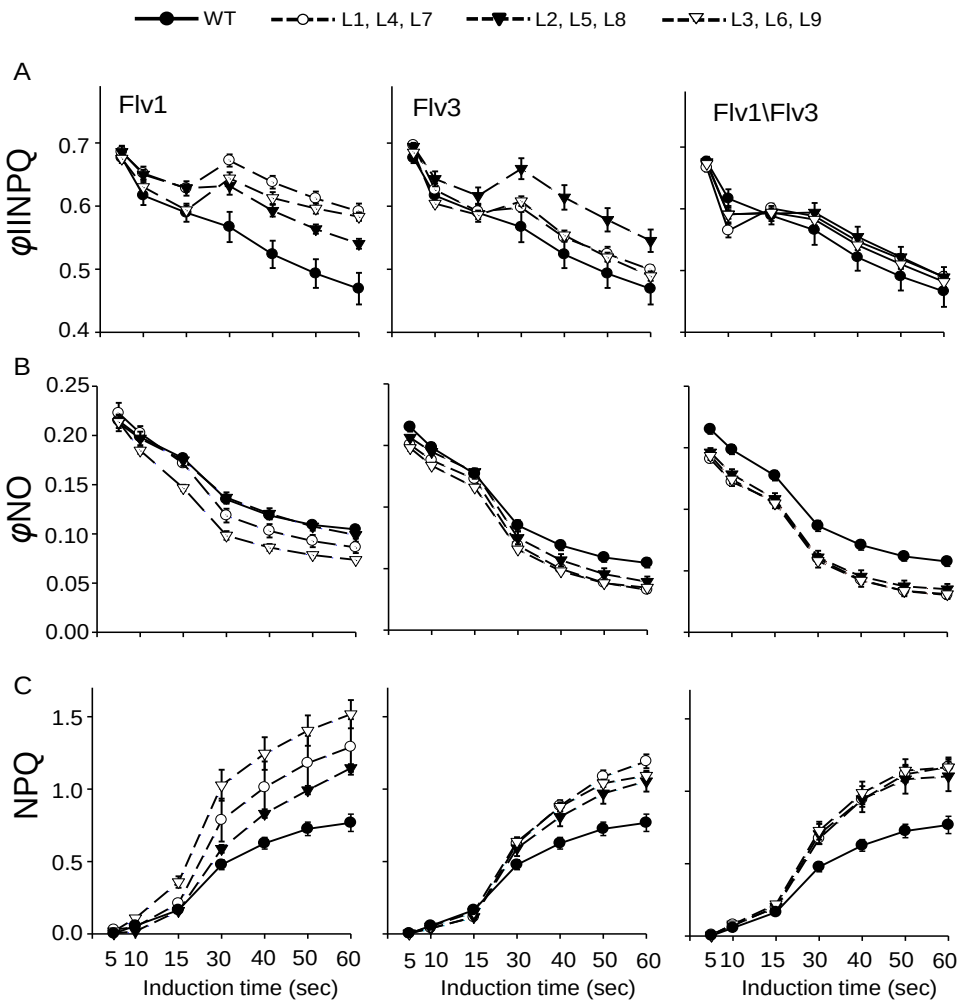

Figure 18. Effect of Flv gene expression on non-photochemical quenching induction in Arabidopsis plants during the first 60 sec of photosynthesis initiation. (A) φIINPQ, quantum yield of regulated non-photochemical energy dissipation in PSII, (B) φNO, quantum yield of non-regulated non-photochemical energy dissipation in PSII and (C) NPQ, non-photochemical quenching. Measurements were carried out in rosette leaves of dark-adapted wild type (black circles) and three independent transgenic lines of Flv1-, Flv3-, Flv1/Flv3-expressing plants: open circles (L1, L4, L7), black triangles (L2, L5, L8) and open triangles (L3, L6, L9) illuminated with actinic light at 150 µmol photons m^{-2} s^{-1}. Data point's represents mean of 8 independent biological replicates ±SE.

Moreover, the NPQ (independent of light-induced quenching) measurements revealed an enhanced induction of photosynthesis in all transgenic plants, being up to 3-fold higher in Flv1- and up to 2-fold in all Flv3- and Flv1/Flv3-expressing lines (Figure 18C). However, the NPQ measurements were lower in Flv2-, Flv4-,and Flv2/Flv4-expressing lines compared to the wild type (Figure 19C). The above measurements strongly support that Flv proteins are functional in higher plants.

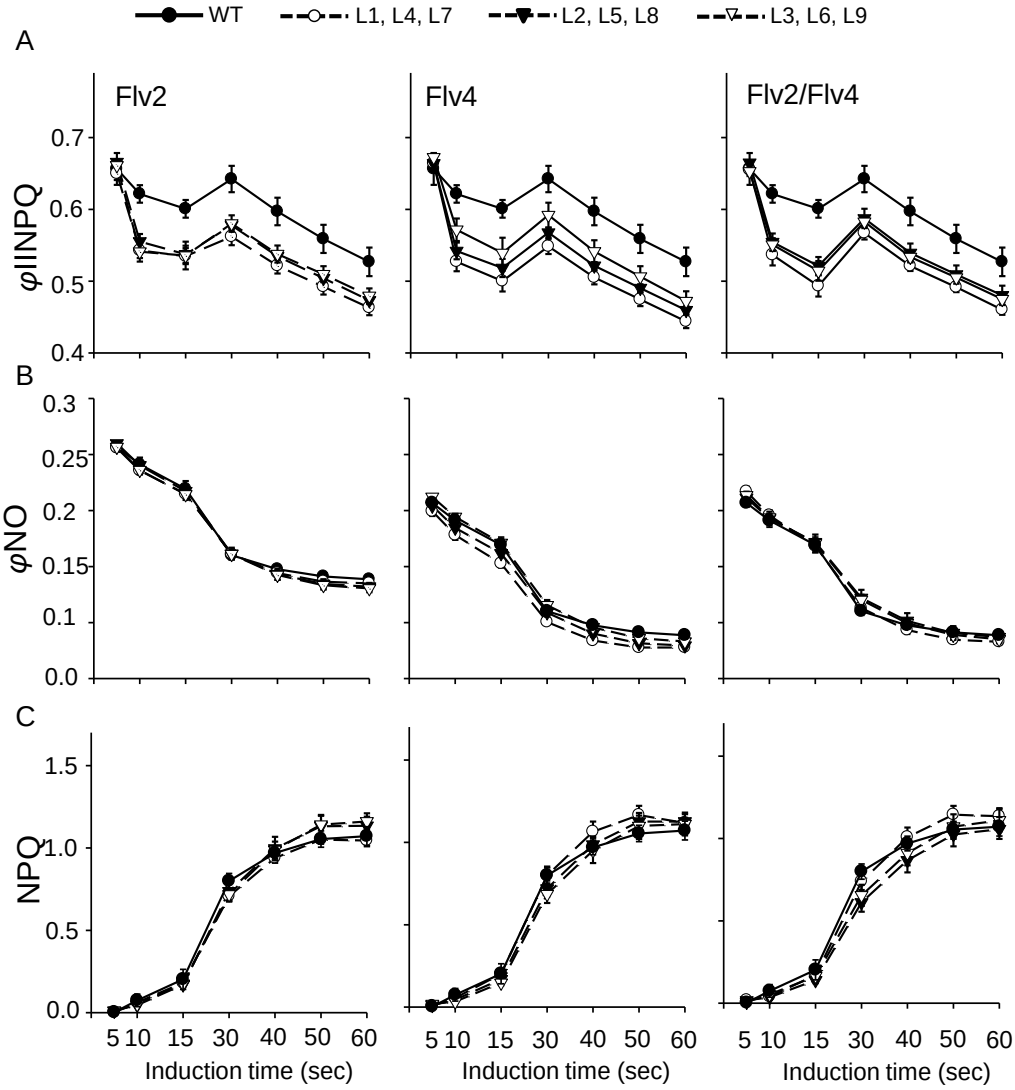

Figure 19. Effect of Flv gene expression on non-photochemical quenching induction in Arabidopsis plants during the first 60 sec of photosynthesis initiation in Flv2-, Flv4-, Flv2/Flv4-expressing lines. (A) φIINPQ, quantum yield of regulated non-photochemical energy dissipation in PSII, (B) φNO, quantum yield of non-regulated non-photochemical energy dissipation in PSII and (C) NPQ, non-photochemical quenching. Measurements were carried out in rosette leaves of dark-adapted wild type (black circles) and three independent transgenic lines of Flv2-, Flv4-, Flv2/Flv4-expressing plants: open circles (L1, L4, L7), black triangles (L2, L5, L8) and open triangles (L3, L6, L9) illuminated with actinic light at 150 μmol photons m^{-2} s^{-1}. Data point's represents mean of 8 independent biological replicates ±SE.

3.4 Altered carbohydrate and amino acid metabolism in Flv-expressing plants

3.4.1 Increased sucrose and starch in Flv-expressing lines

Soluble sugars, sucrose, glucose and fructose, and starch are useful indicators for the photosynthetic performance. Thus, the diurnal rhythm of soluble and insoluble sugar concentrations was determined in wild type, and all Flv-expressing lines (Figure 20 and Figure 21). Compared to the wild type, Flv1-, Flv3-, Flv2-, Flv4-expressing lines showed higher sucrose concentrations, which continuously increased during the light period and dropped to initial values at the end of the dark period. However, there they were still higher than in the wild type (Figure 20A, Figure 21A). The Flv1/Flv3- and Flv2/Flv4-expressing lines showed an increase of sucrose concentrations during the light period while fluctuating during the dark period (Figure 20A, Figure 21A). Starch levels were similar in all Flv-expressing lines at the beginning of illumination, but during the light period they increased faster (up to 1.7-times) in Flv1-, Flv3-, Flv1/Flv3-expressing lines and also in Flv2- Flv4-, and Flv2/Flv4-expressing lines than in WT plants, before declining rapidly in the dark (Figure 20B, Figure 21B).

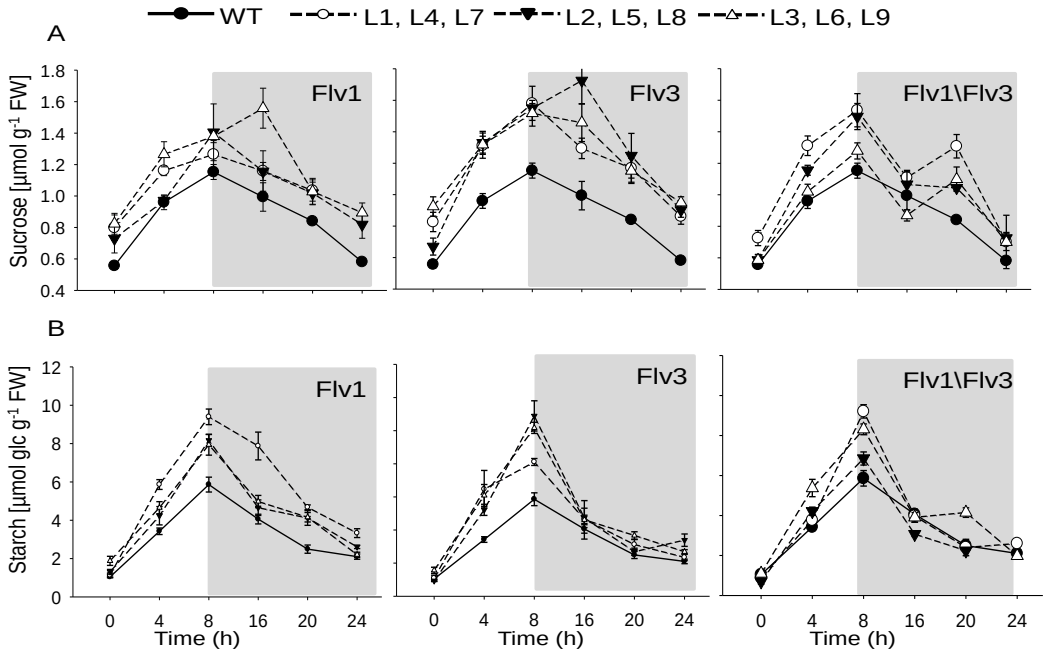

Figure 20. Diurnal changes in sucrose and starch concentrations in Flv-expressing lines. (A) Sucrose concentration, (B) starch concentration. Measurements were carried out in rosette leaves from six weeks old plants collected at different time points (0, 4, 8, 16, 20, 24 h) of WT plants (black circles) and three independent transgenic lines of Flv1-, Flv3- and Flv1/Flv3-expressing lines: open circles (L1, L4, L7), black triangles (L2, L5, L8) and open triangles (L3, L6, L9). Plants were grown in 8h/16h-light/dark regime at 150 µmol photons m^{-2} s^{-1}. Data points represents mean of 5 biological replicates ±SE.

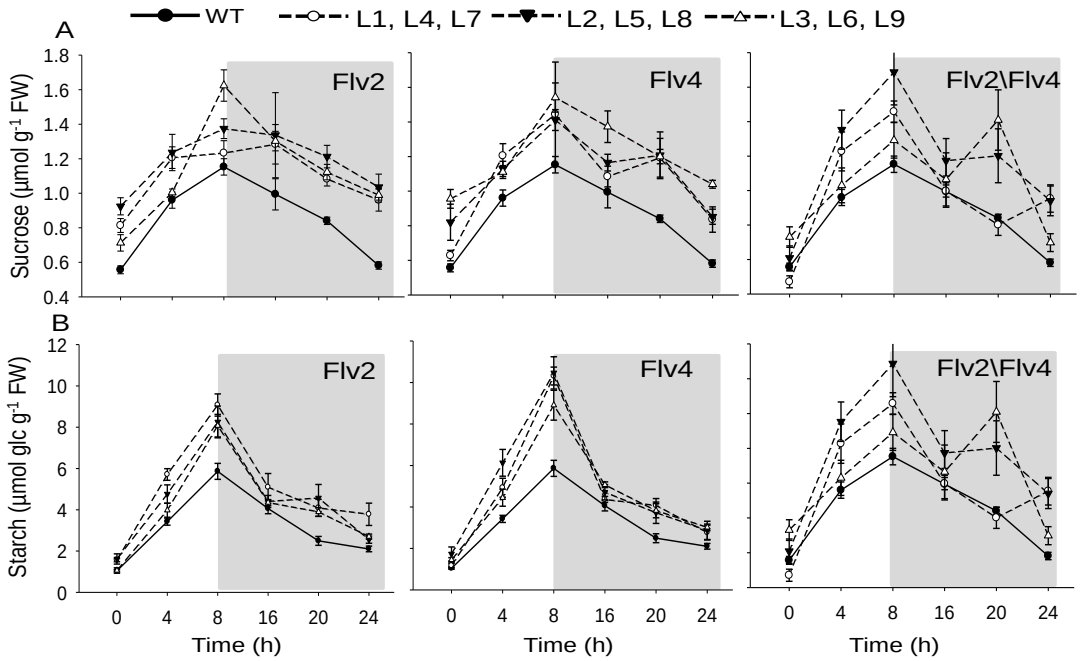

Figure 21. Diurnal changes in sucrose and starch concentrations in Flv-expressing lines. (A) Sucrose concentration, (B) starch concentration. measurements were carried out in rosette leaves from six weeks old plants collected at different time points (0, 4, 8, 16, 20, 24 h) of WT plants (black circles) and three independent transgenic lines of Flv2-, Flv4- and Flv2/Flv4-expressing lines: open circles (L1, L4, L7), black triangles (L2, L5, L8) and open triangles (L3, L6, L9). Plants were grown in 8h/16h-light/dark regime at 150 µmol photons m^{-2} s^{-1}. Data points represents mean of 5 biological replicates ±SE.

3.4.2 Ultrastructural changes in the chloroplasts of Flv-expressing plants

Transmission electron microscopy (TEM) was used to analyze starch granules in individual chloroplasts of source leaves of WT and Flv-expressing lines. The size of the starch granules was similar, while their number was enhanced in Flv1-, Flv3-, Flv1/Flv3-expressing lines (Figure 22A) and Flv2-, Flv4-, Flv2/Flv4-expressing lines (Figure 22B) compared to WT leaves after 5 hours of light illumination (150 µmol photons m^{-2} s^{-1}). This indicated a higher starch accumulation during the light period.

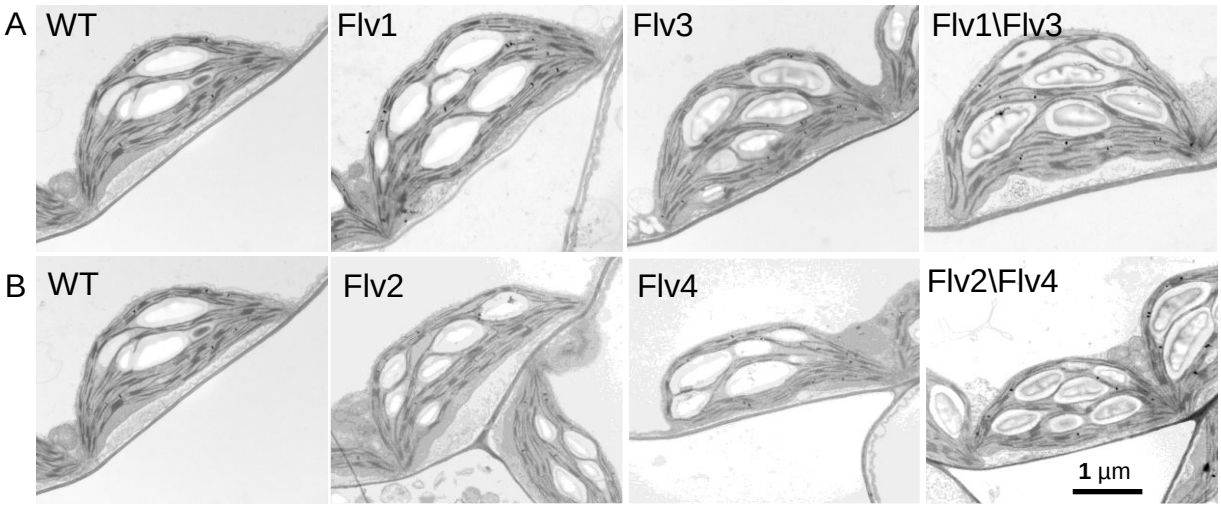

Figure 22. Visualization of starch granules in WT and Flv-expression lines using transmission electron microscopy. (A) Ultrastructural images of WT, Flv1-, Flv3-, Flv1/Flv3-expressing lines, or of (B) WT, Flv2-, Flv4-, Flv2/Flv4-expressing lines. Fully expanded leaves were illuminated for 5h at 150 µmol photons m^{-2} s^{-1} before being imaged.

3.4.3 Glucose and fructose concentrations in Flv-expressing lines

Measurement of glucose and fructose concentrations did not show a consistent pattern and were subject to continuous fluctuations (Figure 23 and Figure 24). Glucose and fructose concentrations were 2 and 3.5-times higher in Flv3-expressing lines during the light period (Figure 23B, E middle graphs) whereas in Flv1- and Flv1/Flv3-expressing lines showed no differences to the wild type (Figure 23A, D, C, F). In Flv2-, and Flv4-expressing lines the glucose concentrations were between 1.6 and 3.3 times higher, while in Flv2/Flv4-expressing lines showed higher toward the end of the day compared to wild type (Figure 24A, B, C). The fructose concentrations were 1.4 and 2.4 times higher in Flv4-expressing lines (Figure 24E middle graph) while in Flv2- and Flv2/Flv4-expressing lines, showed no consistent diurnal pattern of fructose was observed compared to WT (Figure 24D, F).

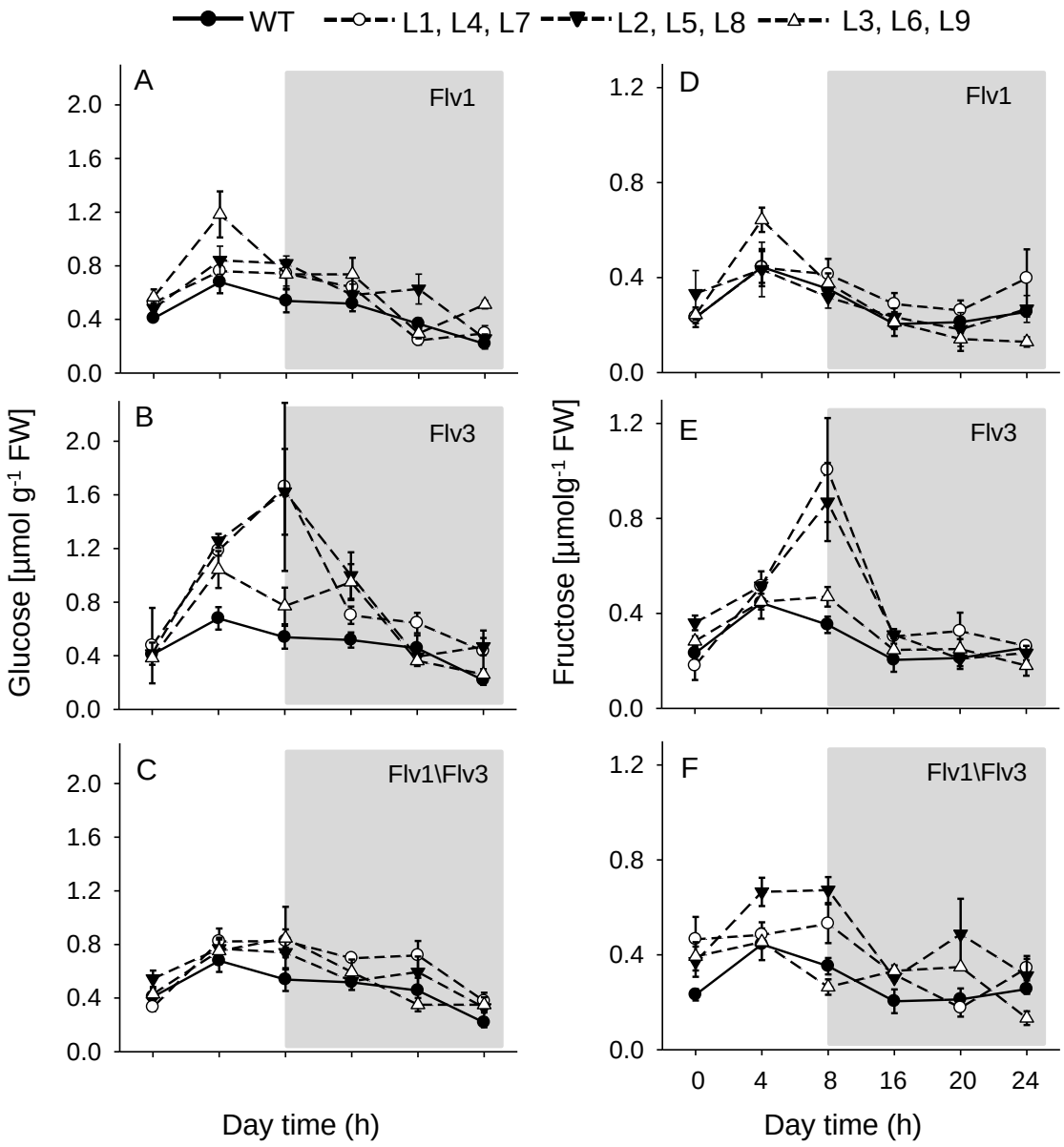

Figure 23. Diurnal changes in glucose and fructose concentrations in Flv-expressing lines. (A-C) Glucose and (D-F) fructose concentrations in Flv1- (A, D), Flv3- (B, E) and Flv1/Flv3- (C, F) expressing lines. Measurements were carried out on six weeks old rosette leaves harvested at different time points (0, 4, 8, 16, 20, 24 h) from WT (black circles) or three independent transgenic lines of Flv1-, Flv3- and Flv1/Flv3-expressing plants: open circles (L1, L4, L7), black triangles (L2, L5, L8) and open triangles (L3, L6, L9) grown at 150 µmol photons m^{-2} s^{-1}. Data points represent means of 5 biological replicates±SE.

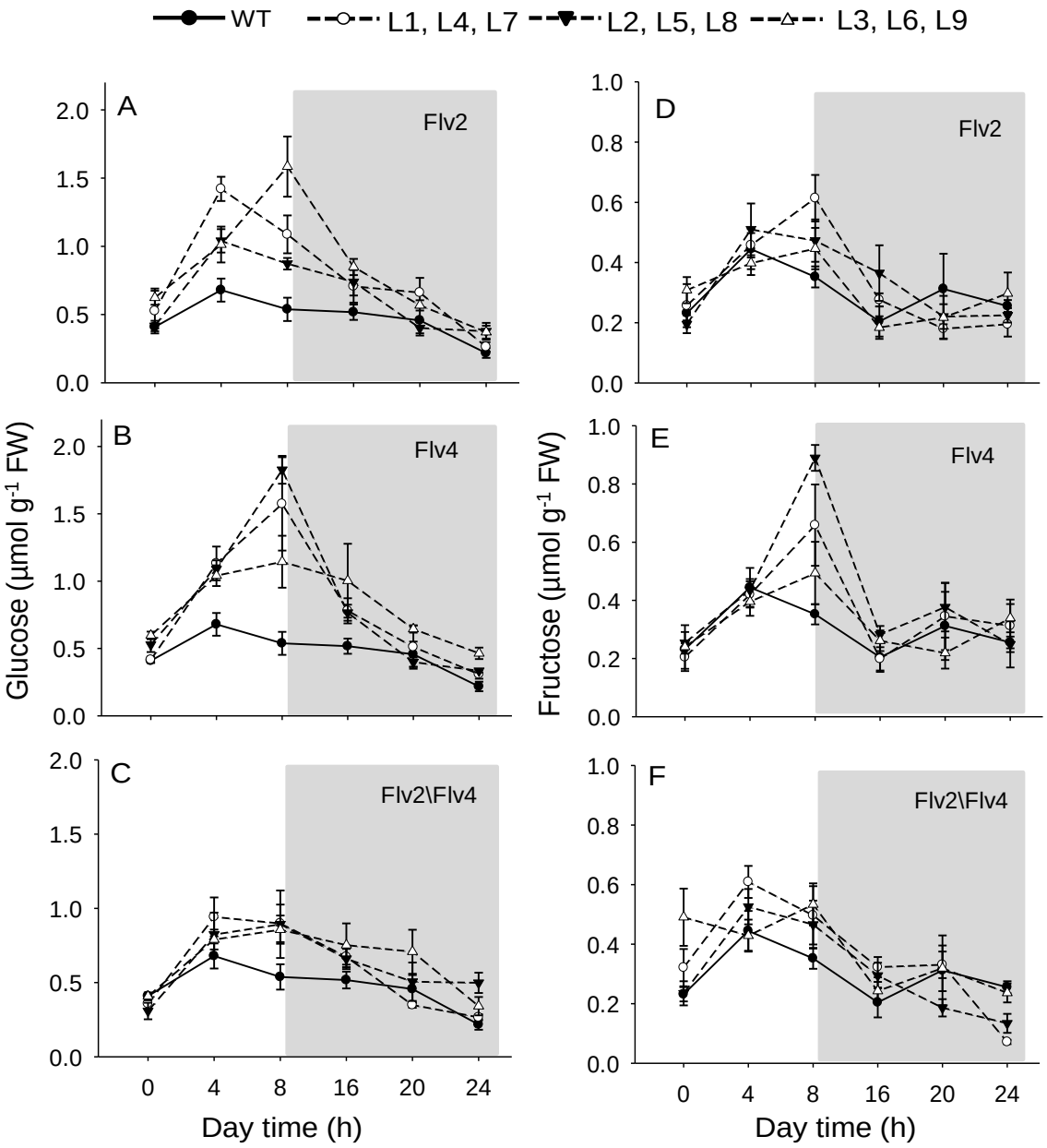

Figure 24. Diurnal changes in glucose and fructose concentrations in Flv-expressing lines. (A-C) Glucose and (D-F) Fructose concentrations in Flv2- (A, D), Flv4- (B, E) and Flv2/Flv4- (C, F) expressing lines. Measurements were carried out on six weeks old rosette leaves harvested at different time points (0, 4, 8, 16, 20, 24 h) from WT (black circles) or three independent transgenic lines of Flv2, Flv4 and Flv2/Flv4 expressing plants: open circles (L1, L4, L7), black triangles (L2, L5, L8) and open triangles (L3, L6, L9) grown at 150 µmol photons m^{-2} s^{-1}. Data points represent means of 5 biological replicates±SE.

3.4.4 Amino acid metabolism in Flv-expressing lines

Amino acids were profiled in Flv-expressing lines at 4h and 8h after onset of light (8h/16h-light/dark regime). Amino acids acts as signaling molecules and nitrogen storing compounds beside used for protein synthesis. In Flv-expressing lines showed no changes in concentration of amino acids after 4 hours of light illumination (Appendix Table. 2 and Table. 3) except for glycine in L1, L2 (Flv1), L9 (Flv1/Flv3) and arginine in L9 Flv2-, Flv2/Flv4-expressing lines, in which values were higher than in the wild type (Appendix Table. 3), indicating that only upstream pathways directly associated with photosynthesis, e.g., sugar metabolism, were influenced during the light period by the expression of Flv genes. In contrast, at the end of the light period (8h of illumination) an increased pool of amino acids including asparagine, glycine, glutamine, proline, and alanine was found in Flv1-, Flv3-, Flv1/Flv3-expressing lines (Table. 1) while asparagine, serine, glycine, glutamine, aspartate, proline, and alanine were higher in Flv2-, Flv4-, Flv2/Flv4-expressing lines compared to wild type (Table. 2). Thus the above result indicates changes in amino acids synthesis may be due to changes in carbohydrate metabolism in Flv-expressing lines.

Table 1. The composition of free amino acids in Flv-expressing lines (Flv1, Flv3, Flv1/Flv3).

Amino acids	Col0		Flv1			Flv3			Flv1/Flv3	
		L1	L2	L3	L4	L5	L6	L7	L8	L9
Asparagine	3,53 ± 0,08	4,41 ± 0,34	4,40 ± 0,26 *	4,51 ± 0,20 **	3,99 ± 0,20	3,98 ± 0,27	3,91 ± 0,10 *	4,34 ± 0,30 *	4,43 ± 0,26 *	4,77 ± 0,60
Serine	13,21 ± 0,23	13,19 ± 0,63	11,27 ± 0,66	11,30 ± 0,67	10,40 ± 1,01	10,05 ± 0,79	10,58 ± 0,41	12,64 ± 1,02	12,88 ± 0,17	12,60 ± 0,29
Arginine	0,17 ± 0,02	0,24 ± 0,02	0,24 ± 0,02 *	0,30 ± 0,03 **	0,21 ± 0,01	0,23 ± 0,01 *	0,22 ± 0,01	0,24 ± 0,01 *	0,19 ± 0,006	0,26 ± 0,02 *
Glycine	0,71 ± 0,06	0,75 ± 0,06	1,32 ± 0,17 *	1,28 ± 0,16 *	1,85 ± 0,20 **	1,79 ± 0,47	1,59 ± 0,33 *	1,15 ± 0,17 *	1,01 ± 0,26	1,28 ± 0,33
Glutamine	14,76 ± 0,49	17,74 ± 0,50 **	18,70 ± 0,54 ***	20,38 ± 0,29 ***	20,67 ± 1,12 **	22,80 ± 1,90 **	20,78 ± 1,12 **	20,03 ± 1,03 **	18,28 ± 0,92 **	19,18 ± 0,44 ***
Aspartate	7,61 ± 0,20	8,73 ± 0,76	9,23 ± 0,30 **	9,11 ± 0,37 **	9,65 ± 0,52 **	8,74 ± 0,67	9,92 ± 0,48 **	9,50 ± 0,68 **	8,21 ± 0,25 **	8,66 ± 0,46 ***
Glutamate	17,00 ± 0,64	19,15 ± 1,63	17,17 ± 0,53	16,48 ± 1,02	15,78 ± 1,39	16,72 ± 1,27	15,62 ± 1,62	15,92 ± 0,76	17,53 ± 0,92	17,34 ± 0,54
Threonine	7,65 ± 0,15	8,72 ± 0,80	7,97 ± 0,49	8,74 ± 0,48	8,21 ± 0,53	8,78 ± 0,79	8,04 ± 0,42	9,34 ± 0,67	8,94 ± 0,35 **	8,80 ± 0,70
Alanine	5,83 ± 0,33	7,70 ± 0,35 **	7,76 ± 0,24 **	8,53 ± 0,45 ***	8,03 ± 0,73 *	9,02 ± 0,81 **	7,61 ± 0,46 **	9,13 ± 0,43 ***	8,03 ± 0,47 **	7,34 ± 0,23 **
GABA	0,31 ± 0,03	0,36 ± 0,08	0,45 ± 0,04	0,70 ± 0,08 **	0,28 ± 0,03	0,32 ± 0,02	0,23 ± 0,04	0,33 ± 0,02	0,42 ± 0,06	0,43 ± 0,06
Proline	5,36 ± 0,32	8,19 ± 0,78 **	6,87 ± 0,50 *	6,32 ± 0,39	7,12 ± 0,82	10,76 ± 0,56 ***	8,16 ± 0,52 **	7,84 ± 0,79 *	8,75 ± 0,86 **	7,34 ± 0,34 **
Lysine	0,3 ± 0,01	0,28 ± 0,07	0,20 ± 0,05	0,29 ± 0,02	0,26 ± 0,02	0,27 ± 0,05	0,19 ± 0,05	0,32 ± 0,01	0,31 ± 0,02	0,37 ± 0,02 *
Valine	0,73 ± 0,01	0,79 ± 0,07	0,95 ± 0,19	0,83 ± 0,05	0,78 ± 0,03	0,88 ± 0,06	0,77 ± 0,04	0,91 ± 0,06 *	0,81 ± 0,03	0,80 ± 0,07
Isoleucine	0,21 ± 0,005	0,24 ± 0,02	0,21 ± 0,007	0,23 ± 0,02	0,20 ± 0,01	0,20 ± 0,01	0,20 ± 0,01	0,24 ± 0,01	0,23 ± 0,01	0,24 ± 0,02
Leucine	0,20 ± 0,009	0,23 ± 0,02	0,34 ± 0,17	0,21 ± 0,03	0,17 ± 0,02	0,19 ± 0,01	0,16 ± 0,01	0,21 ± 0,01	0,22 ± 0,01	0,24 ± 0,03
phenylalanine	0,23 ± 0,07	0,37 ± 0,02	0,49 ± 0,14	0,32 ± 0,07	0,42 ± 0,01 *	0,41 ± 0,02	0,42 ± 0,01 *	0,45 ± 0,03 *	0,40 ± 0,004	0,39 ± 0,02
Histidine	0,05 ± 0,004	0,08 ± 0,008 *	0,11 ± 0,03	0,07 ± 0,01	0,05 ± 0,01	0,05 ± 0,006	0,04 ± 0,007	0,06 ± 0,01	0,04 ± 0,01	0,07 ± 0,01

Measurements were carried out on rosette leaves harvested at the end of the day (8 h) using UPLC and fluorescence detection. All values are in (nmol g^{-1} FW). Values represents means of 4-5 biological replicates±SE. Significant differences to WT are indicated by asterisks according to Student' s t test (* *P*≤0.05, ** P≤0.01, *** P≤0.001).

Table 2. The composition of free amino acids in Flv-expressing lines (Flv2, Flv4, Flv2/Flv4).

Amino acids	Col0		Flv2			Flv4			Flv2/Flv4	
		L1	L2	L3	L4	L5	L6	L7	L8	L9
Asparagine	3,53 ± 0,08	3,90 ± 0,21	4,63 ± 0,36 *	4,43 ± 0,23 **	4,16 ± 0,43	4,28 ± 0,16 ***	4,53 ± 0,27 **	4,36 ± 0,22 **	5,19 ± 0,42 **	4,99 ± 0,43 *
Serine	13,21 ± 0,23	13,15 ± 0,83	11,40 ± 0,67 *	15,22 ± 1,74	10,08 ± 0,76 **	12,51 ± 0,42	15,01 ± 1,29	11,60 ± 0,15 ***	10,80 ± 1,42	10,45 ± 1,09
Arginine	0,17 ± 0,02	0,22 ± 0,02	0,22 ± 0,01	0,26 ± 0,01 **	0,22 ± 0,01	0,26 ± 0,01 **	0,28 ± 0,02 **	0,30 ± 0,03 **	0,26 ± 0,02 *	0,27 ± 0,04
Glycine	0,71 ± 0,06	1,37 ± 0,23 *	2,03 ± 0,44 *	1,76 ± 0,31 *	2,30 ± 0,52 *	2,86 ± 0,55 **	1,46 ± 0,22 *	1,01 ± 0,2	1,38 ± 0,45	0,07 ± 0,006
Glutamine	14,76 ± 0,49	19,21 ± 1,23 **	20,01 ± 2,40	19,44 ± 0,93 ***	21,91 ± 1,27 ***	23,31 ± 0,58 ***	22,00 ± 1,19 **	20,39 ± 1,67 *	24,65 ± 2,80 *	20,86 ± 3,65
Aspartate	7,61 ± 0,20	8,77 ± 0,28 **	9,42 ± 0,21 ***	8,57 ± 0,34 *	9,21 ± 0,78	9,16 ± 0,45 *	9,34 ± 0,74	8,60 ± 0,39	9,19 ± 0,50 *	8,09 ± 0,48
Glutamate	17,00 ± 0,64	15,68 ± 0,78	16,33 ± 0,47	18,87 ± 1,00	14,06 ± 1,20	16,48 ± 0,75	16,66 ± 1,38	14,88 ± 0,38	15,99 ± 1,18	12,35 ± 1,00
Threonine	7,65 ± 0,15	8,33 ± 0,51	8,49 ± 0,76	10,23 ± 0,56 **	7,93 ± 0,39	9,21 ± 0,26 ***	10,38 ± 0,79 *	7,68 ± 0,34	8,59 ± 1,09	6,99 ± 0,58
Alanine	5,83 ± 0,33	7,22 ± 0,65	9,09 ± 0,78 **	7,52 ± 0,57 *	8,88 ± 0,51 ***	9,87 ± 0,37 ***	8,64 ± 0,51 **	9,24 ± 0,90 **	9,97 ± 0,77 **	8,02 ± 1,06
GABA	0,31 ± 0,03	0,51 ± 0,07	0,52 ± 0,06 *	0,60 ± 0,05 **	0,29 ± 0,03	0,36 ± 0,03	0,52 ± 0,03 **	0,39 ± 0,02	0,38 ± 0,04	0,46 ± 0,05 *
Proline	5,36 ± 0,32	6,62 ± 0,76	6,61 ± 1,37 *	8,15 ± 0,87 *	6,48 ± 0,85	8,10 ± 1,01 *	16,41 ± 2,81 **	5,77 ± 0,72 *	10,98 ± 2,82	4,91 ± 0,57
Lysine	0,3 ± 0,01	0,29 ± 0,02	0,26 ± 0,007	0,34 ± 0,05	0,17 ± 0,05	0,24 ± 0,01	0,35 ± 0,04	0,21 ± 0,05	0,20 ± 0,01	0,25 ± 0,03
Valine	0,73 ± 0,01	0,71 ± 0,16	0,65 ± 0,15	0,93 ± 0,07	0,79 ± 0,05	0,87 ± 0,02	0,96 ± 0,09	0,77 ± 0,04	0,81 ± 0,08	0,55 ± 0,16
Isoleucine	0,21 ± 0,005	0,24 ± 0,01	0,22 ± 0,01	0,28 ± 0,03	0,20 ± 0,01	0,22 ± 0,008	0,26 ± 0,03	0,19 ± 0,007	0,19 ± 0,01	0,19 ± 0,02
Leucine	0,20 ± 0,009	0,23 ± 0,01	0,19 ± 0,01	0,26 ± 0,04	0,16 ± 0,01	0,18 ± 0,008	0,24 ± 0,04	0,17 ± 0,008	0,14 ± 0,01	0,18 ± 0,03
phenylalanine	0,23 ± 0,07	0,32 ± 0,06	0,38 ± 0,03	0,43 ± 0,03	0,45 ± 0,02 *	0,40 ± 0,08	0,45 ± 0,03 *	0,33 ± 0,01 *	0,37 ± 0,08	0,29 ± 0,08
Histidine	0,05 ± 0,004	0,10 ± 0,03	0,06 ± 0,01	0,06 ± 0,02	0,05 ± 0,006	0,04 ± 0,005	0,08 ± 0,01	0,03 ± 0,003	0,03 ± 0,005	0,04 ± 0,008

Measurements were carried out on rosette leaves harvested at the end of the day (8h) using uplc and fluorescence detection. All values are in (nmol g^{-1} fw). Values represents means of 4-5 biological replicates±SE. Significant differences to WT are indicated by asterisks according to Student' s t test (* $P \leq 0.05$, ** $P \leq 0.01$, *** $P \leq 0.001$).

3.5 Flv proteins enhance ATP synthesis in Arabidopsis plants

ATP is the energy source for many metabolic reactions and is produced in chloroplasts through photophosphorylation reactions either via the LET or CET. To evaluate whether the expression of Flv genes that accept electrons from ETC influence ATP and/or the energy charge, the single nucleotides (ATP, ADP, and AMP) were measured at different time points 4h, 8h, 16h. The results revealed that ATP concentrations were up to 1.5-times higher throughout the light (4h, 8h) and dark period (16h) in Flv1-, Flv3-, Flv1/Flv3-expressing lines (Figure 25A, B, C), whereas the ATP levels dropped to WT levels in L8, L9 of the Flv1/Flv3-expressing lines during the light-dark transition (Figure 25C). In Flv2-, Flv4-, Flv2/Flv4-expressing lines, the ATP concentration increased by 10-50% (Figure 26A, B, C). The concentrations of ADP and AMP measured at 4h, 8h and 16h were not significantly different in all Flv-expressing lines compared to those of wild type (Appendix Table S6).

The adenylate energy charge, as an functional indicator for the energy status of the cells represents the ratio of ATP, ADP, AMP, was slightly higher, up to 1.3-times in Flv1-expressing lines at three different time points (4h, 8h, 16h) except for L2 at 4h, L3 at 8h (Figure 25D). In Flv3-expressing lines, the energy charge was higher in the transgenic lines L4, L6 (4h), L5 (8h) and L4, L5 (16h) (Figure 25E), while in Flv1/Flv3-expressing lines L7, L9 was higher at 4h after illumination and did not differ at 8h of illumination as well as at 16h during the dark phase (Figure 25F). In Flv2-, and Flv2/Flv4-expressing lines, no differences were observed except in L2 (Flv2) at 8h and L7, L8 (Flv2/Flv4) at 4h during the day (Figure 26D, F), whereas in Flv4-expressing lines the energy charge increased up to 1.3-times compared to the wild type at 4h during the day and in L5, L6 lines during the dark period at 16h (Figure 26E). Above results represent changes in energy charge which is a functionally important indicator than absolute values of ATP is observed in Flv-expression lines at different time points.

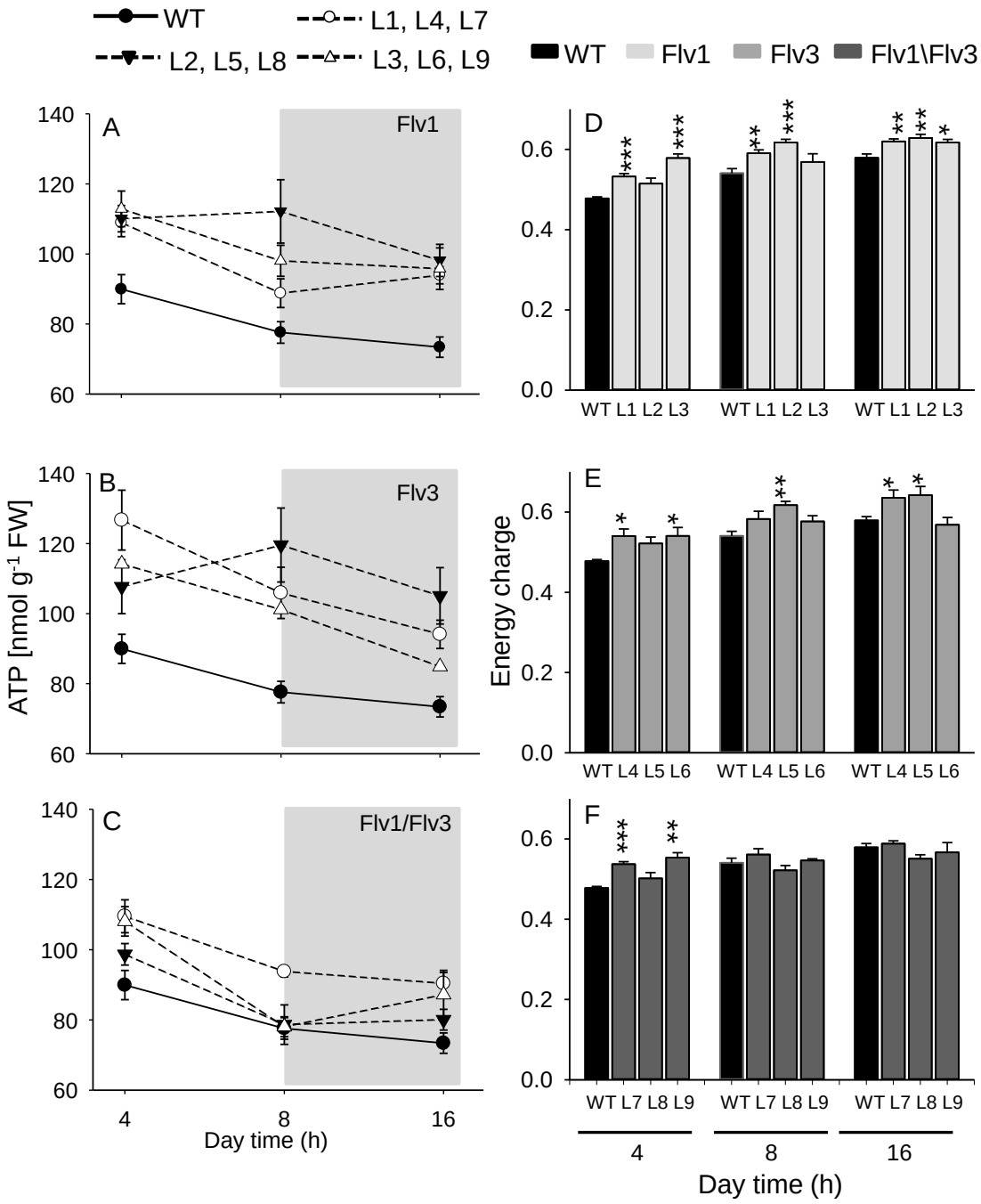

Figure 25. Impact of Flv gene expression on ATP synthesis and energy charge. (A-C) ATP concentration and (D-F) energy charge for Flv1- (A, D), Flv3- (B, E) or Flv1/Flv3- expressing lines (C, F). Measurements were carried out in rosette leaves at three different time points (4h, 8h, 16h) of six weeks-old WT plants (black circles) and three independent transgenic lines expressing Flv1, Flv3, or Flv1/Flv3: open circles (L1, L4, L7), black triangles (L2, L5, L8) and open triangles (L3, L6, L9). Plants were grown at 150 µmol photons m^{-2} s^{-1}. Data points and bars represents means of 5 biological replicates±SE. Significant differences between WT and Flv-expressing lines are indicated by asterisks according to Student's t test (*p≤0.05, **p≤0.01 and ***p≤0.001).

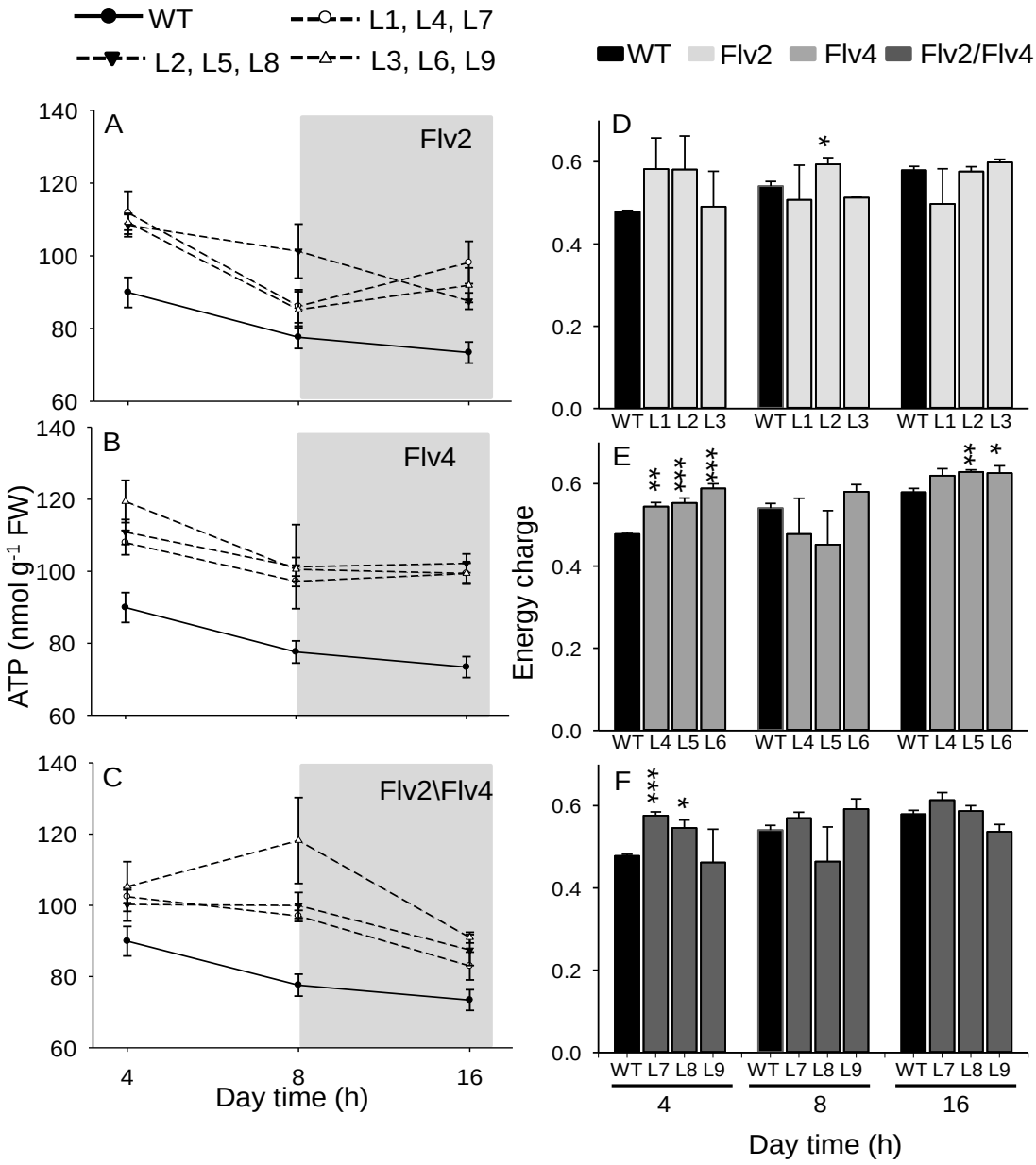

Figure 26. Impact of Flv gene expression on ATP synthesis and energy charge. (A-C) ATP concentration and (D-F) energy charge for Flv2- (A, D), Flv4- (B, E) orFlv2/Flv4- expressing lines (C, F). Measurements were carried out in rosette leaves at three different time points (4h, 8h, 16h) of six weeks-old WT plants (black circles) and three independent transgenic lines expressing Flv2-, Flv4-, and Flv2/Flv4- : open circles (L1, L4, L7), black triangles (L2, L5, L8) and open triangles (L3, L6, L9). Plants grown at 150 µmol photons m^{-2} s^{-1}. Data points and bars represent means of 5 biological replicates±SE. Significant differences between WT and Flv-expressing lines are indicated by asterisks according to Student's t test (*p≤0.05, **p≤0.01 and ***p≤0.001).

3.6 Primary metabolite profiling in Flv expressing plants

To evaluate whether changes in sugar and energy metabolisms in Flv-expressing lines influence the primary metabolism, a detailed metabolite profiling was carried out. Of all measured metabolites, the concentration of hexose-phosphates was higher in all Flv3-expressing lines compared to WT plants 4h after illumination, and no significant changes were observed in Flv1- and Flv1/Flv3-expressing lines except for L2, L9 (Figure 27A respectively). In Flv2-, Flv4-, and Flv2/Flv4-expressing lines, the concentration of hexose phosphates was slightly higher but not statistically significant (Figure 28A).The concentration of the direct precursor of starch synthesis, ADP-Glc increased up to 1.4-times in Flv1-, up to 1.8-times in Flv3- and up to 1.3-times in Flv1/Flv3-expressing lines except for L2, L7, L9 at 4h after illumination compared to WT (Figure 27B). Flv2-, Flv4-, Flv2/Flv4-expressing lines showed an increase of ADP-Glc in Flv2- by up to 2.1 times, Flv4- by up to 1.7 times and Flv2/Flv4-expressing lines by up to 1.5-times except for L2, L4, L7 and L8 (Figure 28B).

With respect to the concentrations of TCA cycle metabolites, citrate and malate are two carbon compounds that frequently accumulate in plants which as carbon reserve and also to run partial TCA cycle for synthesis of amino acids; however; no statistically consistent differences compared to the wild type were observed in citrate and malate concentrations in any of the investigated transgenic plants except for the Flv2/Flv4-expressing L8 (Figure 27C, D and Figure 28C, D). The total chlorophyll and protein concentrations were highly similar in all Flv1-, Flv1/Flv3-, Flv2-, Flv2/Flv4-expressing lines except for Flv3- and Flv4-expressing lines (Figure 27F, E and Figure 28F, E).

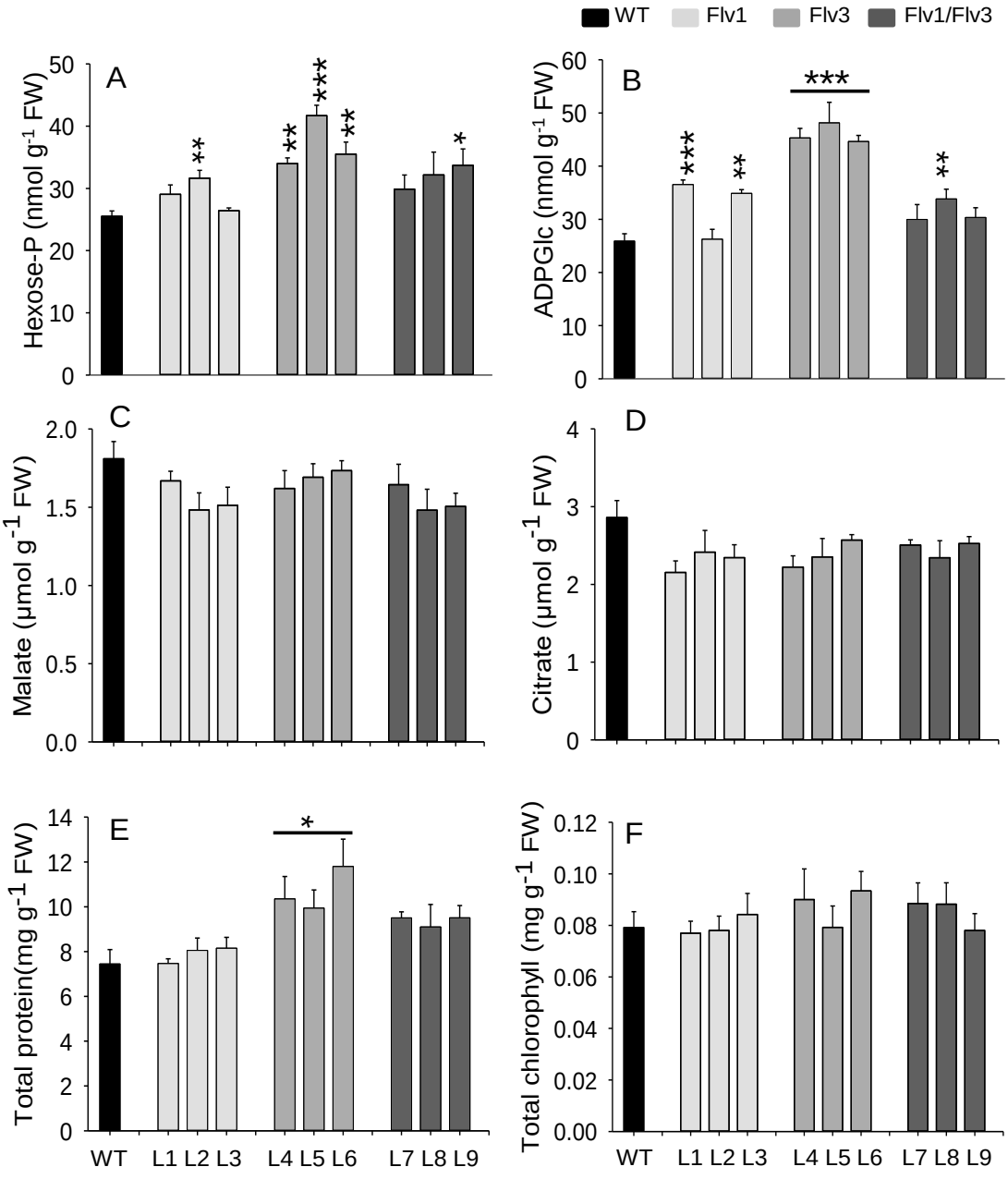

Figure 27. Concentrations of primary metabolites and chlorophyll in Flv-expressing lines (Flv1, Flv3, Flv1/Flv3) at 4h post illumination. (A) Hexose-p concentration, B) ADPGlc, (C) Malate, (D) Citrate, (E) Total protein and (F) Total chlorophyll. Bars represent means of 5 biological replicates±SE. Significant differences between WT and Flv-expressing lines are indicated by asterisks according to Student's t test (*p≤0.05, **p≤0.01 and ***p≤0.001).

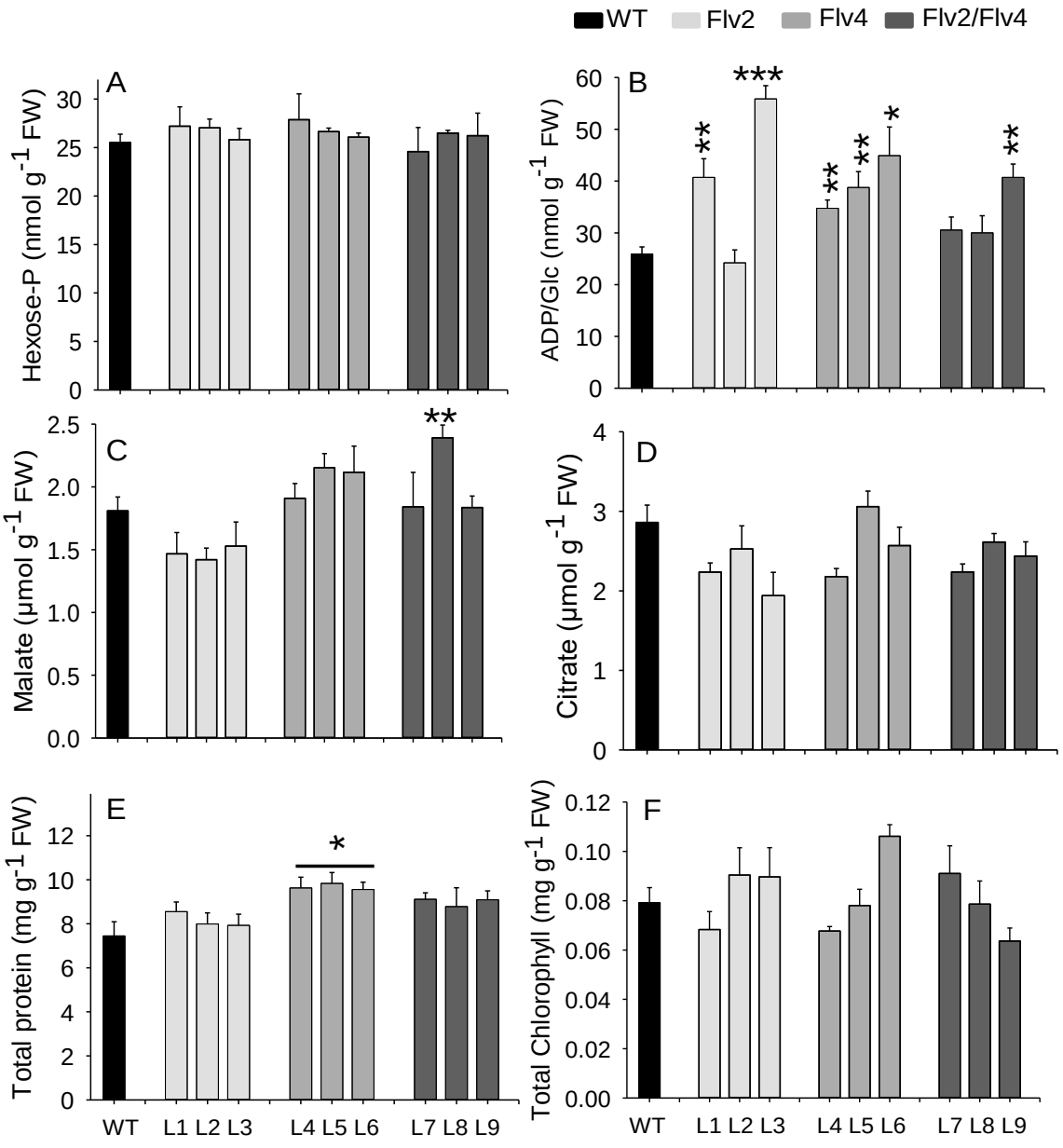

Figure 28. Concentration of primary metabolites and chlorophyll in Flv-expressing lines at 4h post illumination. (A) Hexose-p concentration, (B) ADPGlc, (C) Malate, (D) Citrate, (E) Total protein and (F) Total chlorophyll. Bars represent means of 5 biological replicates±SE. Significant differences between WT and Flv-expressing lines are indicated by asterisks according to Student's t test (*p≤0.05, **p≤0.01 and ***p≤0.001).

3.7 Effect of Flv gene expression on antioxidant metabolism

To investigate whether expression of Flv genes influence the cellular redox state, reduced and oxidized forms of glutathione were measured (Appendix Table S7) and the ratio of reduced to oxidized forms were calculated (Figure 29). The ratio of GSH:GSSG tended to be lower in Flv1-, Flv3-, Flv1/Flv3-expressing lines but they were significantly lower in the lines L3, L5, L6 (Figure 29A), whereas in Flv2-, Flv4-, Flv2/Flv4-expressing lines, the ratio of reduced to oxidized glutathione was significantly lower in all lines except for L4, L5 lines relative to WT plants (Figure 29B). These results predict that the pool of reduced glutathione was maintained at lower levels in Flv-expressing lines avoiding a possible formation of reactive oxygen species or competing for the reducing equivalents

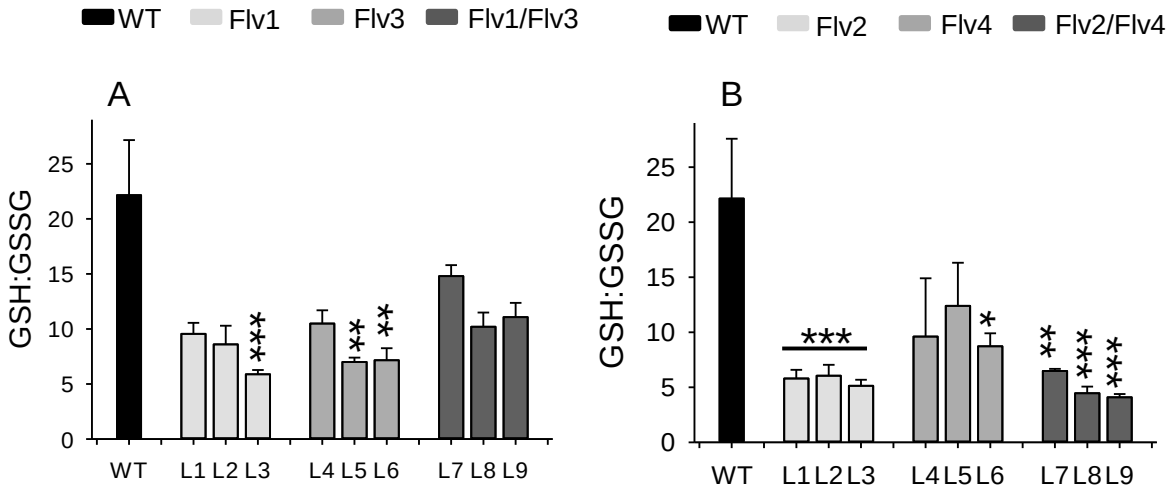

Figure 29. Analysis of antioxidants in Flv-expressing lines. (A) GSH: GSSG of Flv1-, Flv3-, Flv1/Flv3-expressing lines, (B) GSH: GSSG of Flv2-, Flv4-, Flv2/Flv4-expressing lines. Bars represent means of 5 biological replicates±SE. Significant differences between WT and Flv-expressing lines are indicated by asterisks according to Student's t test (*p≤0.05, **p≤0.01 and ***p≤0.001).

4. Discussion

In phototrophic organisms, photosynthesis is the central energy-providing pathway responsible for growth and development. However, it can be seen as an inefficient process in plants as it utilizes only a fraction of 8–10% of the solar spectrum to produce the energy required for the conversion of inorganic carbon to sugars (Long et al., 2006; Zhu et al. 2010). Out of the total energy provided by the spectrum, only about 2-4% of incident light energy is used for plant growth and biomass build-up due to carbon losses through photorespiration and external factors, which in turn activate regulatory photoprotective mechanisms (Long et al., 2006; Zhu et al. 2010). The NPQ activation kinetics reduce photochemistry that results in losses of 7-30% fixed CO_2 based on model simulations in crop canopy during the diurnal period (Long et al., 1994, Werner et al., 2001, Zhu et al., 2004). Kromdijk et al. (2016) showed that changing of the NPQ relaxation kinetics leads to enhanced growth of tobacco under field conditions. Photorespiration is an efficient electron sink that unloads nearly 25% of electron from the electron transport chain under steady-state conditions and is able to detoxify photorespiratory inhibitors that otherwise affect the Calvin cycle efficiency. The absence of a photorespiratory pathway in higher plants affects plant survival under ambient conditions but bypassing the photorespiratory pathways in chloroplasts, which results in increased biomass as demonstrated by Kebeish et al., (2007) in Arabidopsis indicating the importance of photorespiration for proper functioning of electron transport chain in plants.

Algae, cyanobacteria and lower plants possess instead of a photorespiratory pathway other electron sinks downstream of PSI, such as an AEF pathway, which is essential for growth under varying conditions and is executed by flavodiiron (Flv) proteins. In the cyanobacterium *Synechocystis* sp. strain PCC6803, four Flv genes exist in the genome, of which specifically *Flv1* and *Flv3* are induced during fluctuating light and low CO_2 conditions, whereas *Flv2* and *Flv4* genes are induced specifically under low CO_2 conditions (Wang et al., 2004, Eisenhut et al., 2007). These proteins drive oxygen-mediated electron flow like Mehler reaction alleviating over-reduction of the ETC and protect from photoinhibition under fluctuating light conditions (Allahverdiyeva et al. 2015a). Loss-of-function double mutants of Flv1 and Flv3 genes in *Synechocystis* sp. PCC6803 have been shown to display lower rates of O_2 photoreduction, indicating a prominent role of Flv1/Flv3 as heterodimer (Helman et al., 2003). Overexpression of Flv3 in Δ*Flv1* mutant strain partially complemented suppressed growth under fluctuating light, suggesting that Flv3 alone can also photoreduce O_2. Conversely, Flv1 proteins could not be detected and were less

efficient in a Δ*Flv3*/oe*Flv1* strain, even though an improved growth was observed, suggesting that Flv3 requires Flv1 for improved functionality *in vivo* (Mustila et al., 2016). The Flv2 and Flv4 proteins function like a PTOX (plastid terminal oxidase) protecting PSII from photoinhibition. The Δflv2 and Δflv4 Synechocystis sp. PCC6803 mutants showed reduced PSII activity and severe photoinhibition (Zhang et al., 2009). So, in conclusion the Flv proteins are essential for the cyanobacterial strain for maintaining efficient photosynthesis during early induction and protect photosystem from photoinhibition, which are lost in higher plants.

4.1 Expressing Flv proteins in planta allow establishing an AEF pathway to enhance photosynthesis and plant growth

4.1.1 Flv proteins promote early induction of photosynthesis

In the present thesis, the focus was the establishment of an additional electron sink in Arabidopsis plants by the ectopic expression of Flv genes as single genes (Flv1, Flv3, Flv2 or Flv4) or in combination (Flv1/Flv3 or Flv2/Flv4) to study their impact on LET through analysis of chlorophyll *a* fluorescence and on growth parameters under different light regimes. The present work showed that expressing the Flv proteins Flv3 or Flv1/Flv3 kept PSI (P700+) (Figure 16B, C) in a more oxidized state prior to the induction of the dark reaction, while no obvious differences were observed when expressing Flv1 alone (Figure 16B, C). In Flv2-, Flv4-, Flv2/Flv4- expressing lines, the Flv proteins keeps PSII in more oxidized state during early induction of photosynthesis (Figure 17B, C). Further, the higher φPSII and qL values in Flv3-, Flv1/Flv3-, and Flv2-, Flv4-, Flv2/Flv4-expressing lines indicated that Flv proteins dissipate electrons at PSI and PSII.

The increased electron flow in Flv3- and Flv1/Flv3-expressing plants induced luminal acidification and activate NPQ (Figure 18A, B, C). Higher NPQ in photosynthetic organisms indicates dissipation of excess energy that reduces photosynthesis efficiency and slows down the electron flow (Figure 18A, C). In Flv2-, Flv4-, Flv2/Flv4-expressing lines, Flv proteins removed excess electrons directly from PSII and reduced electron accumulation in the electron transport chain and thus enabled the translocation of protons from the stroma to the lumen resulting in lumen acidification and activation of NPQ (Figure 19C).

In addition, φNPQ, the light-dependent dissipation of energy was low in Flv2-, Flv4-, Flv2/Flv4-expressing lines, indicating that in fact these Flv proteins divert electrons from PSII (Figure 19A). In Flv1-expressing lines, the strong NPQ quenching (Figure 18C) obviously suppresses the electron flow as no difference in ϕPSII and qL could be observed (Figure

16B, C). In the ΔMpFlv1 mutant of the bryophytes *Metrosideros polymorpha*, it was illustrated that expression of the Flv1 gene drives AEF by oxidizing PSI and generates a proton motive force that in turn activates NPQ, resulting in the suppression of electron flow (Shimakawa *et al.,* 2017). Likewise*,* Gómez et al. (2018) observed that photosynthetic performance under steady-state illumination was similar in WT and transgenic tobacco plants expressing the cyanobacterial genes Flv1/Flv3 in combination, while the transformants displayed faster recovery of various photosynthetic parameters, including electron transport and NPQ during dark–light transitions. They also kept the PETC in a more oxidized state and enhanced the proton motive force of dark-adapted leaves. The observed results in this thesis clearly demonstrate that the expression of Flv genes Flv1, Flv3 and Flv2, Flv4 as single genes or in combination in Arabidopsis dissipate electrons at PSI, like in the Mehler reaction, or like PTOX at PSII during early induction of photosynthesis indicates enhanced photosynthesis improve plant growth

4.1.2 Expression of Flv proteins in Arabidopsis enhances plant growth

In phototrophic organisms, AEF pathways are induced in the first few seconds after onset of illumination to remove excess electrons accumulated in the electron transport chain and to generate ATP for the activation of the Calvin cycle and photorespiration during dark to light transition. When plants are exposed to fluctuating low- and high-light conditions, they generate an imbalance in the ATP/NADPH ratio in chloroplasts, which is critical for plant growth. As reported earlier, under steady-state conditions, Flvs have restricted access to electron donors, like NADPH or Fd, due to their consumption in the Calvin cycle, which is a major sink for reducing equivalents, whereas Flv proteins are likely functional under highly reduced stromal conditions (Shikanai and Yamamoto, 2017). In this study, Flv-expressing plants grown under different light intensities displayed a positive effect on biomass accumulation until light saturation of photosynthesis was accomplished (Figure 9A, Figure 10A). The low-light conditions reduced photosynthesis efficiency due to less available light for photochemistry while high-light conditions saturated the efficiency of photosynthesis and resulted in improved plant growth (Figure 9B, Figure 10B). Under standard growth conditions, high and moderate light conditions, Flv proteins exerted a positive effect on biomass production (Figure 9B, Figure 10B). A similar increase in growth of Flv-expressing plants was also observed in hydroponic culture (Figure 11, Figure 12). Interestingly under long-day conditions, Flv-expressing lines displayed higher shoot biomass (Figure 13B, E)

and seed yield (Figure 13C, F), illustrating the importance of Flv proteins under conditions where excess electrons may damage the photosynthetic apparatus.

4.2 Expression of Flv proteins in Arabidopsis improves the energy status

The adenylate energy charge is a physiologically important parameter for metabolic activity, where the adenylate nucleotides ATP, ADP and AMP represent the energy status. In plant chlorplasts, ATP is generated through linear electron transport pathway and cyclic electron transport pathway (DalCorso et al., 2008), while the mitochondrial respiratory electron transport chain just partially contributes during the day (Bailleul et al., 2015). The ATP/NADPH ratio adjustment is compensated for by the alternative electron transport pathways (AEF). The cyclic electron transport (CET) is induced specifically under ATP-deficient conditions in cyanobacteria, algae and C4 plants (Carpentier et al., 1984; Maxwell and Biggins, 1976; Herbert et al., 1990; Asada et al., 1993), while in C3 plants the CET pathway is required for protecting PSI specifically under stress conditions.

As reported by Fan et al. (2007), CET rates are low at the very early phase of photosynthetic induction but rise upon illumination, and decline subsequently to <10% of the total electron flux in the steady state. However, the main CET pathway via PGR5/PGRL1 in WT contributes nearly 13% of total ATP synthesis (Avenson et al. 2005a). Recently, Takagi and Miyake (2018) showed that Fd-CET-PSI activity was minor during *in vivo* steady-state photosynthesis in Arabidopsis and that PGR5 and PGRL1 modulate the linear electron flow (LEF) according to electron sink activities around PSI. The Flv-dependent O_2 reduction pathway dissipates 25% of electrons originating from PSII in a *pgr5/pgrl1* mutant background, emphasizing that overexpressing Flv genes can contributes significantly to pmf formation (Shikanai and Yamamoto, 2017).

In the Flv-expressing lines, ATP levels were higher during the day at 4h and 8h after onset of light, indicating that the Flv proteins at PSI dissipate electrons and thus enhance linear electron flow to establish the pH gradient required for ATP synthesis (Figure 25A, B, C). In cyanobacteria Flv3-overexpression enhanced ATP synthesis (Hasunuma et al., 2014). The Flv2 and Flv4 proteins that accept electrons from PSII may enhance oxidation of water and contribute to luminal acidification that in turn promotes ATP synthesis (Figure 26A, B, C). As reported earlier, the cyanobacterial mutants Δ*flv2* and Δ*flv4* of *Synechocystis* sp. PCC6803 showed reduced oxygen evolution rates compared to wild type under low CO_2 conditions (Zhang et al., 2009). The energy charge index calculated from the adenylate nucleotide pools was higher in Flv-expressing lines during the day (Figure 25D, E,

F and Figure 26D, E, F). In Flv-expressing lines at 16h during dark period, the photoassimilates synthesized during the day were obviously used for ATP synthesis during the night that in turn maintained higher ATP production and energy charge (Figure 5), indicating that Flv proteins enhanced photosynthesis efficiency. These results demonstrate that heterologous expression of Flv proteins provides a new alternative electron flow (AEF) pathway that functions independently of cyclic electron transport (CET) or the Mehler reaction and that promotes the generation of the pH gradient across the thylakoid membrane, required for ATP synthesis tand CO2 fixation.

4.3 The expression of Flv genes enhanced metabolic activity in Arabidopsis leaves

The adenylate pool plays a vital role in the regulation of plant metabolism (Geigenberger et al., 2010). CO_2 fixation is dependent on the ATP/NADPH ratio generated through the light reaction of photosynthesis. The unequal ratio of ATP/NADPH generated through LEF, generates ATP limitation in chloroplasts may be due to inefficient ATP synthesis or elevated ATP consumption suppresses the photosynthesis rate and the metabolic reactions in the Calvin cycle. Such conditions leads to stromal reduction intern activates AEF pathway to releave electron pressure from the electron transport chain and compensate for the lacking ATP. In Flv-expressing lines, Flv proteins accept electrons as shown from chlorophyll a fluorescence measurements (Figure 16, Figure 17) and higher ATP availability (Figure 25, Figure 26) enhance Calvin cycle metabolic activity. In Flv-expression lines, the level of hexose phosphates was higher during the middle of the day (Figure 27A, Figure 28A) and also ADPGlc was higher (Figure 27B, Figure 28B). These hexose-phosphates and ADPGlc are crucial precursors for the synthesis of soluble sugars and starch during the day that maintains plant growth during the night (Figure 20A, B and Figure 21A, B). The TCA cycle intermediate citrate can act in the so-called citrate valve under highly reduced conditions in mitochondria operates partial TCA cycle for the synthesis of 2-oxoglutarate and glutamate (Igamberdiev and Gardeström, 2003) and also under photorespiratory conditions. In contrast, malate acts as malate valve that transfers redox equivalents from the chloroplasts to cytosol (Geigenberger and Fernie, 2011; Maurino and Engqvist, 2015). Citrate and malate, the abundant of these organic acids vary in plants that accumulate more starch, did not show significant differences in Flv-expressing lines compared to wild type as Flv-expressing lines observed higher starch (Figure 27C, D and Figure 28C, D).

Interestingly, alteration of the plastidial adenylate kinase through antisense technology enhanced starch and amino acids in transgenic potato plants (Regierer et al., 2002) or resulted in the accumulation of amino acids in Arabidopsis plants, which ended up with improved plant growth (Carrari et al., 2005). Apparently, a tight control of the C:N ratio must be ensured to maintain the balance between carbon sources and nitrogen-containing metabolites such as amino acids. In Flv-expressing plants, no significant changes in amino acid levels could be observed at 4h after illumination, indicating that during the light period the major part of the produced assimilates was converted to starch (Appendix Table 2 and Table 3). However, 8h after illumination nitrogen storage-specific amino acids, like asparagine, glutamine increased (Table 1 and Table 2), suggesting that increased carbon availability enhanced N assimilation that in turn is necessary for protein synthesis and consequently for optimal growth during the night period (Lawlor, 2002). Furthermore, sucrose and ATP levels were higher in Flv-expressing plants, not only during the light period but also during the dark period. Previous studies have shown that sucrose and ATP are closely linked to carbon metabolism during the night (Sharkey et al., 2004) and represent important determinants of higher biomass in several plant species (Graf and Smith, 2011; Sulpice et al., 2009). The above results demonstrate that heterologous expression of Flv genes establishes a new AEF that functions independently of the CET pathway in Arabidopsis contributes to the ATP demand, which supports a higher metabolic activity.

4.4 Effect of Flv genes on antioxidant metabolism in chloroplasts

Another interesting observation in this study was that the ratio of the reduced to the oxidized form of the non-enzymatic anti-oxidant compound glutathione decreased in Flv-expression lines (Figure 29A, Figure 29B). The ratio of oxidized to reduced glutathione represents a major indicator of the cellular redox state (Meister, 1995). Glutathione plays a major role in balancing the redox status mainly in mitochondria and chloroplasts. In the presence of ROS, GSH oxidizes to GSSG and is the rapidly reduced back to form GSH by oxidizing NADPH to $NADP^+$ (Figure 40). This was opposite in Flv-expressing lines, in which the reduced form GSH was low whereas the oxidized form was higher than in the wild type. Considering that glutathione levels in plants do not vary under changing light intensity or day length but increase only under oxidative stress conditions, it is tempting to speculate that Flv proteins may avoid excess electron to leak from the ETC which would prevent ROS production. The glutathione (GSH) reduces oxidized dehydroascorbate (DHA) to form

Figure 30. Introduction of an additional electron sink in Arabidopsis chloroplasts by ectopic expression of Flv proteins improves redox homeostasis and growth. The expression of Flv genes creates an electron sink (Flv1 and Flv3 at PSI; Flv2 and Flv4 at PSI

ascorbate (AA), and oxidized glutathione (GSSG) is reduced by NADPH. Since oxidized glutathione (GSSG) was higher in Flv-expression lines, it may be speculated that Flv proteins induce redox changes (Appendix Figure S7), possible avoid excess ROS production by removing the excess of electrons through Flv proteins. (Figure 30).

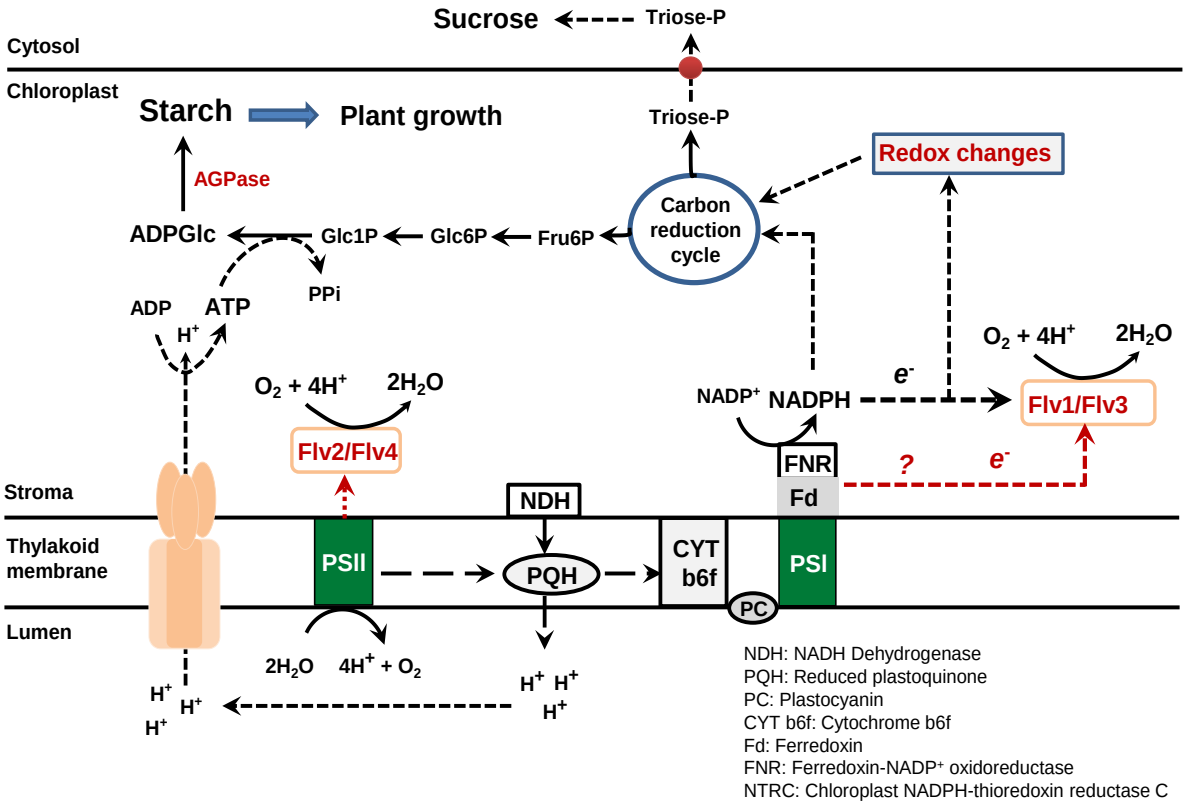

Figure 30. Introduction of an additional electron sink in Arabidopsis chloroplasts by ectopic expression of Flv proteins improves redox homeostasis and growth. The expression of Flv genes creates an electron sink (Flv1 and Flv3 at PSI; Flv2 and Flv4 at PSII) and balances the surplus of electrons flowing through photosystem I and II, by reducing oxygen to water. The continuous flow of electrons results in acidification of the lumen that is the driving force for ATP synthesis. The higher ATP in Flv-expressing lines enhance metabolic activity in chloroplasts. Produced ATP is used for the conversion of Glc1p to ADP Glc via ADP Glc pyrophosphorylase. Increased ADP Glc results finally in the higher starch synthesis that is accumulating during the light period and degraded during the dark phase yielding in improved growth of Arabidopsis plants.

Figure 30. Introduction of an additional electron sink in Arabidopsis chloroplasts by ectopic expression of Flv proteins improves redox homeostasis and growth. The expression of Flv genes creates an electron sink (Flv1 and Flv3 at PSI; Flv2 and Flv4 at PSI

In conclusion, the data demonstrate that establishing alternative electron sinks represents a powerful strategy to protect PETC and that cyanobacterial Flv's provide efficient electron sink as observed from chlorophyll a fluorescence measurements. Based on these investigations, it is hypothesized that expression of Flv's balances excess flow of electrons through PSI and PSII by reducing molecular oxygen to water. Then, the production of redox equivalents in the form of NADPH is maintained and leads to carbon recycling through the Calvin cycle. The latter generates phosphorylated metabolites necessary for starch synthesis. The required energy for this reaction is provided by ATP, which is produced in excess through Flv-aided electron flow and luminal acidification, the driving force for ATP synthesis. ATP is also used for the conversion of Glc1P to ADPGlc via ADPGlc pyrophosphorylase. Increased ADPGlc finally generates a larger pool of starch that builds up during the light period and sustains growth processes for longer during the dark phase, leading to improved growth of Arabidopsis plants (Figure 30).

5. Results

5.1 Impact of drought stress on Flv expression lines

To study the effect of drought stress on Flv-expressing lines, plants were grown in … soil and subjected to a drought stress treatment (Figure 31A). All transgenic lines and WT plants were well watered for 28 days before withholding water. 5% field capacity was attained after 5-8 days and then maintained by adding watering. Phenotypic observations revealed that WT plants were smaller and wilted faster compared to Flv-expressing lines (Figure 31B, C). The aerial parts of the plants were harvested for metabolite analysis. Further, drought recovery experiments were conducted (Appendix Figure 5) but due fungal infections in the green house quantitative data was not measured.

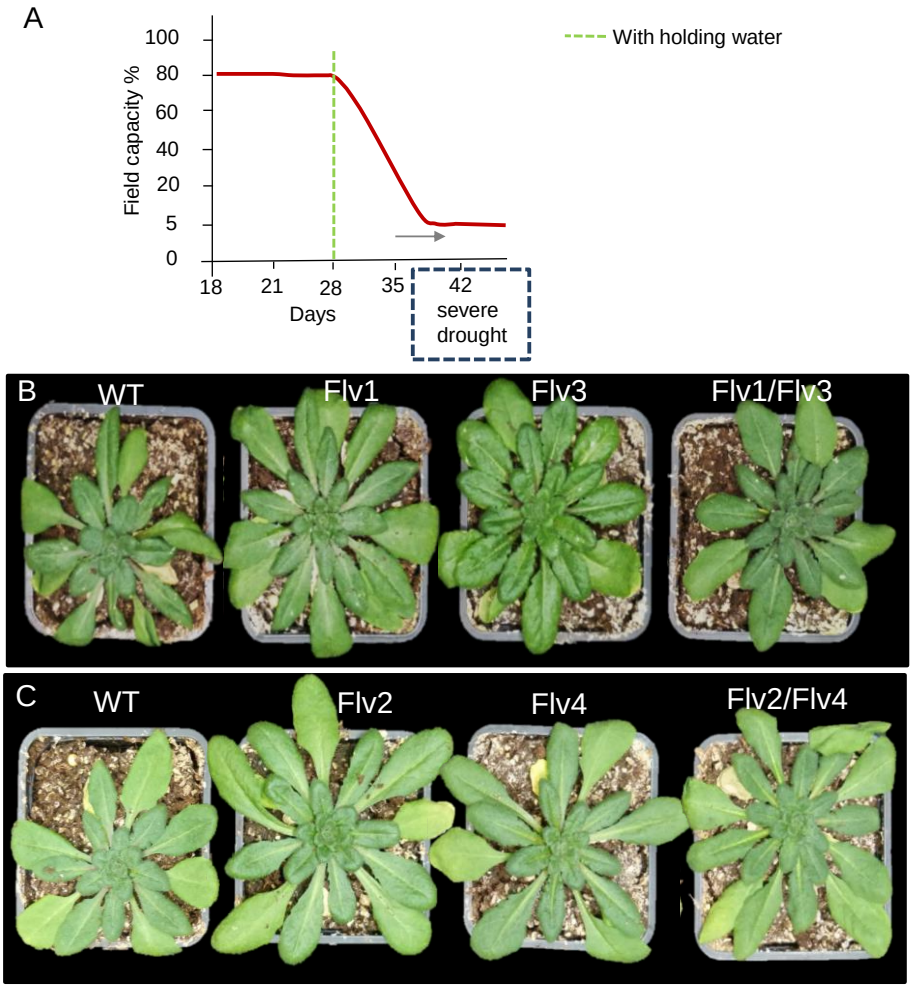

Figure 31. Schematic representation of natural drought stress treatment and sampling of Flv-expressing lines. (A) Drought was imposed after 28 days by withholding water. (B, C) representative photographs of one of the lines were taken before sampling at 37 days. Soil moisture was monitored regularly and maintain 5% field capacity by addition of water. Samples were harvested once wilting was observed.

5.2 Impact of flavodiiron proteins on photosynthesis performance under drought stress

The efficiency of photosynthesis is primarily affected by drought stress in plants, which leads to photoinhibition of photosystems I and II. In the present study, it was investigated whether the expression of Flv genes in Arabidopsis can enhance drought tolerance in Flv-expressing lines.

The photosystem ll parameters, Fv/Fm as indicator for the maximum quantum yield of PSll and φPSII as indicator for operating efficiency of PSll electron transport, were measured in dark-adapted plants. Under drought stress conditions, which were induced by growing plants at at 5% field capacity, the Fv/Fm values did not differ among Flv-expressing lines or between them and WT plants (Figure 32A, Figure 33A). In general, the φPSII values during early induction of photosynthesis increased gradually in all Flv- expressing lines and WT (Figure 32B, Figure 33B). The φPSII values were, however, higher for all Flv1-, Flv3-, and Flv1/Flv3-expressing lines between 1.1–1.4 fold, 1.38 fold, and 1.2-1.4 fold compared to WT, respectively (Figure 32B). In all investigated Flv2-, Flv4-, and Flv2/Flv4-expressing lines, the φPSII values were also higher between 1.2-1.4, 1.3-1.4 and 1.2-1.35 fold compared to WT, respectively (Figure 33B).

The qL parameter, as indicator for active open reaction centers, was 1.3–1.6 fold higher in Flv1-, 1.3–1.5 fold in Flv3-, and 1.0–1.6 fold in Flv1/Flv3-expressing lines compared to WT (Figure 32C). In Flv2-, Flv4-, Flv2/Flv4-expressing lines, the qL was 1.4–2.0 fold higher in Flv2-, Flv4-, 1.6–1.7 fold and Flv2/Flv4-expressing lines 1.4–1.5 fold higher compared to WT (Figure 33C).

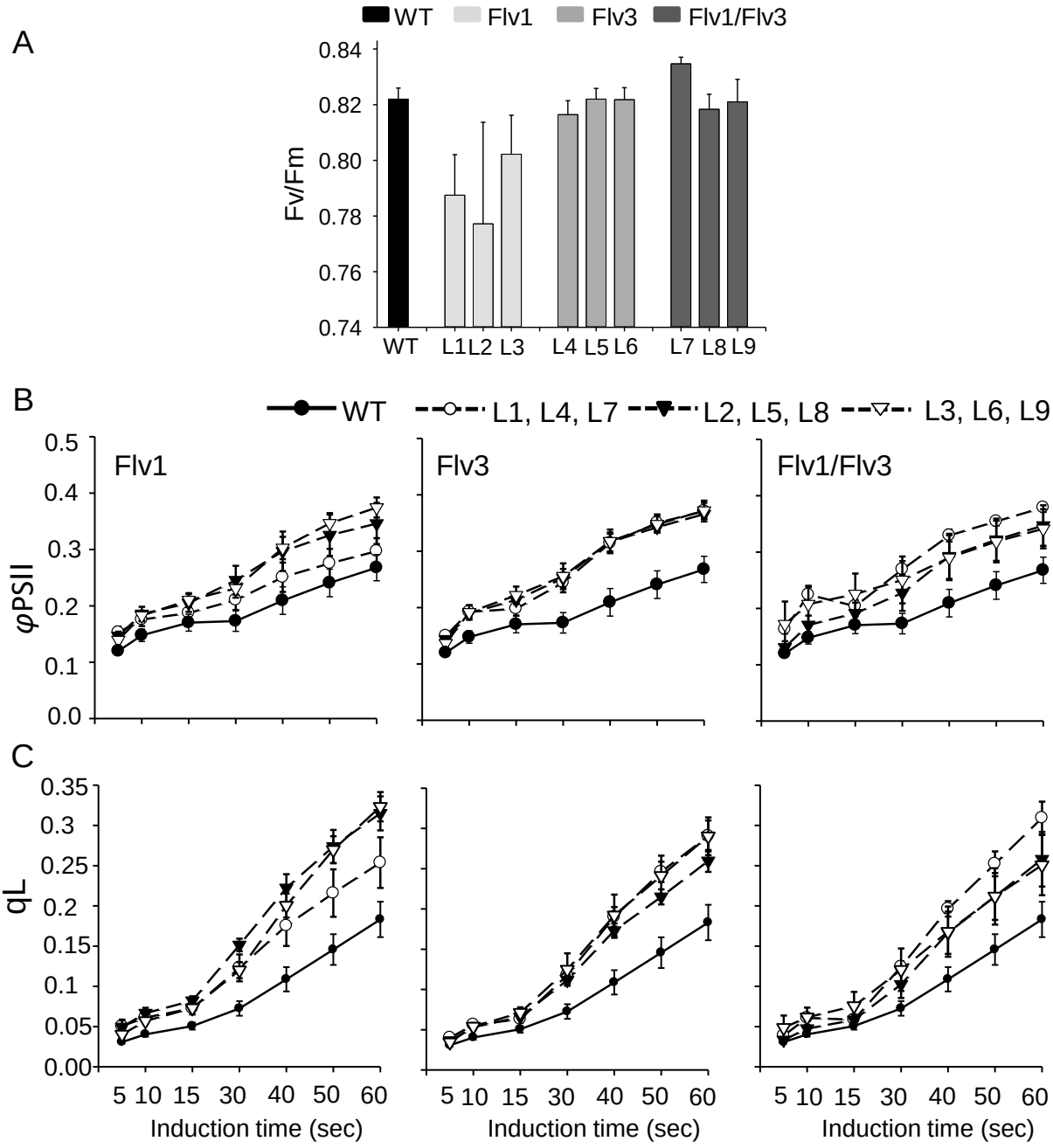

Figure 32. Early photosynthesis induction curves in Flv-expressing lines under drought stress. (A) Fv/Fm, (B) *φ*PSII quantum yield of PSII, (C) open psII reaction centers values were determined at 150 µmol photons m^{-2} s^{-1} of actinic light on dark-adapted leaves of WT (black circles) and three independent lines of Flv1-, Flv3-, and Flv1/Flv3-expressing lines: open circles (L1, L4, L7), black triangles (L2, L5, L8) and open triangles (L3, L6, L9). Data points represent means of 8 biological replicates±SE.

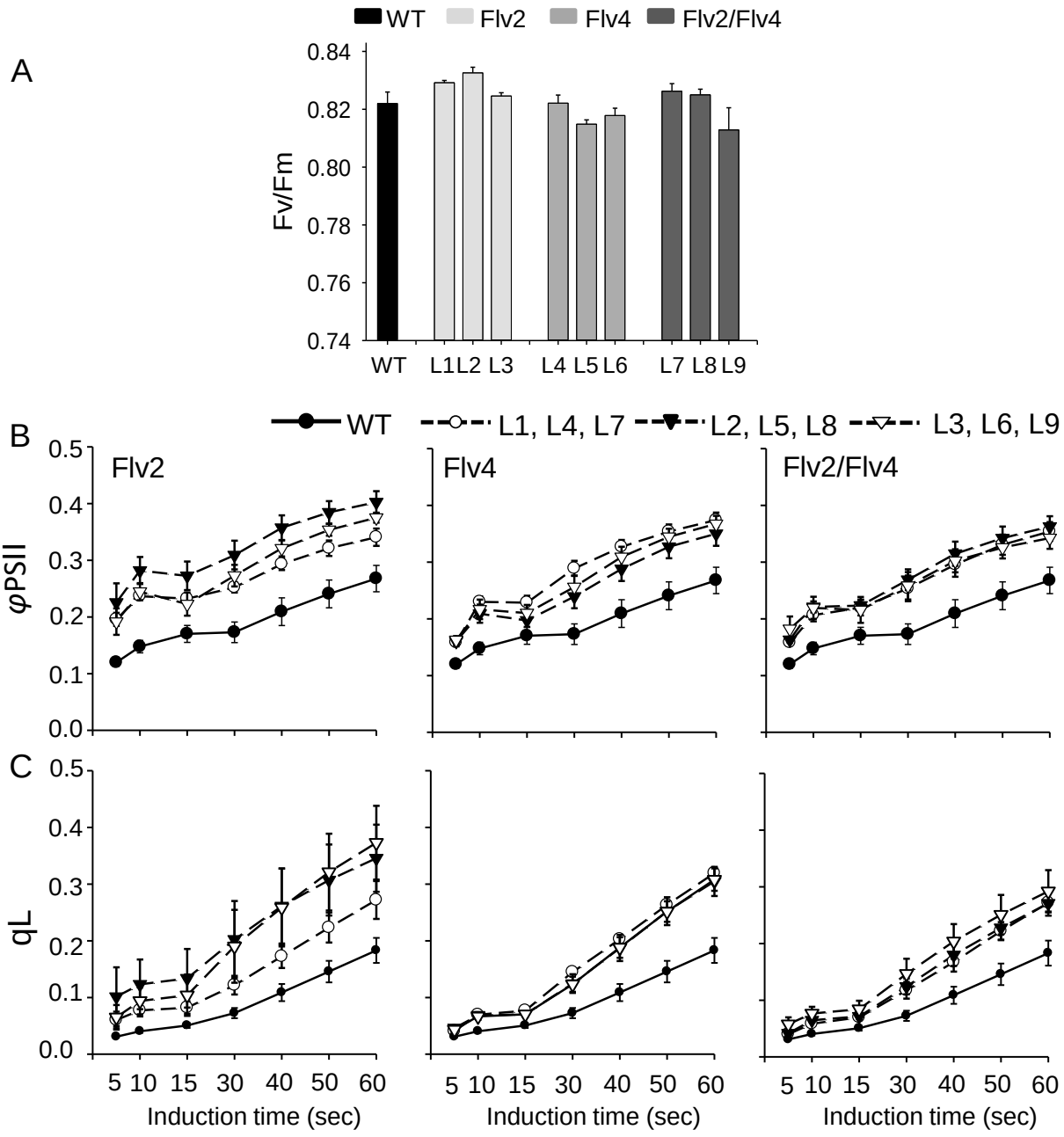

Figure 33. Early photosynthesis induction curves in Flv-expressing lines under drought stress. (A) Fv/Fm, (B) *φ*PSII quantum yield of PSII photochemistry, (C) open PSII reaction centers values were determined at 150 µmol photons m^{-2} s^{-1} of actinic light on dark-adapted leaves of WT (black circles) and three independent lines of Flv1-, Flv3-, and Flv1/Flv3-expressing lines: open circles (L1, L4, L7), black triangles (L2, L5, L8) and open triangles (L3, L6, L9). Data points represent means of 8 biological replicates±SE.

The excess light energy absorbed was dissipated as heat through the regulatory mechanism mediated through xanthophyll cycle (NPQ) so-called non-photochemical quenching (Müller et al., 2001). The light-regulated dissipation of excess energy, as expressed by φIINPQ levels, were lower in all the Flv-expressing lines than in the wild type (Figure 34A, Figure 35A). The φNO, non-regulated energy dissipation, in Flv-expressing lines was similar to WT plants, except for L7 (Flv1/Flv3) (Figure 34B, Figure 35B). The NPQ, the light-independent regulation of energy dissipation did not change in all the Flv-expressing lines (Flv1, Flv3, Flv1/Flv3 and Flv2, Flv4, Flv2/Flv4) except for L7 (Flv1/Flv3), L3 (Flv2) and L8 (Flv2/Flv4) than to WT (Figure 34C, Figure 35C). Thus expression of Flv proteins maintained higher PSII activity and prevented over-reduction of the electron transport chain under drought stress conditions during early induction of photosynthesis.

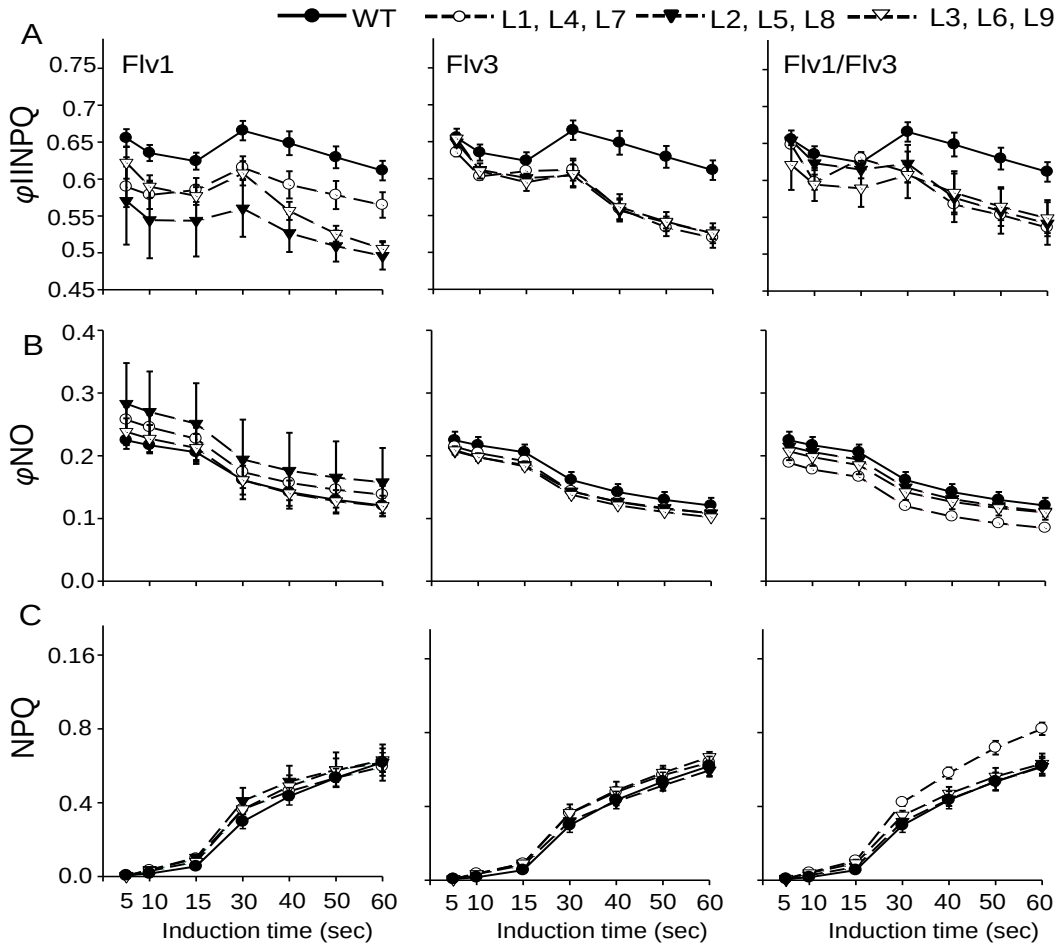

Figure 34. Non-photochemical quenching fluorescence measurements in Flv-expressing Arabidopsis plants under drought stress. (A) *φ*IINPQ, light-dependent non-photochemical energy loss in PSII, (B) *φ*NO, non-regulated energy loss in PSII and (C) NPQ, light-independent non-photochemical quenching. Measurements were carried out in rosette leaves of dark-adapted WT (black circles) and three independent lines of Flv1-, Flv3-, Flv1/Flv3-expressing lines: open circles (L1, L4, L7), black triangles (L2, L5, L8) and open triangles (L3, L6, L9) illuminated with actinic light at 150 µmol photons m^{-2} s^{-1}. Data points represent means of 8 biological replicates±SE.

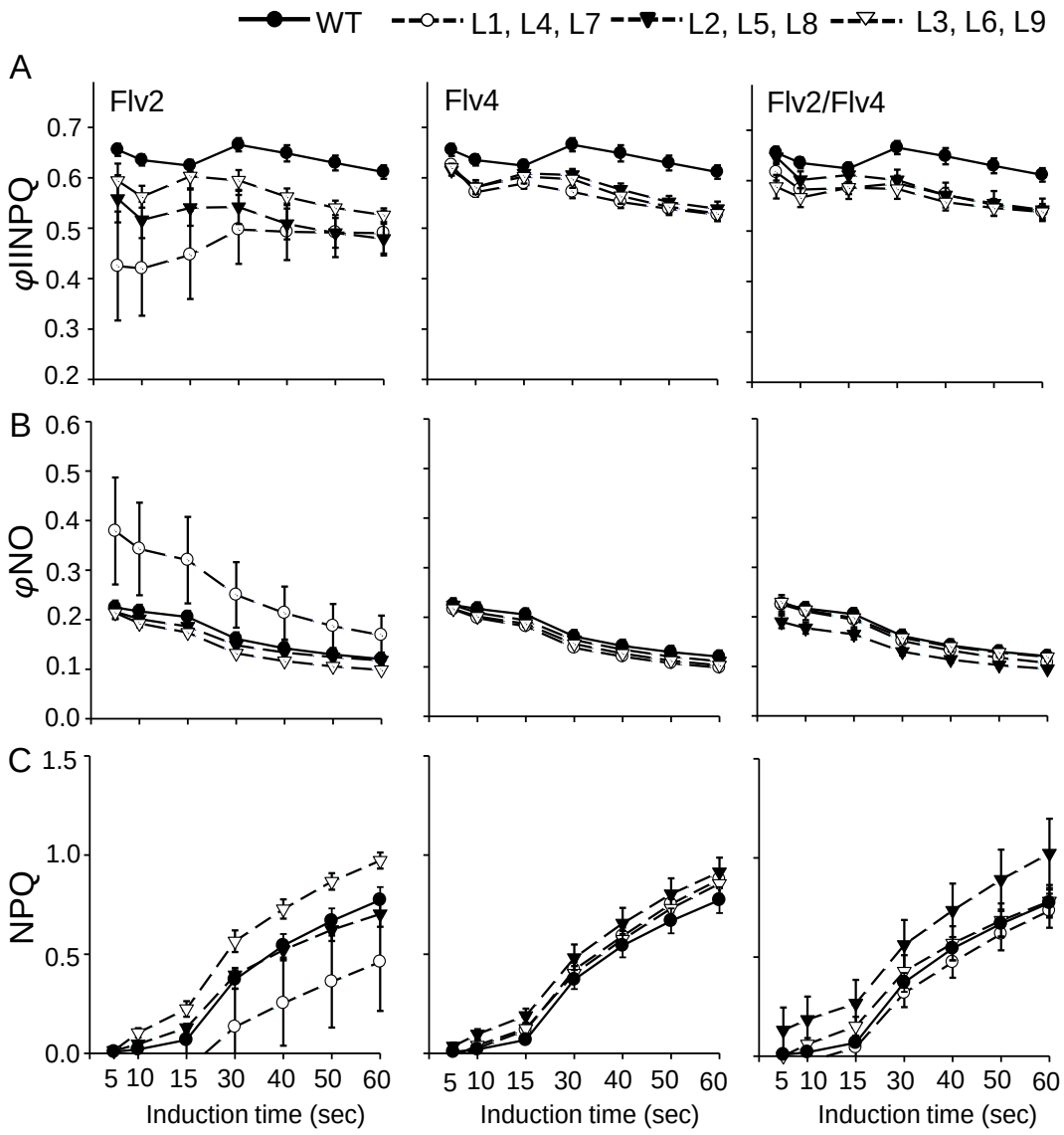

Figure 35. Non photochemical quenching fluorescence measurements in Flv-expressing Arabidopsis plants under drought stress. (A) *φ*IINPQ, light-dependent non-photochemical energy loss in PSII, (B) *φ*-NO, Non regulated energy loss in PSII and (C) NPQ, light-independent non-photochemical quenching. Measurements were carried out in rosette leaves of dark-adapted WT (black circles) and three independent lines of Flv2-, Flv4-, Flv2/Flv4-expressing lines: open circles (L1, L4, L7), black triangles (L2, L5, L8) and open triangles (L3, L6, L9) illuminated with actinic light at 150 μmol photons $m^{-2}s^{-1}$. Data points represent means of 8 biological replicates±SE.

5.3 Effect of drought stress on carbohydrate and amino acid metabolisms in Flv-expressing lines

An elevated carbohydrate status can be seen as indication for the fitness of a plant under drought stress. The changes in soluble sugars and starch concentrations were determined in Flv-expressing lines under drought stress (Figure 36, Figure 37). As shown in the Figure 37A, the sucrose levels were low in all the investigated lines of Flv1-, Flv3-, Flv1/Flv3-expressing lines but significantly lower than the wild type in L1 (Flv1), L4,and L6 (Flv3). In Flv2, Flv4, Flv2/Flv4 lines, sucrose levels were significantly lower in L5, L6 (Flv4), L7 (Flv2/Flv4) lines (Figure 37A). No consistent differences to the wild type in glucose and fructose accumulation was found in any of the Flv-expressing lines (Appendix Figure 3A, B), whereas in Flv3-expressing lines L4 and L6 lower levels of glucose were detected (Appendix Figure 3A). In Flv2-, Flv4-, and Flv2/Flv4-expressing lines, the glucose levels were 2.0–2.9 times higher in all lines compared to WT (Appendix Figure 3C). The fructose levels were higher in L2, L3 (Flv1), L4 (Flv3), L7, L8 (Flv1/Flv3) and L3 (Flv2) compared to WT (Appendix Figure 3B, D). The transitory carbohydrate storage form starch was 1.5 times higher in Flv1-, Flv3-, and Flv1/Flv3-expressing lines except for L2, L3 (Flv1), L5 (Flv3) and L7 (Flv1/Flv3) (Figure 36B) and 1.6 times higher in Flv2-, Flv4-, Flv2/Flv4-expressing lines except for L1 (Flv2), L6 (Flv4) and L8 (Flv2/Flv4) (Figure 37B). The above carbohydrate results indicates Flv proteins maintains photosynthesis under stress conditions.

As drought stress is know to alter amino acid biosynthesis, its influence on the total free amino acid composition in plants as well as on individual specific amino acids were analyzed in Flv-expressing lines. Specific changes could be observed in all Flv-expressing lines at 5% field capacity (Figure 36C,D,E,F, Figure 37C,D,E,F, Appendix: Table 4, Table 5). The aspartate level was higher in all Flv1/Flv3 lines, L3 (Flv1) and L6 (Flv3) expressing lines (Figure 37C) and no changes were observed in Flv2-, Flv4-, Flv2/Flv4-expressing compared to WT (Figure 37C). The glutamate level was higher in lines L4, L6 (Flv3), and in L8, L9 (Flv1/Flv3) (Figure 36D), whereas in Flv2-, Flv4-, and Flv2/Flv4-expressing lines, the glutamate levels were higher in all the lines except for L1 (Flv2) and L4 (Flv4) relative to WT plants (Figure 37D). Proline, which is a stress marker, was markedly lower in the lines L4 (Flv1), L6 (Flv3) and L5 (Flv4) but no differences were observed in Flv1/Flv3-, Flv2-, Flv2/Flv4-expressing lines in comparison to the wild type (Figure 36E, Figure 37E). GABA, another stress-induced amino acid was similar in all Flv1-, Flv3-, Flv1/Flv3-expressing lines except for L4 (Flv3) (Figure 36F), but higher in all Flv2-, Flv4-, and Flv2/Flv4-expressing lines except for L8, L9 (Flv2/Flv4) (Figure 37F). The above results predicts changes in

amino acids levels in Flv-expressing lines but the changes were not tend to be same among the lines and between the Flv genes.

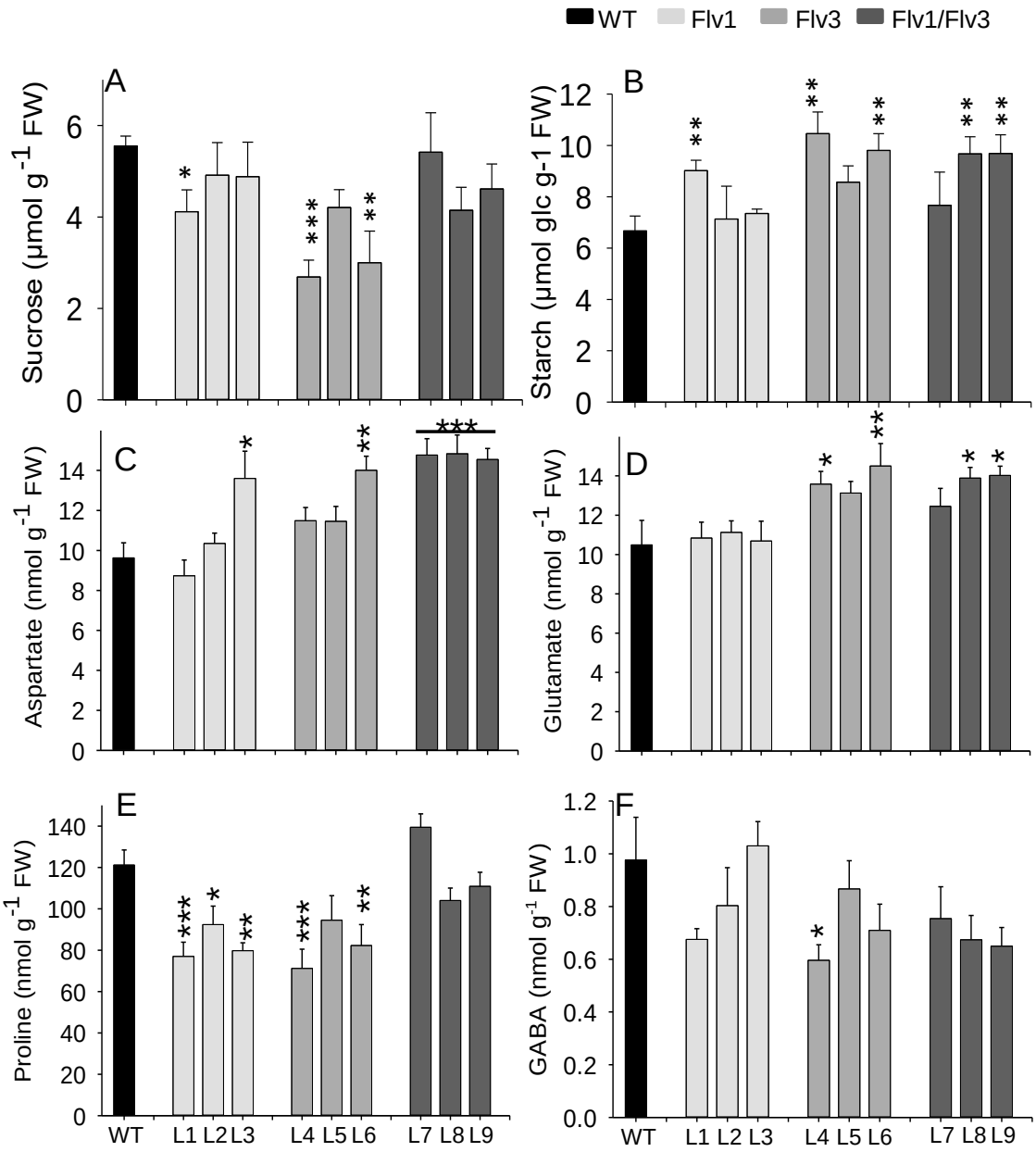

Figure 36. Concentrations of carbohydrates and amino acids in Flv1-, Flv3-, Flv1/Flv3-expressing lines under drought stress.Concentrations of (A) sucrose, (B) starch, (C) aspartate, (D) glutamate, (E) proline, and (F) GABA were measured in three independent lines. Bars represents mean of 7 biological replicates±SE. Significant differences between WT and Flv-expressing lines are indicated by asterisks according to Student's t test (*p≤0.05, **p≤0.01 and ***p≤0.001).

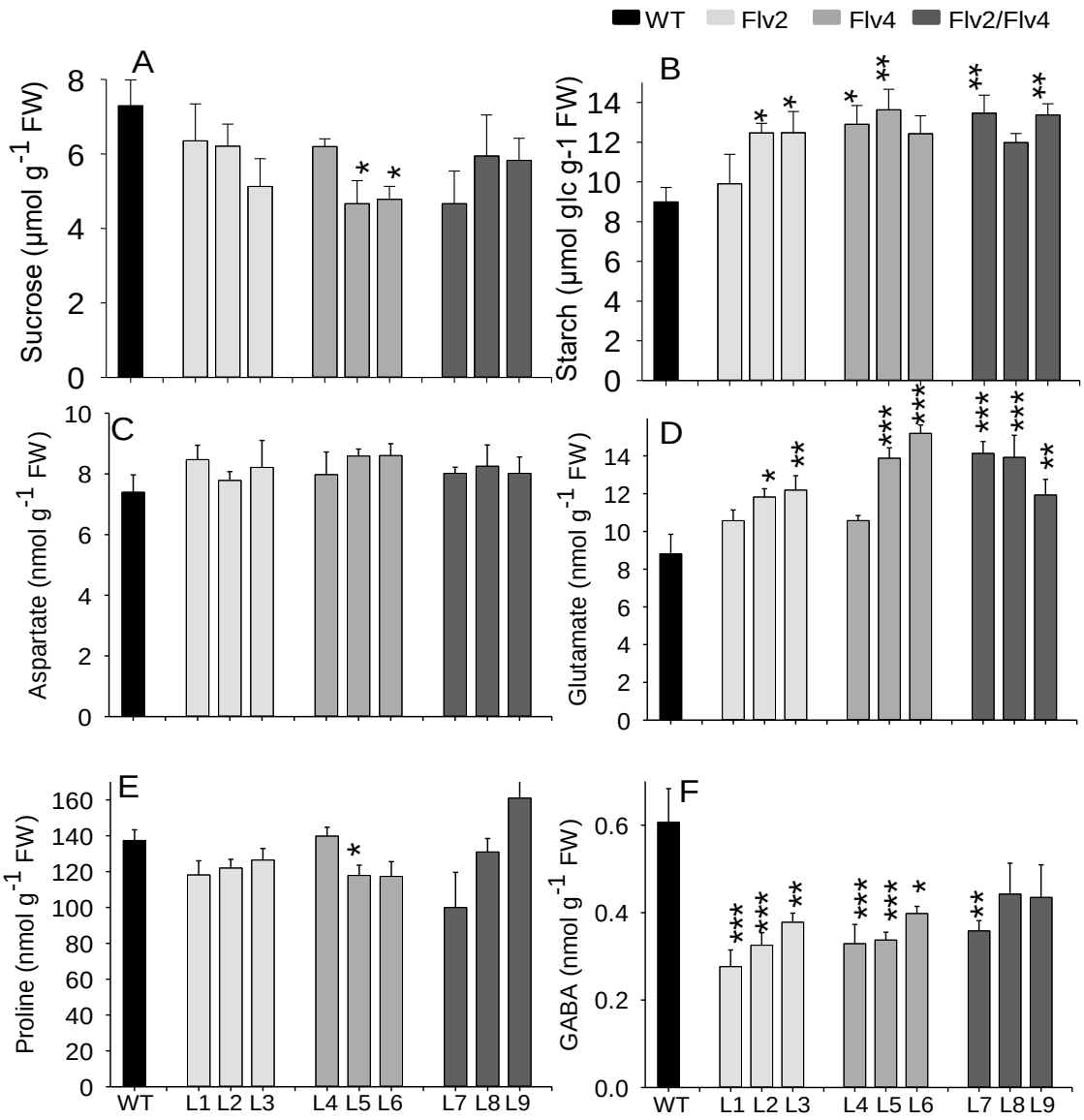

Figure 37. Concentration of carbohydrates and amino acids in Flv-expressing lines Flv2-, Flv4-, Flv2/Flv4-expressing lines under drought stress. Concentration of (A) sucrose, (B) starch, (C) aspartate, (D) glutamate, (E) GABA, and (F) proline were measured in three independent lines. Bars represent means of 7 biological replicates±SE. Significant differences between WT and Flv-expressing lines are indicated by asterisks according to Student's t test (*p≤0.05, **p≤0.01 and ***p≤0.001).

5.4 Expression of Flv genes in the chloroplast enhances ATP levels and energy status under stress conditions

In plants, the ATP levels are essential to maintain growth processes and to prevent cellular damage under stress conditions. As shown in Figure 38A, the ATP levels increased in all Flv1-, Flv3-, and Flv1/Flv3-expressing lines, and the energy charge was higher in all Flv1-, Flv3-, and Flv1/Flv3-expressing lines, except for L3 (Flv1) compared to wild type (Figure 38B). In contrast, the ATP levels were tend to be stable in Flv2-expressing lines but lower in Flv4-, and Flv2/Flv4-expressing lines compared to the wild type (Figure 38C). The AMP and ADP levels in Flv-expressing lines were lower in all lines except Flv1-expressing lines (Appendix figure 4). Interestingly, the energy charge was higher in all lines of Flv2 and in L6 (Flv4) and similar in Flv2/Flv4-expressing lines compared to WT (Figure 38D). These results indicate that Flv proteins (Flv1-, Flv3-, Flv1/Flv3) in chloroplasts relieves electron pressure at PSI and maintains a higher energy status under drought stress conditions.

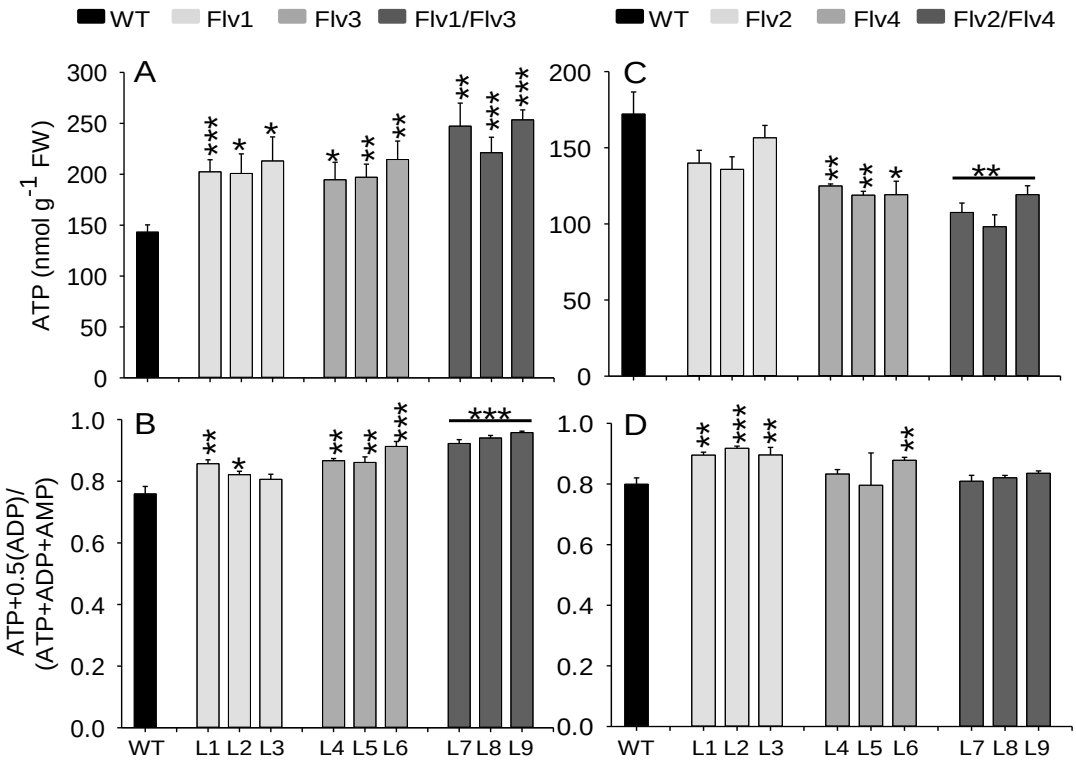

Figure 38. ATP and energy charge in Flv-expressing lines under drought stress conditions. (A) ATP concentration, and (B) energy charge, in Flv1-, Flv3-, Flv1/Flv3-expressing lines, (C) ATP concentration, and (D) energy charge in Flv2-, Flv4-, Flv2/Flv4-expressing lines. Measurements were carried out in three independent lines. Bars represent means of 7 biological replicates±SE. Significant differences between WT and Flv-expressing lines are indicated by asterisks according to Student's t-test (*p≤0.05, **p≤0.01 and ***p≤0.001).

5.5 Flv proteins maintain the redox status under drought stress

The ratio of reduced to oxidized glutathione represents a major indicator of the redox status in plants under stress conditions. As the dioxygen scavenging function of Flv proteins prevents ROS production, glutathione levels were analyzed in Flv-expressing lines under drought stress conditions. The reduced glutathione (GSH) level was significantly lower in Flv1-, Flv3-, and Flv1/Flv3-expressing lines (Figure 39A) and the oxidized glutathione (GSSG) was slightly lower than in WT plants (Figure 39B). In response to drought stress the ratio of GSH:GSSG level was lower in L6 (Flv3) and L9 (Flv1/Flv3) lines than in the WT (Figure 39C). In Flv2-, Flv4-, Flv2/Flv4-expressing lines, the reduced form of glutathione levels higher in Flv2-expressing lines and L4 (Flv4) except for L5, L6 (Flv4) and in all Flv2/Flv4-expressing lines (Figure 39D). The oxidized form of glutathione was lower in L5, L6 (Flv4), L8 (Flv2/Flv4) compared to WT (Figure 39E). Further, the ratio of GSH: GSSG was significantly higher in L1 (Flv2) except Flv4-, and Flv2/Flv4-expressing lines compared to the ratio of WT (Figure 39F). The ratio of GSH:GSSG in Flv1-, Flv3-, Flv1/Flv3-expressing lines indicates that Flv1, Flv3, Flv1/Flv3 proteins which function at PSI in chloroplasts maintains the redox status under stress conditions.

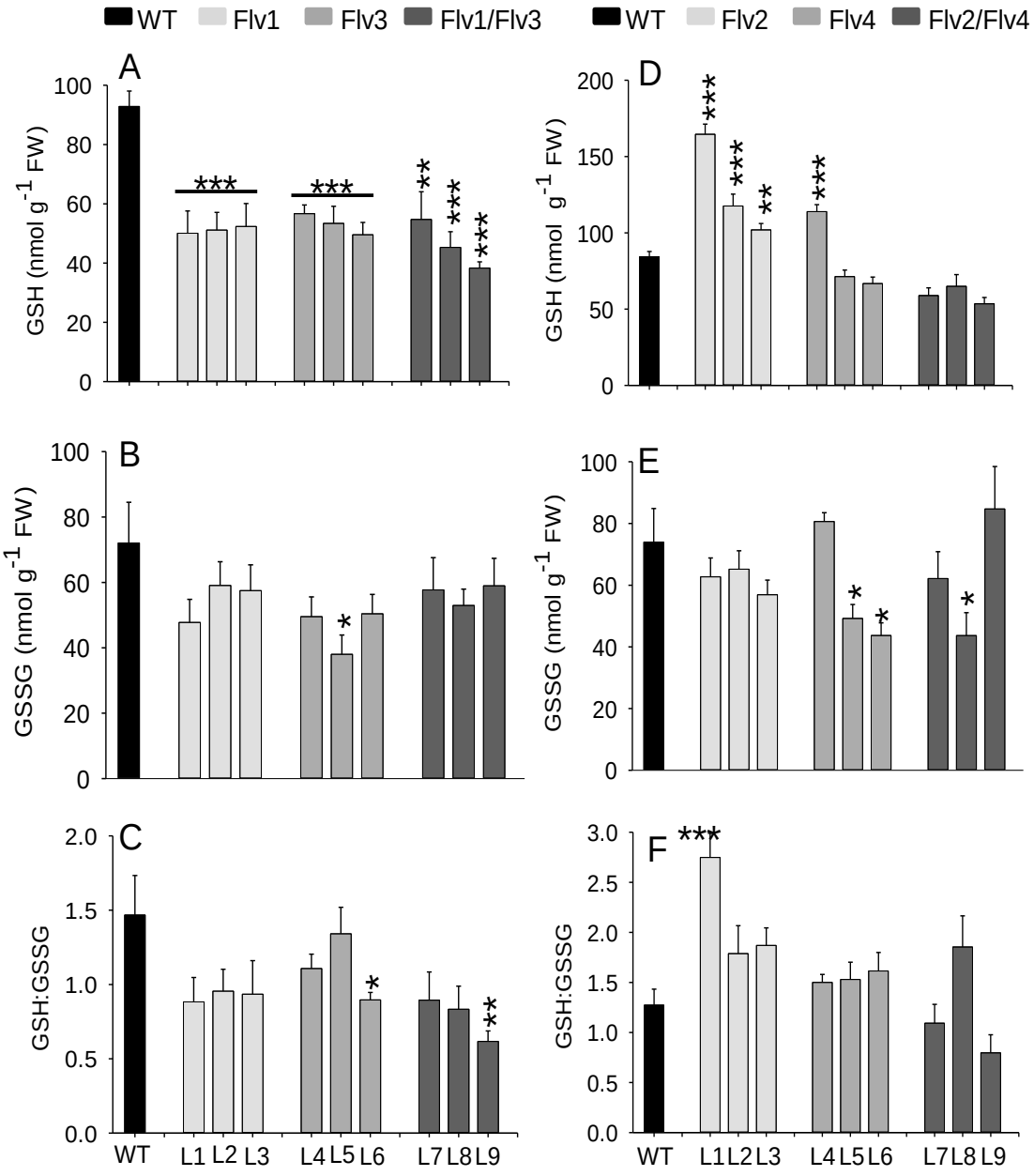

Figure 39. Characterisation of glutathione levels in Flv-expressing lines under drought stress conditions. Concenrations of (A) GSH, and (B) GSSG, and (C) GSH:GSSG ratio in Flv1-, Flv3-, Flv1/Flv3-expressing lines and concentrations of (D) GSH, (E) GSSG, and (F) GSH:GSSG ratio in Flv2-, Flv4-, Flv2/Flv4-expressing lines. Measurements were carried out in three independent lines. Bars represent means of 7 biological replicates±SE. Significant differences between WT and Flv-expressing lines are indicated by asterisks according to Student's t test (*p≤0.05, **p≤0.01 and ***p≤0.001).

6. Discussion

6.1 Flavodiiron proteins alleviate drought tolerance in Flv-expressing lines

Arabidopsis plants harboring different Flv protein isoforms were used to study the impact of an additional electron dissipating pathway in chloroplasts by imposing drought stress. Drought stress is one of the most common stress factors that limits the plant growth and yield by reducing the photosynthesis efficiency and other physiological functions of the cell (Ashraf et al., 2013). Chloroplasts in higher plants evolved several defensive mechanisms to overcome drought stress. The major pathway is photorespiration, which dissipates excess light energy and protects the electron transport chain, as well as photosystems I and II from photoinhibition (Osmond 1981; Osmond & Grace 1995; Osmond et al. 1997; Kozaki & Takeba 1996; Wu et al. 1991). Flavodiiron proteins in photosynthetic organisms and lower plants also act as electron-consuming pathways that protect photosystems from photoinhibition (Allahverdiyeva et al., 2015). These proteins were used in the present study to investigate whether they can protect photosystems I and II also in Arabidopsis under drought stress and thus improve survival of the plant. Flv-transgenic plants performed better than WT plants under drought stress as shown from the two experiments conducted - plant growth at 5% field capacity and drought recovery (Figure 31). Indeed, Flv-expressing lines were able to partially compensate for the water loss, as evident from reduced wilting and bigger size of the rosette, indicating that Flv proteins could effectively maintain the photosynthesis. This in turn resulted in improved plant survival and better growth under drought stress conditions.

6.2 Enhanced photosynthesis efficiency under drought stress in Flv-expressing lines

Photosynthesis is the most affected process when plants are exposed to drought stress (Chaves, 1991). Chlorophyll a fluorescence measurement is an excellent non-invasive method to study the photosynthesis efficiency and it is an indicator for the physiological status of the plant (Strasser et al., 2000). The Fv/Fm ratio (maximum quantum yield of PSII) can be used to estimate the rate of PSII inhibition (Ahmed et al., 2002) but the values of Fv/Fm does not change in the initial stages of drought stress, as PSII is protected from photoinhibition due to its repair mechanism. During short-term drought stress exposure, no differences were observed in Fv/Fm in Flv-expressing lines and WT plants (Figure 32A, Figure 33A). Here, limitation of final electron acceptors at PSI under stress conditions activates CET pathways that induce luminal pH activates NPQ to protect PSII

from photoinhibition. However, the fluorescence parameters φPSII and qL and the electron flow from PSII to PSI were higher in Flv-expressing lines during early induction of photosynthesis (Figure 32B, C, Figure 33B, C) where Flv proteins can act as final electron acceptors. This is in agreement with previous studies that Flv proteins protect the photosystem and prevent over-reduction of the electron transport chain under fluctuating light conditions in *Physcomitrella patens* (Gerotto et al., 2016)or in Flv protein-expressing in rice (Wada et al., 2017). The PGR5/PGRL1-dependent CET-regulated dissipation of excess energy through NPQ (light independent) showed no difference between the Flv-expressing lines and the wild type (Figure 34C, Figure 35C). The φNO (non- light regulated) dissipation of energy was not affected in Flv lines and wild type under stress conditions (Figure 34B, Figure 35B). The φNPQ, light dependent dissipation of energy was low in Flv-expressing lines indicating that the observed light energy was used for the photochemistry (Figure 34A, Figure 35A). This suggests that Flv proteins avoid over-reduction of the ETC and maintain photosynthesis under drought stress conditions.

6.3 Carbohydrate and amino acid metabolism in Flv-expressing lines under drought stress conditions

Drought stress reduces the carbohydrate production in plants either through reduced CO_2 fixation in consequence of closed stomata or ATP limitation due to inhibition of ATP synthase. The carbohydrate synthesis is vital for the plant's adaptation to drought stress conditions (Živković et al., 2005). The transitory carbon storage form starch is synthesized during the day and acts as a critical energy reserve that changes in response to abiotic stress (Thalmann et al., 2017). Under drought, Flv-expressing lines maintained higher starch levels at the end of day period compared to WT plants (Figure 36B, Figure 37B), demonstrating that Flv-expressing plants retained a higher potential to use starch as energy source for better growth (Thalmann et al., 2017).

The soluble sugars glucose, fructose and sucrose synthesized during photosynthesis are used for the cellular metabolism and growth. Sucrose, which is a disaccharide, is used as a carbon supply throughout the plants (Counce and Gravois, 2006) and acts as osmolyte under stress conditions to maintain turgor pressure and to prevent membrane damage (Couée et al., 2006). As shown in figure 36A, 37A, Flv-expressing lines accumulated lower levels of sucrose than WT plants, suggesting that the major sucrose pool was fed into starch at the end of the day period in transgenic plants (Figure 36B, Figure 37B). Thus, Flv

proteins maintained the normal functioning of photosynthesis that supports the production of carbohydrates.

In plants, an increase in free amino acid levels was observed under stress conditions and also considering protein degradation (Usadel et al., 2008). Amino acid accumulation under stress conditions maintains membrane permeability and ion transport (Rai and Sharma., 1991), and also contributes to the energy source (Hildebrandt et al., 2015). In this study, changes were observed in the amino acids glutamate, proline, GABA (γ-aminobutyric acid) and aspartate (Figure 37, Figure 38, Appendix table 4). Glutamate is considered as the central molecule in amino acid metabolism, and also precursor molecule for chlorophyll synthesis (Yaronskaya et al., 2006). It was higher in Flv3-, Flv1/Flv3-expressing lines (Figure 36D) and also in Flv2-, Flv4-, Flv2/Flv4-expressing lines than in the wild type (Figure 37D). Further, proline accumulates under stress conditions in plants and also acts as an osmolyte (Szabados and Savoure, 2010). In plants Proline synthesis and degradation has a role in the redox buffering and energy transfer were low in Flv1-, Flv3-expressing lines and tend to be low in the Flv2-, Flv4-, Flv2/Flv4-expressing lines (Figure 36E, Figure 37E). GABA derives from glutamate, is also induced under environmental stress conditions (Renault et al., 2010) and acts as signaling component that regulates the malate membrane channels (Ramesh et al., 2015). It was also lower in Flv1-, Flv3-, Flv1/Flv3-expressing lines (Figure 36F) with no apparent changes in Flv2-, Flv4-, Flv2/Flv4-expressing lines (Figure 37F). Moreover, aspartate is one of the primary amino acids of the nitrogen assimilation and also generates energy under stress conditions through lysine catabolism. It was higher in Flv1-, Flv3-, Flv1/Flv3-expressing lines (Figure 36C) and slightly higher in Flv2-, Flv4-, Flv2/Flv4-expressing lines (Figure 37C). The low concentrations of drought-related amino acids proline and GABA suggest that due to a better performance of photosynthetic activity, Flv-expressing lines most likely suffered less from drought. Overall, stress-related amino acids were maintained in Flv-expressing lines suggesting that Flv proteins improves the metabolic activity and thus overcome detrimental effects of drought.

6.4 Adenylate pools under drought stress conditions in Flv-expressing lines

ATP levels in plants play a crucial role in maintaining cellular metabolism for growth and survival under stress conditions. Primarily, the CO_2 availability affects the Calvin cycle efficiency in stressed plants (Sharkey et al., 1982). In chloroplasts, a reduced activity of enzymes in the Calvin cycle imbalances energy production and utilization and induces over-reduction of electron transport chain. By limitation of electron acceptors at PSI, electrons

may leak and use O_2 as final electron acceptor generating ROS. Uncontrolled ROS formation inhibits both photosystems (PSII and PSI) and the ATP synthase complex. As reported earlier, low ATP levels are due to the inhibition of ATP synthesis in stressed plants (Lawlor 1995). In Flv-expressing lines, Flv proteins dissipated excess electrons and prevented the inhibition of ATP synthesis that in turn maintained higher ATP levels (Figure 38A, B). Interestingly, the energy status was higher in all lines of Flv2-, L6 Flv4-expressing lines although the ATP levels were low (Figure 38C, D). In Flv2-, Flv4-, Flv2/Flv4-expressing lines, the Flv proteins function at PSII couldn't establish ΔpH for ATP synthesis compared to Flv1, Flv3, Flv1/Flv3 proteins.

6.5 Redox state of glutathione levels in Flv expressing lines

Glutathione (non-enzymatic antioxidant) is a low molecular weight compound that is involved in several functions in plants and supports the growth, primarily in detoxification of ROS under normal and stress conditions (Foyer and Noctor 2005). Enhanced glutathione levels in plants increases tolerance to multiple stresses (Hasanuzzaman and Fujita 2013), and exogenous application of glutathione (GSH) alleviates plant tolerance to abiotic stress conditions (Chen et al. 2012). The Flv proteins remove excess electrons from ETC that prevent ROS production is an additional protective mechanism in Flv-expressing lines. Low levels of reduced and oxidized forms of GSH and the ratio of GSH: GSSG in Flv1-, Flv3-, Flv1/Flv3-expressing lines (Figure 39A, B, C) indicates Flv proteins enhance stress tolerance whereas in Flv2-, Flv4-, Flv2/Flv4-expressing lines, the GSH levels were high in Flv2 all lines and the GSSG and the ratio of GSH:GSSG are fluctuating. (Figure 39D, E, F). Thus, GSH levels in Flv1-, Flv3-, Flv1/Flv3-expressing lines indicate that these Flv proteins function at PSI prevent ROS formation and enhance stress tolerance.

7. Summary

Efficient utilization of light energy through the photosynthetic machinery is of primary importance for growth, especially under fluctuating light conditions when excess electrons may leak from the electron transport chain and produce ROS. To protect against over-reduction of the electron transport chain, plants evolved various mechanisms to overcome electron acceptor limitations at photosystem (PS) I or II. The non-photochemical quenching (NPQ), which dissipates excess energy acts as 'thermal sink' and photorespiration along with other alternative electron flow (AEF) pathways act as 'electron sinks that dissipate electrons in chloroplasts and thus maintain photosynthesis efficiency. This is also the case under stress conditions in which over-reduction of electron transport chain (ETC) is prevented and photosystems are protected from photoinhibition. With the exception of angiosperms, cyanobacteria and lower plants express specific proteins designated as flavodiiron proteins (FlvA, FlvB or Flv1, Flv2, Flv3, Flv4) to prevent photoinhibition of photosystems under fluctuating environmental conditions. Flv proteins form homo- or heterodimers to exert dioxygen scavenging reactions similar to the water-water cycle in chloroplasts that reduces O_2 to H_2O. The loss of Flv proteins in higher plants might be an evolutionary adaptation.

In this study, introducing cyanobacterial Flv proteins in Arabidopsis chloroplasts Flv1, Flv3 and Flv1/Flv3 functions at photosystem I (PSI) and Flv2, Flv4 and Flv2/Flv4 functions at photosystem II (PSII) resulted in maintenance of the electron transport chain in a more oxidized state. The chlorophyll a fluorescence parameters Fv/Fm, φII, qL, φNPQ, φNO, and NPQ measured during early induction of photosynthesis in Flv1-, Flv3-, Flv1/Flv3- and Flv2-, Flv4-, Flv2/Flv4-expressing lines were higher compared to the wild type, indicating that cyanobacterial Flv proteins are functional in higher plants. The Flv-expressing plants were tested under different light intensities ranging from 50, 150, 300 and 600 µE in soil under short-day conditions to evaluate whether an additional electron dissipating pathway in chloroplast could improve plant growth. Flv-expressing lines that were grown under 150 and 300 µmol photons m^{-2} s^{-1} light intensities showed enhanced aerial biomass. Growth analysis in hydroponic culture with full nutrient solution showed also increased shoot and root biomass in all Flv-expressing lines. Further, Flv-expressing lines grown in long-day conditions revealed increased shoot dry weight and yield. Higher carbohydrate and amino acid levels in Flv expressing lines could be due to higher ATP levels. In addition, changes in reduced and oxidized forms of glutathione resulted in a significant shift of the reduced to oxidized (GSH:GSSG) ratio being lower in all investigated transgenic lines compared to the

ratio of wild type indicating that Flv proteins may be an additive effect to maintain the redox status (Figure. 30).

In general, it turned out that the expression of single genes showed similar effect on the metabolism and plant growth as the combination of both genes. Thus, independent of Flv isoforms, dissipating excess energy in Flv lines through Flv proteins enhanced photosynthesis efficiency that was reflected by increased plant growth.

Flv-expressing lines were also tested under drought stress conditions by withholding water. The results showed that Flv plants enhanced drought tolerance and recovered faster after re-watering. The photosynthetic fluorescence induction curves of φII, qL and φNPQ parameters revealed that Flv proteins partially compensated for the loss of electrons under drought conditions. Compared to the wild type, higher ATP, carbohydrate and amino acid levels in Flv-expressing lines indicated stable metabolic activity of the plants enabling them to survive drought stress to some extent. Another evidence for a better tolerance towards drought was the maintenance of redox status predicted from GSH levels in all investigated transgenic plants in the presence of Flv proteins.

Taken together, the results in this thesis provide strong evidence that Flv proteins in chloroplasts introduce additional electron transfer route for dissipating excess electrons that maintain photosynthesis, enhance plant growth and the associated yield and/or protect plants growing under adverse environmental conditions.

8. Zusammenfassung

Die Nutzung der Lichtenergie durch den photosynthetischen Apparat der Pflanze unter ständig wechselnden Umweltbedingungen ist von größter Bedeutung für das Wachstum und den Ertrag. Um eine effiziente Produktion aufrechtzuerhalten, entwickelten die Pflanzen verschiedene Schutzmechanismen, um die Einschränkungen des Photosystems (PS) I oder II zu überwinden.

Das nicht-photochemische Quenching (NPQ), das überschüssige Energie ableitet, wirkt als "thermischer Sink" und die Photorespiration zusammen mit anderen alternativen Elektronenflusswegen (AEF) als "Elektronen-Sink", der Elektronen in Chloroplasten ableitet und damit die Photosyntheseeffizienz aufrechterhält. Dies gilt auch unter Stressbedingungen, bei denen eine Überreduktion der Elektronentransportkette (ETC) verhindert wird und dadurch die Photosysteme vor Photoinhibition geschützt sind. Mit Ausnahme von Angiospermen exprimieren Cyanobakterien und niedere Pflanzen spezifische Proteine, die als Flavodiironproteine bezeichnet werden (FlvA, FlvB oder Flv1, Flv2, Flv3, Flv4), um die Photoinhibition von Photosystemen unter schwankenden Umweltbedingungen zu verhindern. Flvs-Proteine bilden Homo- oder Heterodimere, um eine sauerstoffabfangende Reaktion ähnlich dem Wasser-Wasser-Kreislauf in Chloroplasten auszuüben, der O_2 zu H_2O reduziert. Der Verlust von Flv-Proteinen in höheren Pflanzen könnte eine evolutionäre Anpassung sein.

In dieser Studie führte die Einführung von cyanobakteriellen Flv-Proteinen (Flv1, Flv3 und Flv1/Flv3 am Photosystem I (PSI) und Flv2, Flv4 und Flv2/Flv4 am Photosystem II (PSII)) in den Arabidopsis-Chloroplasten zur Aufrechterhaltung der Elektronentransportkette in einem höheren oxidierten Zustand. Die Chlorophyll- und Fluoreszenzparameter (Fv/Fm, φII, qL, φNPQ, φNO und NPQ), die während der frühen Induktion der Photosynthese in den Linien Flv1, Flv3, Flv1/Flv3 und Flv2, Flv4, Flv2/Flv4 gemessen wurden, waren höher als im Wildtyp, was darauf hinweist, dass die cyanobakteriellen Flv-Proteine in höheren Pflanzen funktionsfähig sind.

Die Flv-exprimierenden Pflanzen wurden unter verschiedenen Lichtintensitäten von 50, 150, 300 und 600 µE unter Kurztagsbedingungen getestet, um zu untersuchen, ob ein zusätzlicher Elektronensink in Chloroplasten das Pflanzenwachstum verbessern könnte. Flv-Linien, die unter 150 µE und 300 µE Lichtintensität kultiviert wurden, zeigten eine verbesserte Biomasse. Weitere Versuche unter hydroponischen Bedingungen mit Vollmedium erbrachten auch erhöhte Trieb- und Wurzelbiomasse in allen repräsentativen Linien. Darüber hinaus zeigten Flv-Linien, die unter Langtag-Bedingungen angebaut

wurden, ein erhöhtes Trockengewicht und einen höheren Ertrag. Erhöhte Kohlenhydrat- und Aminosäure-Gehalte führten zu höheren ATP-Werten in Flv-Linien. Weiterhin führten Veränderungen in reduzierten und oxidierten Formen von Glutathion zu einer signifikanten Verschiebung des Verhältnisses von reduziert zu oxidiert (GSH:GSSG), das in allen untersuchten transgenen Linien niedriger war als das Verhältnis von Wildtyp, was darauf hindeutet, dass Flv-Proteine mit dem antioxidativen Stoffwechsel konkurrieren könnten, um den Redox-Status aufrechtzuerhalten (Abbildung 40).

Im Allgemeinen stellte sich heraus, dass die Expression einzelner Gene einen ähnlichen Einfluss auf den Stoffwechsel und das Pflanzenwachstum hatte wie die Kombination beider Gene. So wird unabhängig von Flv-Isoformen überschüssige Energie in Flv-Linien durch Flv-Proteine abgebaut und die Effizienz der Photosynthese verbessert, was sich in einem erhöhten Pflanzenwachstum widerspiegelt.

Flv-exprimierende Linien wurden auch unter Trockenstressbedingungen getestet, indem Wasser-Mangel erzeugt wurde. Die Ergebnisse zeigten, dass Flv-Pflanzen die Trockenheitstoleranz erhöhen und sich nach der Wässerung schneller erholen. Die photosynthetischen Fluoreszenzinduktionskurven der Parameter φII, qL und φNPQ zeigten, dass Flv-Proteine den Verlust von Elektronen unter Trockenheitsbedingungen teilweise kompensierten. Im Vergleich zum Wildtyp zeigten höhere ATP-Werte, Kohlenhydrate und Aminosäuren-Levels in Flv-Expressionslinien eine stabile Stoffwechselaktivität der Pflanzen, die es ihnen ermöglichte, Trockenstress bis zu einem gewissen Grad zu überstehen. Ein weiterer Beweis für eine bessere Toleranz gegenüber Trockenstress war die Aufrechterhaltung des Redox-Status bei allen untersuchten transgenen Pflanzen in Gegenwart von Flv-Proteinen.

Zusammengenommen liefern die Ergebnisse in dieser Arbeit starke Beweise dafür, dass Flv-Proteine den Verlust von dissipierenden Elektronen teilweise kompensieren und somit das Pflanzenwachstum und den damit verbundenen Ertrag verbessern und/oder Pflanzen unter widrigen Umweltbedingungen schützen können.

9. Literature

Ahkami AH, Melzer M, Ghaffari MR, Pollmann S, Ghorbani Javid M, Shahinnia F, Druege U and Hajirezaei MR. 2013. Distribution of indole-3-acetic acid in Petunia hybrida shoot tip cuttings and relationship between auxin transport, carbohydrate metabolism and adventitious root formation. *Planta* **238**(3): 499-517.

Ahmad N, Michoux F and Nixon PJ. 2012. Investigating the production of foreign membrane proteins in tobacco chloroplasts: expression of an algal plastid terminal oxidase. *PLoSONE* **7**: e41722.

Ahmed S, Nawata E, Hosokawa M, Domae Y and Sakuratani T. 2002. Alterations in photosynthesis and some antioxidant enzymatic activities of mungbean subjected to waterlogging. *Plant Sci.* **163**: 117–123.

Allahverdiyeva Y, Isojärvi J, Zhang P, Aro EM. 2015b. Cyanobacterial oxygenic photosynthesis is protected by flavodiiron proteins. *Life* **5**: 716-743.

Allahverdiyeva Y, Mustila H, Ermakova M, Bersanini L, Richaud P, Ajlani G, Battchikova N, Cournac L, Aro EM. 2013. Flavodiiron proteins Flv1 and Flv3 enable cyanobacterial growth and photosynthesis under fluctuating light. *Proc. Natl. Acad. Sci. USA* **110**: 4111–4116.

Allahverdiyeva Y, Suorsa M, Tikkanen M and Aro EM. 2015a. Photoprotection of photosystems in fluctuating light intensities. *J. Exp. Bot*. **66**: 2427–2436.

Allen JF. 2002. Photosynthesis of ATP-Electrons, Proton Pumps, Rotors, and Poise. *Cell* **110**: 273–276.

Aluru MR, Yu F, Fu AG, Rodermel S. 2006. Arabidopsis variegation mutants: new insights into chloroplast biogenesis. J Exp Bot. **57**(9): 1871-81.

Anderson JM and Andersson B. 1988. The dynamic photosynthetic membrane and regulation of solar energy conversion. *Trends in biochemical sciences* **13**: 351-355.

Asada K, Heber U, Schreiber U. 1993. Electron flow to the intersystem chain from stromal components and cyclic electron flow in maize chloroplasts, as detected in intact leaves by monitoring redox change of P700 and chlorophyll fluorescence. *Plant Cell Physiol*. **34**: 39–50.

Asada K. 1999. THE WATER-WATER CYCLE IN CHLOROPLASTS: Scavenging of Active Oxygens and Dissipation of Excess Photons. *Annu Rev Plant Physiol Plant* Mol Biol. **50**: 601–639.

Ashraf M, Harris PJC. 2013. Photosynthesis under stressful environments: An overview. Photosynthetica. **51**: 163–190.

Atkin OK, Macherel D. 2009. The crucial role of plant mitochondria in orchestrating drought tolerance, *Annals of Botany* **103**: 581-597.

Avenson TJ, Cruz JA, Kanazawa A. and Kramer DM. 2005a. Regulating the proton budget of higher plant photosynthesis. *Proc Natl Acad Sci USA*. **102:** 9709–9713.

Badawia GH, Kawanoa N, Yamauchia Y, Shimadaa E, Sasakia R, Kubo A and Tanakaa K. 2004. Over-expression of ascorbate peroxidase in tobacco chloroplasts enhances the tolerance to salt stress and water deficit. *Physiologia Plantarum* **121**: 231–238.

Bailleul B, Berne N, Murik O, Petroutsos D, Prihoda J, Tanaka A et al. 2015. Energetic coupling between plastids and mitochondria drives CO2 assimilation in diatoms. *Nature* **524**: 366–369.

Baker NR. 2008. Chlorophyll fluorescence: a probe of photosynthesis in vivo. *Annu. Rev. Plant Biol.* **59**: 89-113.

Baniulis D et al. **2008**. Structure–function of the cytochrome b_6f complex. *Photochem. Photobiol*. **84**: 1349–1358.

Bauwe H, Hagemann M, Fernie AR. 2010. Photorespiration: players, partners and origin. *Trends in Plant Science* **15**: 330–336.

Bendall DS, Manasse RS. 1995. Cyclic photophosphorylation and electron transport. Biochim. Biophys. Acta. **1229**: 23-38.

Bersanini L, Battchikova N, Jokel M, Rehman A, Vass I, Allahverdiyeva Y, Aro EM. 2013. Flavodiiron protein Flv2/Flv4-related photoprotective mechanism dissipates excitation pressure of photosystem II in cooperation with phycobilisomes in cyanobacteria. *Plant Physiol.* **164**: 805–818.

Blankenship RE. **2013**. Molecular Mechanisms of Photosynthesis. John Wiley & Sons.

Boldt R, Edner C, Kolukisaoglu U, Hagemann M, Weckwerth W, Wienkoop S, Morgenthal K and Bauwe H. 2005. D-GLYCERATE 3-KINASE, the last unknown enzyme in the photorespiratory cycle in Arabidopsis, belongs to a novel kinase family. *The Plant Cell* **17**: 2413–2420.

Bonardi V, Pesaresi P, Becker T, Schleiff E, Wagner R, Pfannschmidt T, Leister D. 2005. Photosystem II core phosphorylation and photosynthetic acclimation require two different protein kinases. *Nature* **437**: 1179– 1182.

Bowyer JR, Camilleri P and Vermaas WFJ. 1991. Photosystem II and its interaction with herbicides. In Herbicides. Edited by Baker, NR and Percival MP. **10**: 27-85. *Elsevier Science Publishers*, Amsterdam.

Cape JL et al. 2006. Understanding the cytochrome bc complexes by what they don't do. The Q-cycle at 30. *Trends Plant Sci*. **11**: 46–55.

Carol P, Stevenson D, Bisanz C, Breitenbach J, Sandmann G, Mache R, Coupland G, Kuntz M. 1999. Mutations in the Arabidopsis gene *IMMUTANS* cause a variegated phenotype by inactivating a chloroplast terminal oxidase associated with phytoene desaturation. The *Plant Cell* **11**: 57–68.

Carpentier R, LaRue B, Leblanc RM. 1984. Photoacoustic spectroscopy of *Anacystis nidulans*: III. Detection of photosynthetic activities. *Arch*. *Biochem. Biophys*. **228**: 534–543.

Carraretto L, Teardo E, Checchetto V, Finazzi G, Uozumi N & Szabo I. 2016. Ion Channels in Plant Bioenergetic Organelles, Chloroplasts and Mitochondria: From Molecular Identification to Function. *Mol Plant* **9**: 371–395.

Carrari F, Coll-Garcia D, Schauer N, Lytovchenko A, Palacios-Rojas N, Balbo I et al. 2005. Deficiency of a plastidial adenylate kinase in *Arabidopsis* results in elevated photosynthetic amino acid biosynthesis and enhanced growth. *Plant Physiol.* **137**: 70–82.

Cassier-Chauvat C, Chauvat F. 2014. Function and regulation of ferredoxins in the cyanobacterium, Synechocystis PCC 6803: recent advances. *Life* **4**: 666-680.

Chaux F, Peltier G, Johnson X. 2015. A security network in PSI photoprotection: regulation of photosynthesis control, NPQ and O_2 photoreduction by cyclic electron flow. *Front. Plant Sci.* **6**: 875.

Chaves MM. 1991. Effects of water deficits on carbon assimilation. *J. Exp. Bot.* **42**: 1–16.

Chen JH, Jiang HW, Hsieh EJ, Chen HY, Chien CT, Hsieh HL, Lin TP. 2012. Drought and salt stress tolerance of an *Arabidopsis* glutathione *S*-transferase U17 knockout mutant are attributed to the combined effect of glutathione and abscisic acid. *Plant Physiol.* **158**: 340–351.

Chen M and Blankenship RE. 2011. Expanding the solar spectrum used by photosynthesis. *Trends Plant Sci.* **16**: 427–431.

Chen YE, Liub WJ, Suc YQ, Cuia JM, Zhangd ZW, Yuana M, Zhanga HY and Yuand S. 2016. Different response of photosystem II to short and long-term drought stress in Arabidopsis thaliana. *Physiologia Plantarum* **158**: 225–235.

Clough SJ and Bent AF. 1998. Floral dip: a simplified method for Agrobacterium mediated transformation of *Arabidopsis thaliana*. *Plant J*. **16**: 735–743.

Colombo M, Suorsa M, Rossi F, Ferrari R, Tadini L, Barbato R and Pesaresi P. 2016. Photosynthesis Control: An underrated short-term regulatory mechanism essential for plant viability. *Plant Signaling & Behavior* **11**: e1165382.

Cotton CA, Douglass JS, De Causmaecker S, Brinkert K, Cardona T, Fantuzzi A. et al. 2015. Photosynthetic constraints on fuel from microbes. *Front. Bioeng. Biotechnol*. **3**: 36.

Couée I, Sulmon C, Gouesbet G, Amrani AEI. 2006. Involvement of soluble sugars in reactive oxygen species balance and responses to oxidative stress in plants. *J. Expt. Bot.* **57**: 449–459.

Counce PA, Gravois KA. 2006. Sucrose synthase activity as a potential indicator of high rice grain yield. *Crop Sci.* **46**:1501–1507.

Cramer WA et al. 2011. The Q cycle of cytochrome bc complexes: a structure perspective. *Biochim. Biophys. Acta*. **1807**: 788–802.

Crofts AR and Wraight CA. 1983. The electrochemical domain of photosynthesis. *Biochim. Biophys.* Ada **726**: 149-185.

Crofts AR, Barquera B, Gennis RB, Kuras R, Guergova-Kuras M and Berry EA. 1999. Mechanism of Ubiquinol Oxidation by the bc1 Complex: Different Domains of the Quinol Binding Pocket and Their Role in the Mechanism and Binding of Inhibitors. *Biochemistry* **38**: 15807–15826.

Cruz de Carvalho MH. 2008. Drought stress and reactive oxygen species: production, scavenging and signaling. *Plant Signalling and Behaviour* **3**: 156–165.

DalCorso G, Pesaresi P, Masiero S, Aseeva E, Schünemann D, Finazzi G, Leister D. 2008. A Complex Containing PGRL1 and PGR5 Is Involved in the Switch between Linear and Cyclic Electron Flow in Arabidopsis. *Cell* **132**: 273–285.

Dang KV, Plet J, Tolleter D, Jokel M, Cuiné S, Carrier P, Auroy P, Richaud P, Johnson X, Alric J, Allahverdiyeva Y, Peltier G. 2014. Combined Increases in Mitochondrial Cooperation and Oxygen Photoreduction Compensate for Deficiency in Cyclic Electron Flow in Chlamydomonas reinhardtii. *The Plant Cell* **26**: 3036-50.

Davis GA, Kanazawa A, Schöttler MA, Kohzuma K, Froehlich JE, Rutherford AW, Sayre R. 2016. Limitations to photosynthesis by proton motive forceinducedphotosystem II photodamage. *eLife,* **5**: 27–39.

Dekker JP and Boekema EJ. 2005. Supramolecular organization of thylakoid membrane proteins in green plants. *Biochim. Biophys. Acta.* **1706**: 12–39.

Demmig-Adams B, Adams WW III 1992. Carotenoid composition in sun and shade leaves of plants with different life forms. Plant Cell Environ. **15**: 411–419.

Demmig-Adams B. 1998. Survey of thermal energy dissipation and pigment composition in sun and shade leaves. Plant Cell Physiol. **39**: 474–482.

Demmig-Adams B, Garab G, William Adams III, Govindgee. 2014. Non-photochemical quenching and energy dissipation in plants, algae and cyanobacteria. *Advances in Photosynthesis and Respiration* **40**: Springer Science+Business Media Dordrecht.

Dreher F, Modjtahedi BS, Modjtahedi SP, Maibach HI. 2005. Quantification of stratum corneum removal by adhesive tape stripping by total protein assay in 96-well microplates. *Skin Research and Technology* 11: 97 – 101. *Ecotoxicology.* **22**(3): 584-96.

Eisenhut M, Aguirre von Wobeser E, Jonas L, Schubert H, Ibelings BW, Bauwe H et al. 2007. Long-term response toward inorganic carbon limitation in wild type and glycolate turnover mutants of the cyanobacterium *Synechocystis* sp. strain PCC 6803. *Plant Physiol.* **144**: 1946–1959.

Emlyn-Jones D, Ashby MK, Mullineaux CW. 1999. A gene required for the regulation of photosynthetic light harvesting in the cyanobacterium *Synechocystis* 6803. *Mol Microbiol*. **33**: 1050–1058.

Fan DY, Nie Q, Hope AB, Hillier W, Pogson BJ, Chow WS. 2007. Quantification of cyclic electron flow around Photosystem I in spinach leaves during photosynthetic induction. *Photosynth Res.* **94**: 347.

Farooq M, Wahid A, Kobayashi N, Fujita D and Basra SMA. 2009. Plant drought stress: effects, mechanisms and management. *Agron. Sustain. Dev*. **29**: 185–212.

Fernandez AP, Strand A. 2008. Retrograde signaling and plant stress: plastid signals initiate cellular stress responses. *Curr. Opin. Plant Biol.* **11**: 509–513.

Finazzi G, Barbagallo RP, Bergo E, Barbato R, Forti G. 2001. Photoinhibition of Chlamydomonas reinhardtii in State 1 and State 2: Damages to the photosynthetic apparatus under linear and cyclic electron flow. *J Biol Chem.* **276**(25): 22251–22257.

Flexas J, Bota J, Loreto F, Cornic G, Sharkey TD. 2004. Diffusive and metabolic limitations to photosynthesis under drought and salinity in C3 plants. *Plant Biology* **6**: 269-279.

Flexas J, Galmes J, Ribas-Carbo M, Medrano H. Lambers H, Ribas-Carbo M. 2005. The effects of water stress on plant respiration, Plant respiration: from cell to ecosystem, Dordrecht Springer-Verlag 85-94.

Flexas J, Ribas-Carbó M, Bota J, Galmés J, Henkle M, Martínez-Cañellas S, Medrano H. 2006. Decreased Rubisco activity during water stress is not induced by decreased relative water content but related to conditions of low stomatal conductance and chloroplast CO2concentration. *New Phytologist* **172**: 73-82.

Foudree A, Putarjunan A, Kambakam S, Nolan T, Fussell J, Pogorelko G and Rodermel S. 2012. The mechanism of variegation in immutans provides insight into chloroplast biogenesis. Front. *Plant Sci*. **3**: 260.

Foyer CH, Noctor G. 2005. Redox homeostasis and antioxidant signaling: a metabolic interface between stress perception and physiological responses. *The Plant Cell* **17**: 1866–1875.

Franziska F, Timm S, Arrivault S, Florian A, Stitt M, Fernie AR, Bauwe H. 2017. The Photorespiratory Metabolite 2-Phosphoglycolate Regulates Photosynthesis and Starch Accumulation in Arabidopsis. *The Plant Cell* **29**: 2537–2551

Garg BK, Kathju S and Burman U. 2001. Influence of water stress on water relations, photosynthetic parameters and nitrogen metabolism of moth bean genotypes. *Biol. Plant.* **44**: 289–292.

Geigenberger P, Riewe D, Fernie AR. 2010. The central regulation of plant physiology by adenylates. *Trends Plant Sci.* **15**: 98–105.

Geigenberger P, Fernie AR. 2011. Metabolic control of redox and redox control of metabolism in plants. *Antiox. Redox Signal.* **21**: 1389–1421.

Geiger DR and Servaites JC. 1994. Diurnal regulation of photosynthetic carbon metabolism in C3 plants. Annu. Rev. Plant Physiol. *Plant Mol. Biol.* **45**: 235–256.

Gerotto C, Alboresi A, Meneghesso A, Jokel M, Suorsa M, Aro EM, Morosinotto T. 2016. Flavodiiron proteins act as safety valve for electrons in *Physcomitrella patens*. Proc Natl Acad Sci USA **113**: 12322–12327.

Ghaffari MR, Shahinnia F, Usadel B, Junker B, Schreiber F, Sreenivasulu N and Hajirezaei MR. 2016. The metabolic signature of biomass formation in barley. *Plant Cell Physiol*. **57**: 1943-1960.

Gietl C. 1992. Malate dehydrogenase isoenzymes: cellular locations and role in the flow of metabolites between the cytoplasm and cell organelles. *Biochim Biophys Acta* **1100**: 217–234.

Gómez R, Carrillo N, Morelli MP, Tula S, Shahinnia F, Hajirezaei MR and Lodeyro AF. 2018. Faster photosynthetic induction in tobacco by expressing cyanobacterial flavodiiron proteins in chloroplasts. *Photosynth Res.* **136**: 129–138.

Goncalves VL, Saraiva LM, Teixeira M. 2011. Gene expression study of the flavodiiron proteins from the cyanobacterium *Synechocystis* sp. PCC 6803. *Biochem. Soc. Trans.* **39**: 216–218.

Govindjee and Coleman W. 1990. How does photosynthesis make oxygen? *Scientific American* **262**: 50–58.

Graf A, Smith AM. 2011. Starch and the clock: the dark side of plant productivity. *Trends Plant Sci.* **16**: 169–175.

Gu JF, Zhou ZX, Li ZK, Chen Y, Wang ZQ and Zhang H. 2017. Rice (*Oryza sativa* L.) with reduced chlorophyll content exhibit higher photosynthetic rate and efficiency, improved canopy light distribution, and greater yields than normally pigmented plants. *Field Crop Res*. **200**: 58–70.

Haink G, Deussen A. 2003. Liquid chromatography method for the analysis of adenosine compounds. *J. Chromatogr.* **784**: 189–193.

Hanawa H, Ishizaki K, Nohira K, Takagi D, Shimakawa G, Sejima T, Shaku K, Makino A, Miyake C. 2017. Land plants drive photorespiration as higher electron-sink: comparative study of post-illumination transient O_2-uptake rates from liverworts to angiosperms through ferns and gymnosperms. *Physiol Plant.* **161**(1):138-149.

Hasanuzzaman M, Fujita M. 2013. Exogenous sodium nitroprusside alleviates arsenic-induced oxidative stress in wheat (Triticum aestivum L.) seedlings by enhancing antioxidant defense and glyoxalase system. *Ecotoxicology*. **22**: 584–596.

Hasunuma T, Matsuda M, Senga Y, Aikawa S, Toyoshima M, Shimakawa G, Miyake C and Kondo A. 2014. Overexpression of flv3 improves photosynthesis in the cyanobacterium Synechocystis sp. PCC6803 by enhancement of alternative electron flow. *Biotechnology for Biofuels* **7**: 493.

Helman Y, Tchernov D, Reinhold L, Shibata M, Ogawa T, Schwarz R, Ohad I, Kaplan A. 2003. Genes encoding A-type flavoproteins are essential for photoreduction of O2 in cyanobacteria. *Curr. Biol.* **13**: 230–235.

Herbert SK, Fork DC, Malkin S. 1990. Photoaccoustic measurements *in vivo* of energy storage by cyclic electron flow in algae and higher plants. *Plant Physiol*. **94**: 926–934.

Hertle AP, Blunder T, Wunder T, Pesaresi P, Pribil M, Armbruster U & Leister D. 2013. PGRL1 Is the Elusive Ferredoxin-Plastoquinone Reductase in PhotosyntheticCyclic Electron Flow. *Molecular Cell* **49**: 511–523.

Heyno E, Innocenti G, Lemaire SD, Issakidis-Bourguet E, KriegerLiszkay A. 2014. Putative role of the malate valve enzyme NADP–malate dehydrogenase in H_2O_2 signalling in Arabidopsis. *Philos. Trans R Soc Lond B Biol Sci.* **369**: 20130228.

Heyno E,Gross CM, Laureau C, Culcasi M, Pietri S and Krieger- Liszkay A. 2009. Plastid alternative oxidase (PTOX) promotes oxidative stress when overexpressed in tobacco. *J.Biol.Chem.* **284**: 31174–31180.

Hildebrandt TM, Nunes Nesi A, Arau´ jo WL and Braun HP. 2015. Amino Acid Catabolism in Plants. *Mol. Plant.* **8**: 1563–1579.

Hillman F, Fischer RJ, Caranto JD, Mot A, Kurtz DM, Bahl H. 2009. Reductive dioxygen scavenging of flavodiiron proteins of Clostridium acetobutylicum. *FEBS Lett* **583**: 241-245.

Holsters M, de Waele D, Depicker A, Messens E, van Montagu M, Schell J. 1978. Transfection and transformation of Agrobacterium tumefaciens. Mol Gen Genet. **163**:181-187.

Ilík P, Pavlovič A, Kouřil R, Alboresi A, Morosinotto T, Allahverdiyeva Y, Shikanai T. 2017. Alternative electron transport mediated by flavodiiron proteins is operational in organisms from cyanobacteria up to gymnosperms. *New Phytologist* **214**: 967–972.

Igamberdiev AU, Gardeström P. 2003. Regulation of NAD- and NADP-dependent isocitrate dehydrogenases by reduction levels of pyridine nucleotides in mitochondria and cytosol of pea leaves. *Biochim. Biophys. Acta.* **1606**: 117–125.

Jansson S. 1999. A guide to the *Lhc* genes and their relatives in *Arabidopsis*. **Trends Plant Sci**. **4**: 236–240.

Jin HL, Li MS, Duan SJ, Fu M, Dong XX, Liu B. et al. 2016. Optimization of light-harvesting pigment improves photosynthetic efficiency. *Plant Physiol*. **172**: 1720–1731.

Kebeish R, Niessen M, Thiruveedhi K, Bari R, Hirsch HJ, Rosenkranz R, Stäbler N, Schönfeld B, Kreuzaler F, Peterhänsel C. 2007. Chloroplastic photorespiratory bypass increases photosynthesis and biomass production in Arabidopsis thaliana. *Nat Biotechnol*. **25**: 593–599.

Kirst H, Formighieri C, Melis A. 2014. Maximizing photosynthetic efficiency and culture productivity in cyanobacteria upon minimizing the phycobilisome light-harvesting antenna size. *Biochim Biophys Acta Bioenerg* **1837**: 1653–1664.

Kirst H, Stephane TG, Niyogi KK, Lemaux PG, Melis A. 2017. Photosynthetic antenna engineering to improve crop yields. *Planta* **245**: 1009-1020.

Kozaki A. & Takeba G. 1996. Photorespiration protects C3 plants from photooxidation. *Nature* **384**: 557-560.

Kramer DM, Cruz JA, & Kanazawa A. 2003. Balancing the central roles of the thylakoid proton gradient. *Trends in Plant Science* **8**: 27–32.

Kramer DM, Johnson G, Kiirats O, Edwards GE. 2004. New fluorescence parameters for the determination of Q A redox state and excitation energy fluxes. *Photosynth Res.* **79**: 209–218.

Kraner ME, Link K, Melzer M, Ekici AB, Uebe S, Tarazona P et al. 2017. Choline transporter-like1 (CHER1) is crucial for plasmodesmata maturation in Arabidopsis thaliana. *Plant J.* **89**: 394–406.

Krapp A, Hofmann B, Schäfer C, Stitt M. 1993. Regulation of the expression of rbcS and other photosynthetic genes by carbohydrates: a mechanism for the 'sink regulation' of photosynthesis? *The Plant Journal* **3**: 817–828.

Kromdijk J, Glowacka K, Leonelli L, Gabilly ST, Iwai M, Niyogi KK. 2016. Improving photosynthesis and crop productivity by accelerating recovery from photoprotection. *Science* **354**: 857–861.

Kuhlgert S, Austic G, Zegarac R, Osei-Bonsu I, Hoh D, Chilvers MI, Roth MG, Bi K, TerAvest D, Weebadde P. 2016. MultispeQ Beta: a tool for large-scale plant phenotyping connected to the open PhotosynQ network. *Royal Soc Open Sci.* **3**: 160592.

Laureau C, De Paepe R, Latouche G, Moreno-Chacon M, Finazzi G, Kuntz M, Cornic G, Streb P. 2013. Plastid terminal oxidase (PTOX) has the potential to act as a safety valve for excess excitation energy in the alpine plant species Ranunculus glacialis L. *Plant Cell Environ*. **36**: 1296-1310.

Lawlor DW, Tezara W. 2009. Causes of decreased photosynthetic rate and metabolic capacity in water-deficient leaf cells: a critical evaluation of mechanisms and integration of processes. *Annals of Botany* **103**: 561–579.

Lawlor DW. 2002. Carbon and nitrogen assimilation in relation to yield: mechanisms are the key to understanding production systems. *J. Exp. Bot.* **53**: 773–787.

Lawlor DW. 2002. Limitations to photosynthesis in water-stressed leaves: stomatal vs metabolism and the role of ATP. *Annals of Botany* **89**: 871–885.

Lawlor DW.1995. In Environment and Plant Metabolism (ed. Smirnoff, N.) 129–160 (Bios Scientific, Oxford.

Lehtimaki N, Lintala M, Allahverdiyeva Y, Aro EM, Mulo P. 2010. Drought stress-induced upregulation of components involved in ferredoxin-dependent cyclic electron transfer. *J. Plant Physiol.* **167**: 1018–1022.

Lennon AM, Prommeenate P, Nixon PJ. 2003. Location, expression and orientation of the putative chlororespiratory enzymes, ndh and immutans, in higher-plant plastids. Planta **218**: 254–260.

Leonardos ED, Savitch LV, Huner NPA, O¨ quist G, Grodzinski B. 2003. Daily photosynthetic and C-export patterns in winter wheat leaves during cold stress and acclimation. *Physiol Plant.* **117**: 521–531.

Levitt J. 1980. Responses of Plants to Environmental Stresses. **Vol 2**. Water, Radiation, Salt and other Stresses.Academic Press, New York, 93–128.

Li XP, Muller-Moule P, Gilmore AM, Niyogi KK. 2002. PsbS-dependent enhancement of feedback de-excitation protects photosystem II from photoinhibition. *Proc Natl Acad Sci USA* **99**: 15222–7.

Li Z, Wakao S, Fischer BB, Niyogi KK. 2009. Sensing and responding to excess light. *Annu Rev Plant Biol*. **60**: 239–260.

Logemann J, Shell J, Willmitzer L. 1987. Improved method for the isolation of RNA from plant tissues, *Anal Biochem.* **20**: 16–20.

Long SP, Humphries S, Falkowski PG. 1994. Photoinhibition of photosynthesis in nature. *Annu. Rev. Plant Biol.* **45**: 633–662.

Long SP, Zhu XG, Naidu SL, Ort DR. 2006. Can improvement in photosynthesis increase crop yields? *Plant Cell Physiol*. **29**: 315–330.

Long TA, Okegawa Y, Shikanai T, Schmidt GW, Covert SF. 2008. Conserved role of proton gradient regulation 5 in the regulation of PSI cyclic electron transport. *Planta* **228**: 907–918.

Ludwig J and Canvin DT. 1971. The rate of photorespiration during photosynthesis and the relationship of the substrate of light respiration to the products of photosynthesis in sunflower leaves. *Plant Physiol.* **48:** 712–719.

Lunde C, Jensen PE, Rosgaard L, Haldrup A, Gilpin MJ and Scheller HV. 2003. Plants impaired in state transitions can to a large degree compensate for their defect. *Plant Cell Physiol.* **4444**–54.

Lvanov AG, Rosso D, Savitch LV, Stachula P, Rosembert M, Oquist G, Hurry V, Huner NP. 2012. Implications of alternative electron sinks in increased resistance of PSII and PSI photochemistry to high light stress in cold-acclimated Arabidopsis thaliana. Photosynth. Res. **113**: 191-206.

Maier A, Fahnenstich H, von Caemmer S, Engqvist MKM, Weber APM, Flügge U-I, Maurino VG . 2012. Transgenic introduction of a glycolate oxidative cycle into A. thaliana chloroplasts leads to growth improvement. Frontiers in Plant Science **3**: 1–12.

Matthew J. Paul Till K. Pellny. 2003. Carbon metabolite feedback regulation of leaf photosynthesis and development. *J Exp Bot.* **54**(382): 539–547.

Matsubara S, Krause GH, Seltmann M, Virgo A, Kursar TA, Jahns P, Winter K. 2008. Lutein epoxide cycle, light harvesting and photoprotection in species of the tropical tree genus Inga. Plant Cell Environ. **31**: 548–561.

Maurino VG, Engqvist MK. 2015. 2-Hydroxy acids in plant metabolism. *Arabidopsis Book* **13**:e0182.

Maxwell PC, Biggins J. 1976. Role of cyclic electron transport in photosynthesis as measured by the photoinduced turnover of P_{700} in vivo, *Biochemistry* **15**: 3975–398.

Mayta ML, Lodeyro AF, Guiamet JJ, Tognetti VB, Melzer M, Hajirezaei MR and Carrillo N. 2018. Expression of a Plastid-Targeted Flavodoxin Decreases Chloroplast Reactive Oxygen Species Accumulation and Delays Senescence in Aging Tobacco Leaves, *Front. Plant Sci*. **17.**

Mehler AH. 1951. Studies on reactions of illuminated chloroplasts. *Archives of Biochemistry and Biophysics* **33**: 65–77.

Meister A. 1995. Glutathione biosynthesis and its inhibition. *Methods in Enzymology* **252**: 26–39.

Melis A, Neidhardt J, Benemann JR. 1999. Dunaliella salina (Chlorophyta) with small chlorophyll antenna sizes exhibit higher photosynthetic productivities and photon use efficiencies than normally pigmented cells. *J Appl Phycol.* **10**: 515–525.

Minagawa J. 2011. State transitions—the molecular remodeling of photosynthetic supercomplexes that controls energy flow in the chloroplast. *Biochim Biophys Acta.* **1807**(8): 897–905.

Mitchell P. 1966. Chemiosmotic coupling in oxidative and photosynthetic phosphorylation. *Biol. Rev.* **41**: 445–502.

Mitchell PJ. 1976. Possible molecular mechanisms of the proton motive function of cytochrome systems. *Theor. Biol*. **62:** 327–367.

Miyake C & Asada K. 1992. Thylakoid-Bound Ascorbate Peroxidase in Spinach Chloroplasts and Photoreduction of Its Primary Oxidation Product Monodehydroascorbate Radicals in Thylakoids. *Plant and Cell Physiology* **33**: 541–553.

Mulkidjanian AY. 2010. Activated Q-cycle as a common mechanism for cytochrome bc1 and cytochrome $b_6f$complexes. *Biochim. Biophys. Acta*.**17971**: 858–1868.

Müller P, Li XP, Niyogi KK. 2001. Non-photochemical quenching. A response to excess light energy. *Plant Physiol.* **125**: 1558–1566.

Mullineaux CW and Daniel Emlyn-Jones. 2004. State transitions: an example of acclimation to low-light stress. *J Exp Bot.* **56**: 411.

Munekage Y, Hashimoto M, Miyake C, Tomizawa KI, Endo T, Tasaka M & Shikanai T. 2004. Cyclic electron flow around photosystem I is essential for photosynthesis. *Nature*, **429**: 579–582.

Munekage Y, Hojo M, Meurer J, Endo T, Tasaka M & Shikanai T. 2002. PGR5 Is Involved in Cyclic Electron Flow around Photosystem I and Is Essential for Photoprotection in Arabidopsis. *Cell* **110**: 361–371.

Murata N. 1969. Control of excitation transfer in photosynthesis I. Light-induced change of chlorophyll a fluoresence in Porphyridium cruentum. *Biochimica et Biophysica Acta (BBA) – Bioenergetics* **172**: 242–251.

Mussgnug JH, Thomas-Hall S, Rupprecht J, Foo A, Klassen V, McDowall A, Schenk PM, Kruse O, Hankamer B. 2007. Engineering photosynthetic light capture: impacts on improved solar energy to biomass conversion. *Plant Biotechnol J* **5**: 802–814.

Mustila H, Paananen P, Battchikova N, Santana-Sánchez A, Muth-Pawlak D, Hagemann M, Aro EM. and Allahverdiyeva Y. 2016. The Flavodiiron Protein Flv3 Functions as a Homo-Oligomer during Stress Acclimation and is Distinct from the Flv1/Flv3 Hetero-Oligomer Specific to the O2 Photoreduction Pathway. *Plant Cell Physiol.* **57**(7): 1468–1483.

Nakajima Y, Tsuzuki M, Ueda R. 2001. Improved productivity by reduction of the content of light-harvesting pigment in *Chlamydomonas perigranulata*. *J Appl Phycol.* **13**: 95–101.

Nakajima Y, Ueda R. 1997. Improvement of photosynthesis in dense microalgal suspension by reduction of light harvesting pigments. *J Appl Phycol.* **9**: 503–510.

Nakajima Y, Ueda R. 1999. Improvement of microalgal photosynthetic productivity by reducing the content of light harvesting pigments. *J Appl Phycol***. 11**: 195–201.

Nandha B, Finazzi G, Joliot P, Hald S, Johnson GN. 2007. The role of PGR5 in the redox poising of photosynthetic electron transport. *Biochim Biophys Acta* **1767**: 1252–1259.

Nawrocki WJ, Tourasse NJ, Taly A, Rappaport F and Wollman FA. 2015. The plastid terminal oxidase: its elusive function points to multiple contributions to plastid physiology. Annu. Rev. Plant Biol. **66:** 49–74.

Nishio JN, and Whitmarsh J. 1993. Dissipation of the Proton Electrochemical Potential in Intact Chloroplasts (II. The pH Gradient Monitored by Cytochrome f Reduction Kinetics). *Plant Physiol.* **101**: 89–96.

Niyogi KK, and Truong TB. 2013. Evolution of flexible non-photochemical quenching mechanisms that regulate light harvesting in oxygenic photosynthesis. *Current Opinion in Plant Biology* **16**: 307–314.

Niyogi KK, Li XP, Rosenberg V, Jung HS. 2005. Is PsbS the site of non-photochemical quenching in photosynthesis. *J Exp Bot.* **56** (411): 375–382.

Nugent J (ed.) 2001. Photosynthetic water oxidation. *Biochimica et Biophysica Acta* **1503**: 1–259.

Ogawa T. 1991. A gene homologous to the subunit-2 gene of NADH dehydrogenase is essential to inorganic carbon transport of Synechocystis PCC6803. *Proc Natl Acad Sci USA* **88**: 4275–9.

Ort DR & Baker NR. 2002. A photoprotective role for O2 as an alternative electron sink in photosynthesis? *Current Opinion in Plant Biology* **5**: 193–198.

Ort DR & Yocum CF. 1996. In Oxygenic Photosynthesis: The Light Reactions, ed. Yocum CF. Kluwe, Dordrecht, The Netherlands: 1-9.

Ort DR, Merchant SS, Alric J, Barkan A, Blankenship RE, Bock R. et al. 2015. Redesigning photosynthesis to sustainably meet global food and bioenergy demand *Proc Natl Acad Sci USA* **112**: 8529–8536.

Osmond CB & Grace SC. 1995. Perspectives on photoinhibition and photorespiration in the ¢eld: quintessential ine¤ciencies of the light and dark reactions of photosynthesis? *J. Exp. Bot.* **46**: 1351-1362.

Osmond CB, Badger M, Maxwell K, BjÎrkman O & Leegood RC. 1997. Too many photons: photorespiration, photoinhibition and photooxidation. *Trends Plant Sci.* **2**: 119-121.

Osmond CB. 1981. Photorespiration and photoinhibition. Some implications for the energetics of photosynthesis. *Biochim. Biophys. Acta* **639**: 77-98.

Pakrasi HB and Vermaas WFJ. 1992. Protein engineering of photosystem II. In The Photosystems: Structure, Function and Molecular Biology. Edited by Barber, J. **11**: 231-258. *Elsevier Science Publishers*, Amsterdam.

Pathi KM, Tula S and Tuteja N. 2013. High frequency regeneration via direct somatic embryogenesis and efficient *Agrobacterium*- mediated genetic transformation of tobacco. *Plant Signal Behav.* **8**(6): e24354.

Peltier G & Cournac L. 2002. CHLORORESPIRATION. *Annual Review of Plant Biology* **53**: 523–550.

Peltier G, Aro EM & Shikanai T. 2016. NDH- 1 and NDH-2 Plastoquinone Reductases in Oxygenic Photosynthesis. *Annual Review of Plant Biology* **67**: 55–80.

Peltier G, Tolleter D, Billon E, Cournac L. 2010. Auxiliary electron transport pathways in chloroplasts of microalgae. *Photosynth. Res*. **106**: 19–31.

Peng L, Shimizu H & Shikanai T. 2008. The chloroplast NAD(P)H dehydrogenase complex interacts with photosystem I in Arabidopsis. *The Journal of Biological Chemistry* **283**: 34873–9.

Peshev D. & Van den Ende W. 2013. Sugars as antioxidants in plants. In Crop Improvement under Adverse Conditions (eds N. Tuteja & S.S. Gill) 285–308. Springer-Verlag, Berlin, Heidelberg, Germany.

Pfannschmidt T, Brautigam K, Wagner R, Dietzel L, Schroter Y, Steiner S et al. 2009. Potential regulation of gene expression in photosynthetic cells by redox and energy state: approaches towards better understanding. *Ann. Bot.* **103**: 599–607.

Pinheiro C, Chaves MM. 2011. Photosynthesis and drought: can we make metabolic connections from available data? *J Exp Bot*. **62**: 869-882.

Polle JE, Kanakagiri SD, Melis A. 2003. tla1, a DNA insertional transformant of the green alga Chlamydomonas reinhardtii with a truncated light-harvesting chlorophyll antenna size. *Planta* **217**: 49–59.

Porra RJ, Thompson WA, Kriedemann PE . 1989. Determination of accurate extinction coefficients and simultaneous-equations for assaying chlorophyll a and chlorophyll b extracted with four different solvents: verification of the concentration of chlorophyll standards by atomic-absorption spectroscopy. *Biochimica et Biophysica Acta* **975**: 384–394.

Pribil M, Pesaresi P, Hertle A, Barbato R and Leister D. 2010. Role of Plastid Protein Phosphatase TAP38 in LHCII Dephosphorylation and Thylakoid Electron Flow. *PLoS Biology* **8:** e1000288.

Price AH, Cairns JE, Horton P, Jones HG, Griffiths H. 2002. Linking drought-resistance mechanisms to drought avoidance in upland rice using a QTL approach: progress and new opportunities to integrate stomatal and mesophyll responses. J Exp Bot. **53**: 989–1004.

Putarjunan A, Liu X, Nolan T, Yu F and Rodermel S. 2013. Understanding chloroplast biogenesis using second-site suppressors of immutans and var2. Photosynth. Res. **116**: 437–453.

Quick W. and Neuhaus HE. 1997. A molecular approach to primary metabolism in higher plants. In The Regulation and Control of Photosynthetic Carbon Assimilation. *Taylor and Francis Ltd*, London. 41–62.

Quiles MJ. 2006. Stimulation of chlororespiration by heat and highlight intensity in oat plants. *Plant Cell Environ.* **29**: 1463–1470.

Rai VK, Sharma UD. 1991. Amino acids can modulate ABA induced stomatal closure, stomatal resistance and K+ fluxes in *Vicia faba* leaves. *–Beitr, Biol, Pflanz*. **66**: 393-405.

Raines CA. 2003. The Calvin cycle revisited. *Photosynth Res***. 75**: 1–10.

Ramesh SA, Tyerman SD, Xu B, Bose J, Kaur S, Conn V et al. 2015. GABA signalling modulates plant growth by directly regulating the activity of plant-specific anion transporters. *Nat. Commun.* **6**: 7879.

Ray DK, Mueller ND, West PC and Foley JA. 2013. Yield trends are insufficient to double global crop production by 2050. *PLoS ONE* **8**: e66428.

Ray DK, Ramankutty N, Mueller ND, West PC and Foley JA. 2012. Recent patterns of crop yield growth and stagnation. *Nat. Commun*. **3**: 1293.

Regierer B, Fernie AR, Springer F, Perez-Melis A, Leisse A, Koehl K et al. 2002. Starch content and yield increase as a result of altering adenylate pools in transgenic plants. *Nat. Biotechnol.* **20**: 1256–1260.

Renault H, Roussel V, El Amrani A, Arzel M, Renault D, Bouchereau A, Deleu C. 2010. The Arabidopsis *pop2-1* mutant reveals the involvement of GABA transaminase in salt stress tolerance. *BMC Plant Biology* **10**: 20.

Rhodes D, Handa S, Bressan RA. 1986. Metabolic changes associated with adaptation of plant-cells to water-stress. *Plant Physiol*. **82**: 890–903.

Rochaix JD. 2011. Assembly of the photosynthetic apparatus. *Plant Physiol.* **155**: 1493–500.

Rochaix JD. 2013. Fine-Tuning Photosynthesis. *Science* **342**: 6154.

Rodrigues R, Vicente JB, Félix R, Oliveira S, Teixeira M and Rodrigues-Pousada C. 2006. Desulfovibrio gigas flavodiiron protein affords protection against nitrosative stress in vivo. Journal of Bacteriology **188**: 2745–51.

Rosso D, Ivanov AG, Fu A, Geisler-Lee J, Hendrickson L, Geisler M et al. 2006. IMMUTANS does not act as a stress-induced safety valve in the protection of the photosynthetic apparatus of Arabidopsis during steady-state photosynthesis. *Plant Physiol.* **142**: 574–585.

Roychoudhury A, Ghosh S. 2013. Physiological and biochemical responses of mungbean (*Vigna radiata* L. Wilczek) to varying concentrations of cadmium chloride or sodium chloride. *Unique J. Pharm. Biol. Sci.* 1: 11–21.

Ruban AV, Johnson MP, Duffy CDP. 2012. The photoprotective molecular switch in the photosystem II antenna. *Biochim Biophys Acta.* **1817**(1): 167–181.

Rumberg B and Siggel U. 1969. pH changes in the inner phase of the thylakoids during photosynthesis. *Die Naturwissenschaften* **56**: 130–132.

Sacksteder C A, Kanazawa A, Jacoby M E & Kramer DM. 2000. The proton to electron stoichiometry of steady-state photosynthesis in living plants: A proton-pumping Q cycle is continuously engaged. *Proc Natl Acad Sci USA* **97**: 14283–8.

Saglio PH, Pradet A. 1980. Soluble sugars, respiration, and energy charge during aging of excised maize root tips. *Plant Physiol.* **66**: 516-519.

Samol I, Shapiguzov A, Ingelsson B, Fucile G, Crèvecoeur M, Vener AV, Goldschmidt-Clermont M. 2012. Identification of a photosystem II phosphatase involved in light acclimation in Arabidopsis. *The Plant Cell* **24**: 2596–609.

Saraiva LM, Vicente JB, Teixeira M. 2004. The role of the flavodiiron proteins in microbial nitric oxide detoxification. *Adv. Microb. Physiol*. **49**: 77–129.

Sayed OH. 2003. Chlorophyll fluorescence as a tool in cereal crop research. *Photosynthetica* **41**(3): 321–330.

Scheibe R, Backhausen JE, Emmerlich V, Holtgrefe S. 2005. Strategies to maintain redox homeostasis during photosynthesis under changing conditions. *J Exp Bot*. **56**: 1481–1489.

Schreiber U and Neubauer C. 1990. 02-dependent electron flow, membrane energetisation and the mechanism of non-photochemical quenching of chlorophyll fluorescence. Photosynth. Res. **25:** 279-293.

Shapiguzov A, Ingelsson B, Samol I, Andres C, Kessler F, Rochaix JD, GoldschmidtClermont M. 2010. The PPH1 phosphatase is specifically involved in LHCII dephosphorylation and state transitions in Arabidopsis. *Proc Natl Acad Sci USA* **107**: 4782–7.

Sharkey TD & Badger MR. 1982. Effects of water stress on photosynthetic electron transport, photophosphorylation and metabolite levels of Xanthium strumarium cells. *Planta* **156**: 199–206.

Sharkey TD, Laporte MM, Lu Y, Weise SE, Weber APM. 2004. Engineering plants for elevated CO2: a relationship between sugar sensing and starch degradation. *Plant Biology* **6**: 280-288.

Sharkey TD. 1985. Photosynthesis in intact leaves of C3 plants: physics, physiology and rate limitations. *Bot. Rev.* **51**: 53–105.

Shikanai T & Yamamoto H. 2017. Contribution of Cyclic and Pseudo-cyclic Electron Transport to the Formation of Proton Motive Force in Chloroplasts. *Molecular Plant* **10**: 20–29.

Shikanai T. 2007. *Annu. Rev. Plant Biol.* 58: 199-217.

Shimakawa G, Shaku K, Nishi A, Hayashi R, Yamamoto H, Sakamoto K, Makino A, Miyake C. 2015. FLAVODIIRON2 and FLAVODIIRON4 proteins mediate an oxygen-dependent alternative electron flow in Synechocystis sp. PCC 6803 under CO2-limited conditions. *Plant Physiol*. **167**: 472-480.

Shimakawa G, Ishizaki K, Tsukamoto S, Tanaka M, Sejima T, Miyake C. 2017. The liverwort, *Marchantia*, drives alternative electron flow using a flavodiiron protein to protect PSI. *Plant Physiol.* **173**: 1636-1647.

Silaghi-Dumitrescu R, Kurtz DM, Jr Ljungdahl, LG, Lanzilotta, WN. 2005. X-ray crystal structures of *Moorella thermoacetica* FprA. Novel diiron site structure and mechanistic insights into a scavenging nitric oxide reductase. *Biochemistry* **44**: 6492–6501.

Somerville C and Ogren WL. 1982. Genetic modification of photorespiration. Trends Biochem. Sci. **7**: 171-174.

Spetea C, Herdean A, Allorent G, Carraretto L, Finazzi G & Szabo I. 2017. An update on the regulation of photosynthesis by thylakoid ion channels and transporters in Arabidopsis. *Physiol. Plant*. **161**: 16-27.

Stepien P and Johnson GN. 2009. Contrasting responses of photosynthesis to salt stress in the glycophyte Arabidopsis and the halophyte thellungiella: role of the plastid terminaloxidase as an alternative electron sink. *Plant Physiol.* **149**: 1154–1165.

Stitt M. 1991. Rising CO2 levels and their potential significance for carbon flow in photosynthetic cells. *Plant Cell Environ.* **14**:741–762.

Strand Å, Foyer C, Gustafsson P, Gardeström P, Hurry V. 2003. Altering flux through the sucrose biosynthesis pathway in transgenic *Arabidopsis thaliana* modifies photosynthetic acclimation at low temperatures and the development of freezing tolerance. *Plant Cell Environ*. **26**: 523–535.

Strasser RJ, Srivastava A, Tsimilli-Michael M. 2000. The fluorescence transient as a tool to characterize and screen photosynthetic samples. In: Mohanty P, Yunus U, Pathre M, editors. Probing Photosynthesis: Mechanism, Regulation and Adaptation. London: *Taylor and Francis*. 443–480.

Sulpice R, Eva-Theresa Pyl, Ishihara H, Trenkamp S, Steinfath M, Witucka-Wall H, Gibon Y, Usadel B, Poree F, Conceição Piques M, Korff MV, Steinhauser MC, Joost JB. Keurentjes, Guenther M, Hoehne M, Selbig J, Alisdair R, Fernie Altmann T. and Stitt M. 2009. Starch as a major integrator in the regulation of plant growth, *Proc Natl Acad Sci USA* **106** (25): 10348-10353.

Sun X., Wen T. 2011. Physiological roles of plastid terminal oxidase in plant stress responses. *J. Biosci*. **36**: 951–956.

Suorsa M, Järvi S, Grieco M, Nurmi M, Pietrzykowska M, Rantala M, Aro EM. 2012. PROTON GRADIENT REGULATION5 is essential for proper acclimation of Arabidopsis photosystem I to naturally and artificially fluctuating light conditions. *The Plant Cell* **24**: 2934–48.

Szabados L, Savoure A. 2010. Proline: a multifunctional amino acids. *Trends Plant Sci.* **15**: 89-97.

Takahashi S, Milward SE, Fan DY, Chow WS, Badger MR. 2009. How does cyclic electron flow alleviate photoinhibition in Arabidopsis? *Plant Physiol.* **149**: 1560–1567.

Takagi D, Miyake C. 2018. PROTON GRADIENT REGULATION 5 supports linear electron flow to oxidize photosystem 1. *Physiol. Plant*. doi:10.1111/ppl.12723

Taniguchi M, Miyake H. 2012. Redox-shuttling between chloroplast and cytosol: integration of intra-chloroplast and extra-chloroplast metabolism. *Curr Opin Plant Biol.* **15**: 252–260.

Tardy F, Havaux M. 1997. Thylakoid membrane fluidity and thermostability during the operation of the xanthophyll cycle in higher-plant chloroplasts. *Biochim Biophys Acta*. **1330**: 179-193.

Tausz M, Kranner I, Grill D. 1996. Simultaneous determination of ascorbic acid and dehydroascorbic acid in plant materials by HPLC, *Phytochem. Anal*. **7**: 69–72.

Thalmann M and Santelia D. 2017. Starch as a determinant of plant fitness under abiotic stress. *New Phytologist* **214**: 943-951.

Tikhonov A, Khomutov G, Ruuge E, Blumenfeld L. 1981. Electron-Transport Control in Chloroplasts - Effects of Photosynthetic Control Monitored by the Intrathylakoid Ph. *Biochim Biophys Acta.* **637**: 321-333.

Tilman D, Balzer C, Hill J and Befort BL. 2011. Global food demand and the sustainable intensification of agriculture. *Proc Natl Acad Sci USA* **108**(50): 20260-20264.

Tyystjärvi E, Aro EM. 1996. The rate constant of photoinhibition, measured in lincomycin-treated leaves, is directly proportional to light intensity. *Proc Natl Acad Sci USA* **93**: 2213–2218.

Usadel B, Bläsing OE, Gibon Y, Poree F, Höhne M, Günter M, Trethewey R, Kamlage B, Poorter H, Stitt M 2008. Multilevel genomic analysis of the response of transcripts, enzyme activities and metabolites in Arabidopsis rosettes to a progressive decrease of temperature in the non-freezing range. *Plant Cell Environ.* **31**(4): 518-47.

Van Oosten JJ, Besford RT. 1994. Sugar feeding mimics effect of acclimation to high CO2: rapid downregulation of RuBisCO small subunit transcripts, but not of the large subunit transcripts. Journal of Plant Physiology **143**: 306–312.

Vanlerberghe GC, McIntosh L. 1997. Alternative oxidase: from gene to function. *Annu Rev Plant Physiol Plant Mol Biol.* **48**: 703–734.

Vermaas WFJ. 1993. Molecular-biological approaches to analyze photosystem II structure and function. *Annu. Rev. Plant Physiol. Plant Mol. Biol*. **44**: 457-481.

Vicente JB, Carrondo MA, Teixeira M, Frazão C. 2008a. Structural studies on flavodiiron proteins. *Methods Enzymol*. **437**: 3–19.

Vicente JB, Gomes CM, Wasserfallen A, Teixeira M. 2002. Module fusion in an A-type flavoprotein from the cyanobacterium *Synechocystis* condenses a multiple-component pathway in a single polypeptide chain. *Biochem. Biophys. Res. Commun*. **294**: 82–87.

Vicente JB, Justino MC, Gonçalves VL, Saraiva LM, Teixeira M. 2008b. Biochemical, spectroscopic, and thermodynamic properties of flavodiiron proteins. *Methods Enzymol*. **437**: 21–45.

Vollmar M, Schlieper D, Winn M, Büchner C & Groth G. 2009. Structure of the c14 rotor ring of the proton translocating chloroplast ATP synthase. *The Journal of Biological Chemistry* **284**: 18228–35.

Wada S, Yamamoto H, Suzuki Y, Yamori W, Shikanai T, Makino A. 2017. Flavodiiron Protein Substitutes for Cyclic Electron Flow without Competing CO2 Assimilation in Rice. *Plant Physiol*. **176**: 1509–1518.

Wang HL, Postier BL, Burnap RL. 2004. Alterations in global patterns of gene expression in *Synechocystis* sp. PCC 6803 in response to inorganic carbon limitation and the inactivation of *ndhR*, a LysR family regulator. *J. Biol. Chem.* **279**: 5739–5751.

Wang X, Cai J, Jiang D, Liu F, Dai T, Cao W. 2011. Pre-anthesis high-temperature acclimation alleviates damage to the flag leaf caused by post-anthesis heat stress in wheat. *Journal of Plant Physiology* **168**: 585–593.

Wang Y, Ying Y, Chen J, Wang XC. 2004. Transgenic Arabidopsis overexpressing Mn-SOD enhanced salt- tolerance. *Plant Sci*. **167**: 671-677.

Wasserfallen A, Ragettli S, Jouanneau Y, Leisinger T. 1998. A family of flavoproteins in the domains Archaea and Bacteria. *Eur. J. Biochem*. **254**: 325–332.

Weigel D and Glazebrook J. 2006b. Transformation of Agrobacterium using the freeze-thaw method. CSH Protoc. 2006(**7**): 1031-1036.

Werner C, Ryel RJ, Correia O, Beyschlag W. 2001. Effects of photoinhibition on whole-plant carbon gain assessed with a photosynthesis model. *Plant Cell Environ*. **24**: 27–40.

Wollman FA. 2001. State transitions reveal the dynamics and flexibility of the photosynthetic apparatus. *The EMBO Journal* **20**: 3623–30.

Woodrow IE and Berry JA. 1988. Enzymic regulation of photosynthetic CO2 fixation in C3 plants. *Annu. Rev. Plant Physiol. Plant Mol. Biol.* **39**: 533–594.

Wu J, Neimanis S & Heber U. 1991. Photorespiration is more e¡ective than the Mehler reaction in protecting the photosynthetic apparatus against photoinhibition. *Bot. Acta* **104**: 283-291.

Xu ZZ, and Zhou GS. 2005. Effects of water stress on photosynthesis and nitrogen metabolism in vegetative and reproductive shoots of *Leymus chinensis*. *Photosynthetica* **43**: 29–35.

Yadav KNS, Semchonok DA, Nosek L, Kouřil R, Fucile G, Boekema EJ & Eichacker LA. 2017. Supercomplexes of plant photosystem I with cytochrome b6f, lightharvesting complex II and NDH. *Biochimica et Biophysica Acta (BBA) - Bioenergetics* **1858**:12–20.

Yamamoto H, Peng L, Fukao Y, Shikanai T. 2011. An Src homology 3 domain-like fold protein forms a ferredoxin binding site for the chloroplast NADH dehydrogenase-like complex in Arabidopsis. *Plant Cell* **23**: 1480-1493.

Yamamoto H, Takahashi S, Badger MR, Shikanai T. 2016. Artificial remodelling of alternative electron flow by flavodiiron proteins in Arabidopsis. *Nat. Plants* **2**:16012.

Yaronskaya E, Vershilovskaya I, Poers Y, Alawady AE, Averina N, Grimm B. 2006. Cytokinin effects on tetrapyrrole biosynthesis and photosynthetic activity in barley seedlings, *Planta* **224**: 700-709.

Zhang P, Allahverdiyeva Y, Eisenhut M, Aro EM. 2009. Flavodiiron proteins in oxygenic photosynthetic organisms: photoprotection of photosystem II by Flv2 and Flv4 in *Synechocystis* sp. PCC 6803. *PLoS ONE* **4**: e5331.

Zhang P, Eisenhut M, Brandt AM, Carmel D, Silen HM, Vass I, Allahverdiyeva Y,Salminen TA, Aro EM. 2012. Operon *flv4-flv2* provides cyanobacterial photosystem II with flexibility of electron transfer. *The Plant Cell* **24**: 1952–1971.

Zhu XG, Long SP and Ort DR. 2010. Improving photosynthetic efficiency for greater yield. *Annu. Rev. Plant Biol.* **61**: 235–261.

Zhu XG, Ort DR, Whitmarsh J, Long SP. 2004. The slow reversibility of photosystem II thermal energy dissipation on transfer from high to low light may cause large losses in carbon gain by crop canopies: A theoretical analysis. *J. Exp. Bot.* **55**: 1167–1175.

Živković T, Quartacci MF, Stevanović F, Marinone F, Navari-Izzo F. 2005. Low-molecular weight substances in the poikilohydric plant Ramonda serbica during dehydration and rehydration. *Plant Sci.* **168**: 105–111.

10. Appendix

Appendix Table 1. Gene specific primers used for PCR analysis

Gene	Forward primer	Reverse primer
Flv1	ATGGGAATCCATGCAAAACTGGAGAC	ATAATGATCGCCAGATTTCCGGTG
Flv2	ATGATTTCTCCAATTGGTGGTC	ATATTGTCCCCCCGATTTGC
Flv3	ATGTTCACTACCCCCCTCCCCCCCCAAAAGC	GTAATAATTGCCGACTTTGCGAT
Flv4	ATGGTTACCCTAATTGATTCTCCAACC	GTAGTGGTTGCCCAGTTTGCGGT
Flv1-RT	TGTTTGGTTCCTTCGGTTGG	TTCAAAGTTTGGTCGGTGGG
Flv2-RT	TAGCCAGACCCTCAAAGTAGC	CAGGGTAGGAGAACCGACAAT
Flv3-RT	TAAAAACCCAAACCGCAAGCA	CCTTCTGCTTTAGCTACCCGA
Flv4-RT	ACCGCTTTGCCGGAGTTA	GGTGGTGAGTGGCGGTTA
UBQ10	CTTCGTCAAGACTTTGACCG	CTTCTTAAGCATAACAGAGACGAG

Appendix Table 2. The composition of free amino acids in Flv-erexpression lines.

Amino acids	Col0		Flv1			Flv3			Flv1/Flv3	
		L1	L2	L3	L4	L5	L6	L7	L8	L9
Asparagine	4,93 ±0,36	4,32 ±0,17	3,81 ±0,49	3,85 ±0,23	3,75 ±0,21	3,83 ±0,25	4,74 ±0,51	4,23 ±0,35	5,77 ±0,85	4,71 ±0,31
Serine	15,96 ±1,45	14,91 ±0,73	13,47 ±1,55	16,05 ±1,55	14,39 ±1,14	16,59 ±0,39	20,92 ±2,65	17,85 ±0,69	22,47 ±3,82	17,39 ±1,78
Arginine	0,29 ±0,01	0,25 ±0,01	0,25 ±0,01	0,25 ±0,01	0,24 ±0,01	0,29 ±0,03	0,30 ±0,02	0,27 ±0,02	0,39 ±0,05	0,63 ±0,26
Glycine	0,14 ±0,03	0,07 ±0,01	0,09 ±0,02	0,06 ±0,01	0,24 ±0,04	0,22 ±0,05	0,29 ±0,03	0,18 ±0,02	0,14 ±0,01	0,07 ±0,02
Glutamine	12,04 ±1,26	9,97 ±0,60	10,69 ±1,49	10,14 ±0,88	14,25 ±0,62	12,98 ±0,85	17,52 ±1,92	11,23 ±0,63	15,17 ±2,69	11,19 ±0,27
Aspartate	10,03 ±0,86	8,31 ±0,77	9,42 ±0,67	8,46 ±0,61	11,13 ±0,62	10,28 ±0,48	13,22 ±0,83	9,63 ±0,77	13,73 ±2,24	11,44 ±1,57
Glutamate	23,23 ±1,75	23,36 ±1,39	23,09 ±1,66	22,90 ±1,37	21,95 ±1,38	22,73 ±0,49	26,05 ±1,75	21,68 ±1,56	27,13 ±4,14	22,91 ±0,68
Threonine	8,66 ±0,87	8,32 ±0,51	7,74 ±1,07	9,76 ±0,92	8,25 ±0,34	8,31 ±0,35	10,49 ±1,28	8,38 ±0,56	11,71 ±1,75	9,77 ±0,29
Alanine	8,38 ±0,66	8,35 ±0,60	7,43 ±0,83	6,25 ±0,64	6,34 ±0,50	6,63 ±0,35	8,13 ±0,89	6,37 ±0,31	8,13 ±1,29	6,48 ±0,42
GABA	0,52 ±0,10	0,51 ±0,03	0,45 ±0,11	0,61 ±0,06	0,40 ±0,02	0,54 ±0,05	0,58 ±0,05	0,63 ±0,07	0,89 ±0,10	1,04 ±0,18
Proline	8,46 ±1,51	9,10 ±0,73	7,20 ±1,41	10,03 ±2,06	7,29 ±0,27	9,44 ±2,08	8,33 ±1,13	8,61 ±0,89	8,01 ±0,14	8,04 ±1,08
Lysine	0,84 ±0,06	0,82 ±0,06	0,90 ±0,11	0,78 ±0,16	1,13 ±0,10	0,72 ±0,06	1,25 ±0,12	0,78 ±0,08	0,90 ±0,12	1,21 ±0,23
Valine	0,71 ±0,06	0,64 ±0,01	0,63 ±0,06	0,71 ±0,05	0,67 ±0,02	0,79 ±0,02	0,81 ±0,09	0,76 ±0,06	0,90 ±0,15	0,86 ±0,06
Isoleucine	0,23 ±0,020	0,20 ±0,002	0,20 ±0,02	0,23 ±0,01	0,21 ±0,01	0,25 ±0,008	0,26 ±0,03	0,24 ±0,02	0,30 ±0,05	0,23 ±0,07
Leucine	0,19 ±0,01	0,18 ±0,005	0,17 ±0,02	0,20 ±0,01	0,15 ±0,01	0,23 ±0,01	0,19 ±0,03	0,22 ±0,03	0,25 ±0,05	0,23 ±0,06
phenylalanine	0,39 ±0,04	0,33 ±0,01	0,33 ±0,05	0,35 ±0,02	0,39 ±0,02	0,43 ±0,02	0,52 ±0,09	0,35 ±0,02	0,45 ±0,08	0,95 ±0,59
Histidine	2,19 ±0,14	1,42 ±0,07	1,44 ±0,22	1,34 ±0,41	2,75 ±0,12	2,40 ±0,08	2,54 ±0,17	0,91 ±0,32	1,27 ±0,46	2,01 ±0,68

Measurements were carried out on rosette leaves harvested at the middle of the day (4 h) using uplc and fluorescence detection. All values are in (nmol g^{-1} fw). values represents means of 4-5 biological replicates±SE. Significant differences to WT are indicated by asterisks according to student' s t test (* $p \leq 0.05$, ** $p \leq 0.01$, *** $p \leq 0.001$).

Ap pendix Table 3. The composition of free amino acids in Flv-erexpression lines.

Amino acids	Col0		Flv2			Flv4			Flv2/Flv4	
		L1	L2	L3	L4	L5	L6	L7	L8	L9
Asparagine	4,93 ±0,36	4,01 ±0,22	4,80 ±0,21	4,27 ±0,69	3,80 ±0,45	4,07 ±0,47	5,58 ±0,58	4,01 ±0,38	4,33 ±0,77	4,07 ±0,20
Serine	15,96 ±1,45	18,47 ±1,35	14,92 ±1,04	16,32 ±2,74	16,62 ±1,33	15,38 ±1,36	18,27 ±0,84	12,80 ±0,52	15,42 ±1,83	14,70 ±0,81
Arginine	0,29 ±0,01	0,28 ±0,02	0,25 ±0,01	0,29 ±0,03	0,20 ±0,03	0,24 ±0,009	0,32 ±0,03	0,50 ±0,09	0,39 ±0,10	0,67 ±0,04 ***
Glycine	0,14 ±0,03	0,30 ±0,04 *	0,28 ±0,04 *	0,13 ±0,01	0,29 ±0,09	0,20 ±0,04	0,17 ±0,05	1,12 ±0,39	0,51 ±0,24	1,11 ±0,08 ***
Glutamine	12,04 ±1,26	14,41 ±1,17	13,78 ±0,72	12,4 ±2,32	11,67 ±1,17	13,37 ±1,49	12,67 ±0,63	11,51 ±0,91	14,27 ±2,38	9,87 ±0,56
Aspartate	10,03 ±0,86	9,63 ±0,64	9,33 ±0,53	10,32 ±1,57	8,38 ±0,81	9,32 ±0,48	11,23 ±0,49	8,34 ±0,47	9,94 ±1,23	8,04 ±0,18
Glutamate	23,23 ±1,75	23,36 ±1,84	22,45 ±0,76	24,37 ±3,39	21,17 ±2,11	21,42 ±1,85	26,23 ±0,68	16,88 ±0,86	22,79 ±3,57	19,14 ±1,19
Threonine	8,66 ±0,87	8,66 ±0,54	10,30 ±0,32	8,36 ±1,27	8,12 ±1,11	7,71 ±0,69	10,31 ±0,7328	6,53 ±0,42	9,92 ±1,65	7,54 ±0,66
Alanine	8,38 ±0,66	9,61 ±1,03	9,58 ±0,52	8,04 ±1,45	7,69 ±0,82	9,29 ±1,34	8,63 ±0,58	8,48 ±1,05	10,36 ±1,94	8,17 ±0,26
GABA	0,52 ±0,10	0,73 ±0,06	0,74 ±0,11	0,67 ±0,04	0,36 ±0,05	0,45 ±0,03	0,54 ±0,03	0,62 ±0,07	0,46 ±0,08	0,66 ±0,08
Proline	8,46 ±1,51	7,49 ±0,66	12,50 ±1,55	7,04 ±1,72	12,84 ±2,52	8,39 ±1,04	18,55 ±2,9 *	6,05 ±1,06	11,96 ±2,68	6,87 ±0,29
Lysine	0,84 ±0,06	0,95 ±0,22	1,21 ±0,09	0,99 ±0,11	0,85 ±0,19	0,78 ±0,05	0,77 ±0,05	0,64 ±0,03	0,94 ±0,19	0,81 ±0,08
Valine	0,71 ±0,06	0,73 ±0,06	0,75 ±0,05	0,75 ±0,13	0,67 ±0,08	0,70 ±0,06	0,93 ±0,04	0,60 ±0,04	0,78 ±0,13	0,65 ±0,04
Isoleucine	0,23 ±0,020	0,23 ±0,01	0,23 ±0,01	0,23 ±0,03	0,20 ±0,02	0,21 ±0,01	0,29 ±0,01	0,16 ±0,01	0,22 ±0,04	0,20 ±0,01
Leucine	0,19 ±0,01	0,18 ±0,01	0,19 ±0,02	0,22 ±0,04	0,19 ±0,02	0,16 ±0,01	0,27 ±0,01	0,15 ±0,01	0,18 ±0,03	0,17 ±0,01
phenylalanine	0,39 ±0,04	0,42 ±0,03	0,34 ±0,02	0,30 ±0,05	0,32 ±0,03	0,36 ±0,02	0,36 ±0,01	0,26 ±0,01	0,38 ±0,07	0,30 ±0,01
Histidine	2,19 ±0,14	2,33 ±0,51	2,62 ±0,08	1,85 ±0,33	1,11 ±0,31	1,11 ±0,47	1,34 ±0,37	1,25 ±0,22	1,22 ±0,31	1,30 ±0,21

Measurements were carried out on rosette leaves harvested at the middle of the day (4 h) using uplc and fluorescence detection. All values are in (nmol g^{-1} fw). Values represents means of 4-5 biological replicates±SE. Significant differences to WT are indicated by asterisks according to student' s t test (* $p \leq 0.05$, ** $p \leq 0.01$, *** $p \leq 0.001$).

Appendix Table 4. The composition of free amino acids in Flv-erexpression lines under drought stress.

Amino acids	Col0		Flv1			Flv3			Flv1/Flv3	
		L1	L2	L3	L4	L5	L6	L7	L8	L9
Asparagine	4,99 ±0,43	4,84 ±0,28	4,99 ±0,43	5,72 ±0,30	4,90 ±0,30	5,52 ±0,63	5,44 ±0,33	5,63 ±0,82	6,07 ±0,40	4,90 ±0,19
Serine	9,62 ±0,54	10,10 ±0,66	11,22 ±0,67	13,69 ±1,17 **	13,36 ±0,74 ***	13,70 ±1,26 **	14,20 ±0,70 ***	11,96 ±1,18	12,42 ±0,87	11,46 ±0,50 *
Arginine	0,92 ±0,12	0,60 ±0,06	0,80 ±0,09	0,89 ±0,08	0,68 ±0,02	0,88 ±0,10	0,74 ±0,04	0,84 ±0,07	0,78 ±0,05	0,67 ±0,03
Glycine	3,54 ±0,27	2,95 ±0,37	2,80 ±0,29	4,04 ±0,47	4,49 ±0,36 **	4,82 ±0,55	3,76 ±0,62	4,43 ±0,34	3,82 ±0,16	3,14 ±0,19
Glutamine	6,61 ±0,27	5,22 ±0,51	6,09 ±0,55	6,55 ±0,52	7,43 ±0,51	6,91 ±0,75	6,32 ±0,51	7,84 ±0,77	8,19 ±0,76	6,39 ±0,35
Aspartate	8,42 ±0,54	8,73 ±0,78	10,35 ±0,51 *	13,60 ±1,36 **	11,49 ±0,65 **	11,45 ±0,74 **	14,00 ±0,70 ***	14,76 ±0,81 ***	14,83 ±0,94 ***	14,54 ±0,55 ***
Glutamate	9,59 ±0,79	10,83 ±0,80	11,12 ±0,58	10,68 ±1,00	13,58 ±0,64 ***	13,12 ±0,58 **	14,50 ±1,14 **	12,45 ±0,91 *	13,88 ±0,54 ***	14,02 ±0,46 ***
Threonine	11,37 ±0,42	10,86 ±0,66	11,63 ±0,51	10,72 ±0,36	12,66 ±0,53	11,29 ±0,40	12,46 ±0,38	13,36 ±0,46 **	12,07 ±0,50	12,73 ±0,49 *
Alanine	5,54 ±0,27	5,31 ±0,22	6,03 ±0,41	6,38 ±0,19 *	7,15 ±0,37 **	6,81 ±0,34 **	6,56 ±0,20 **	8,21 ±0,34 ***	7,60 ±0,32 ***	7,64 ±0,36 ***
GABA	0,79 ±0,10	0,67 ±0,04	0,80 ±0,14	1,03 ±0,04	0,59 ±0,05	0,86 ±0,10	0,70 ±0,09	0,75 ±0,12	0,67 ±0,09	0,64 ±0,07
Proline	129,30 ±5,03	77,02 ±6,88	92,41 ±8,91	79,76 ±3,81	71,22 ±9,28	94,53 ±11,82	82,28 ±10,11	139,45 ±6,47	104,96 ±6,01	110,92 ±6,74
Lysine	0,40 ±0,01	0,33 ±0,01	0,34 ±0,01	0,36 ±0,01	0,34 ±0,007	0,38 ±0,01	0,36 ±0,009	0,41 ±0,01	0,36 ±0,01	0,35 ±0,01
Valine	3,16 ±0,33	2,46 ±0,16	2,98 ±0,51	3,39 ±0,32	1,79 ±0,21	2,87 ±0,45	2,18 ±0,49	3,12 ±0,43	2,23 ±0,33	2,35 ±0,15
Isoleucine	1,60 ±0,20	0,92 ±0,12	1,29 ±0,26	1,48 ±0,15	0,71 ±0,09	1,22 ±0,23	0,87 ±0,25	1,38 ±0,26	0,86 ±0,18	0,90 ±0,11
Leucine	1,34 ±0,18	0,80 ±0,11	1,18 ±0,28	1,50 ±0,19	0,58 ±0,06	1,01 ±0,20	0,67 ±0,22	1,06 ±0,19	0,76 ±0,17	0,80 ±0,10
phenylalanine	2,10 ±0,34	1,23 ±0,20	1,47 ±0,27	2,26±0,31	0,99 ±0,10	1,60 ±0,29	1,19 ±0,35	1,36 ±0,19	1,04 ±0,12	1,02 ±0,14
Histidine	1,59 ±0,14	1,41 ±0,18	1,81 ±0,29	1,99 ±0,15	1,03 ±0,13	1,43 ±0,23	1,10 ±0,25	1,71 ±0,21	1,11 ±0,13	1,16 ±0,13

Measurements were carried out on rosette leaves using uplc and fluorescence detection. All values are in (nmol g^{-1} fw). Values represents means of 5-7 biological replicates±SE. Significant differences to WT are indicated by asterisks according to student' s t test (* $p \leq 0.05$, ** ** $p \leq 0.01$, *** $p \leq 0.001$).

Appendix Table 5. The composition of free amino acids in Flv-erexpression lines under drought stress.

Amino acids	Col0		Flv2			Flv4			Flv2/Flv4	
		L1	L2	L3	L4	L5	L6	L7	L8	L9
Asparagine	4,99 ±0,43	4,11 ±0,59	3,21 ±0,09	5,72 ±0,30 **	3,30 ±0,29	3,90 ±0,18	4,02 ±0,22	3,70 ±027	3,90 ±0,31	3,69 ±0,19
Serine	9,62 ±0,54	8,69 ±0,74	8,93 ±0,21	9,72 ±0,42	7,49 ±0,54	9,25 ±0,30	10,24 ±0,59	9,37 ±0,78	9,70 ±0,89 *	9,27 ±0,52
Arginine	0,92 ±0,12	0,80 ±0,15	0,63 ±0,04	0,67 ±0,03	0,70 ±0,10	0,75 ±0,04	0,70 ±0,08	0,65 ±0,05	0,58 ±0,02	0,68 ±0,06
Glycine	3,54 ±0,27	5,44 ±0,50 **	3,97 ±0,29	4,03 ±0,15	5,09 ±0,45 **	4,60 ±0,06 **	4,47 ±0,10 **	7,30 ±0,43 ***	5,50 ±0,47	4,64 ±0,28 **
Glutamine	6,61 ±0,27	8,54 ±0,67 *	7,01 ±0,27	7,85 ±0,15 ***	7,71 ±0,49	8,93 ±0,34 ***	8,99 ±0,56 **	9,73 ±0,77 **	9,41 ±0,95 *	8,40 ±0,53 **
Aspartate	8,42 ±0,54	8,47 ±0,47	7,78 ±0,29	8,21 ±0,89	7,97 ±0,74	8,58 ±0,22	8,60 ±0,39	8,02 ±0,19	8,25 ±0,69	8,02 ±0,53
Glutamate	9,59 ±0,79	10,56 ±0,57	11,28 ±0,43	12,18 ±0,76 *	10,57 ±0,26	13,87 ±0,55 ***	15,19 ±0,44 ***	14,13 ±0,62 ***	17,32 ±3,54	11,92 ±0,82*
Threonine	11,37 ±0,42	12,51 ±0,61	11,75 ±0,16	11,85 ±0,24	12,04 ±0,76	14,03 ±0,49 ***	13,56 ±0,59 **	12,83 ±0,42 *	12,63 ±0,96 ***	12,76 ±0,40 *
Alanine	5,54 ±0,27	5,42 ±0,38	5,68 ±0,20	6,16 ±0,19 *	5,65 ±0,32	7,28 ±0,27 ***	6,82 ±0,34 **	7,73 ±0,44 ***	8,20 ±1,02	6,66 ±0,26 **
GABA	0,79 ±0,10	0,27 ±0,03	0,32 ±0,02	0,37 ±0,02	0,32 ±0,04	0,33 ±0,01	0,39 ±0,01	0,35 ±0,02	0,44 ±0,07	0,43 ±0,07
Proline	129,30 ±5,03	118,17 ±7,85	121,98 ±4,86	126,76 ±6,41	139,80 ±4,91	117,87 ±5,69	117,33 ±8,19	99,97 ±19,60	130,95 ±7,51	160,98 ±9,30 **
Lysine	0,40 ±0,01	0,37 ±0,01	0,37 ±0,01	0,39 ±0,008	0,38 ±0,01	0,38 ±0,01	0,38 ±0,01	0,40 ±0,01	0,31 ±0,03	0,25 ±0,01
Valine	3,16 ±0,33	1,88 ±0,22	2,05 ±0,22	1,99 ±0,19	2,04 ±0,19	1,50 ±0,10	1,70 ±0,09	1,88 ±0,29	1,84 ±0,21	2,75 ±0,29
Isoleucine	1,60 ±0,20	0,77 ±0,14	0,86 ±0,13	0,81 ±0,12	0,86 ±0,10	0,51 ±0,05	0,60 ±0,04	0,77 ±0,15	0,67 ±0,13	1,18 ±0,17
Leucine	1,34 ±0,18	0,55 ±0,07	0,60 ±0,09	0,67 ±0,11	0,65 ±0,07	0,47 ±0,07	0,53 ±0,05	0,57 ±0,14	0,58 ±0,11	0,84 ±0,11
phenylalanine	2,10 ±0,34	1,20 ±0120	1,18 ±0,13	1,33±0,21	1,44 ±0,14	0,95 ±0,09	1,05 ±0,07	1,02 ±0,16	1,04 ±0,15	1,47 ±0,18
Histidine	1,59 ±0,14	1,02 ±0,10	1,04 ±0,07	1,05 ±0,13	0,96 ±0,14	0,78 ±0,05	0,84 ±0,06	0,94 ±0,11	0,68 ±0,15	1,19 ±0,20

Measurements were carried out on rosette leaves using uplc and fluorescence detection. All values are in (nmol g^{-1} fw). Values represents means of 5-7 biological replicates±SE. Significant differences to WT are indicated by asterisks according to student' s t test (* $p \leq 0.05$, ** ** $p \leq 0.01$, *** $p \leq 0.001$).

Appendix Table 6. The concentration of AMP, ADP in WT and Flv-expressing lines.

AMP	WT	Flv1			Flv3			Flv1/Flv3		
		L1	L2	L3	L1	L2	L3	L1	L2	L3
4 h	111.96±8.70	93.68±2.92	99.07±5.70	77.07±2.24	99.54±7.06	99.29±4.75	89.22±8.99	91.92±2.96	98.23±4.79	84.51±5.23
8 h	64.41±4.33	57.67±4.96	64.13±5.27	71.14±5.17	69.07±3.05	64.58±3.51	73.88±5.71	70.38±4.88	63.31±7.36	62.81±2.00
16 h	49.06± 1.01	52.29±0.96	52.10±1.32	52.92±1.21	49.01±4.83	53.32±7.71	59.16±5.79	60.09±3.22	63.37±1.80	63.04±7.19
ADP		L1	L2	L3	L1	L2	L3	L1	L2	L3
4 h	31.74±2.04	36.26±2.22	31.58±3.90	36.20±1.52	39.30±2.75	35.93±2.95	31.33±2.72	31.48±0.78	30.25±3.09	29.06±2.45
8 h	23.75±1.53	28.95±1.34	28.33±2.46	28.26±0.94	29.96±3.02	32.51±1.93	30.00±3.25	29.43±1.63	28.53±2.50	22.88±1.54
16 h	30.15±2.57	26.89±1.46	27.40±1.64	31.90±2.23	26.84±1.20	26.88±1.77	28.20±1.01	25.59±0.90	22.37±0.13	26.42±3.39

AMP	WT	Flv2			Flv4			Flv2/Flv4		
		L1	L2	L3	L1	L2	L3	L1	L2	L3
2nd	111,96±8,70	103,63±4,63	109,81±3,98	76,08±5,09	88,29±4,81	87,26±5,99	77,82±2,71	72,35±3,22	80,67±3,97	86,53±4,89
3rd	64,41±4,33	54,03±4,01	61,51±4,86	80,41±5,01	70,36±5,12	82,86±4,43	68,80±5,21	70,69±6,42	78,86±2,81	76,03±6,19
4th	49,06± 1,01	62,22±3,77	62,12±4.38	58,22±1.69	56,73±5,96	54,76±2,49	53,90±5,39	47,95±2,61	58,01±4,15	77,79±6,05
ADP		L1	L2	L3	L1	L2	L3	L1	L2	L3
2nd	31,74±2,04	33,03±2,45	30,33±2,77	26,06±1,06	28,61±0,57	29,58±2,39	35,18±2,14	24,58±0,94	30,26±2,09	28,97±1,58
3rd	23,75±1,53	29,01±1,01	26,15±1,55	25,64±2,86	25,85±1,11	30,18±2,32	28,72±2,67	26,95±0,80	28,89±2,10	27,26±3,15
4th	30,15±2,57	30,33±2,61	24,41±1,58	24,03±1,46	27,00±1,70	26,67±0,79	29,86±1,52	23,59±1,06	24,88±1,85	21,41±0,55

Measurements were carried out at 4 h post illumination (2nd time point), 8 h at the end of day light (3rd time point) and 16 h dark period (4th time point). Plants were six weeks old. Data represent means of 5 biological replicates±SE.

Appendix Table 7. The concentration of GSH and GSSG in WT and Flv-expressing lines.

	WT	Flv1			Flv3			Flv1/Flv3		
		L1	L2	L3	L1	L2	L3	L1	L2	L3
GSH	114,51±4,02	96,60±4,79	86,24±3,17	107,38±4,62	113,89±7,26	108,50±4,07	99,73±8,81	107,75±2,70	100,91±5,88	79,44±5,59
GSSG	6,28±1,18	9,40±7,003	11,62±2,24	18,13±1,08	11,21±1,19	15,71±0,92	14,68±1,34	7,27±0,3	10,54±1,40	7,45±0,66
	WT	**Flv2**			**Flv4**			**Flv2/Flv4**		
		L1	L2	L3	L1	L2	L3	L1	L2	L3
GSH	114,51±4,02	0,105±0,004	0,09±0,002	0,09±0,002	0,10±0,006	0,104±0,003	0,105±0,008	0,09±0,003	0,07±0,002	0,060±0,006
GSSG	6,28±1,18	0,01±0,002	0,01±0,002	0,01±0,001	0,005±0,001	0,01±0,001	0,01±0,001	0,01±0,0005	0,01±0,002	0,01±0,001

Measurements were carried out in rosette leaves at the end of the day at 8 h post illumination All values are in (nmol g^{-1} fw). Values represents means of 4-5 biological replicates±SE.

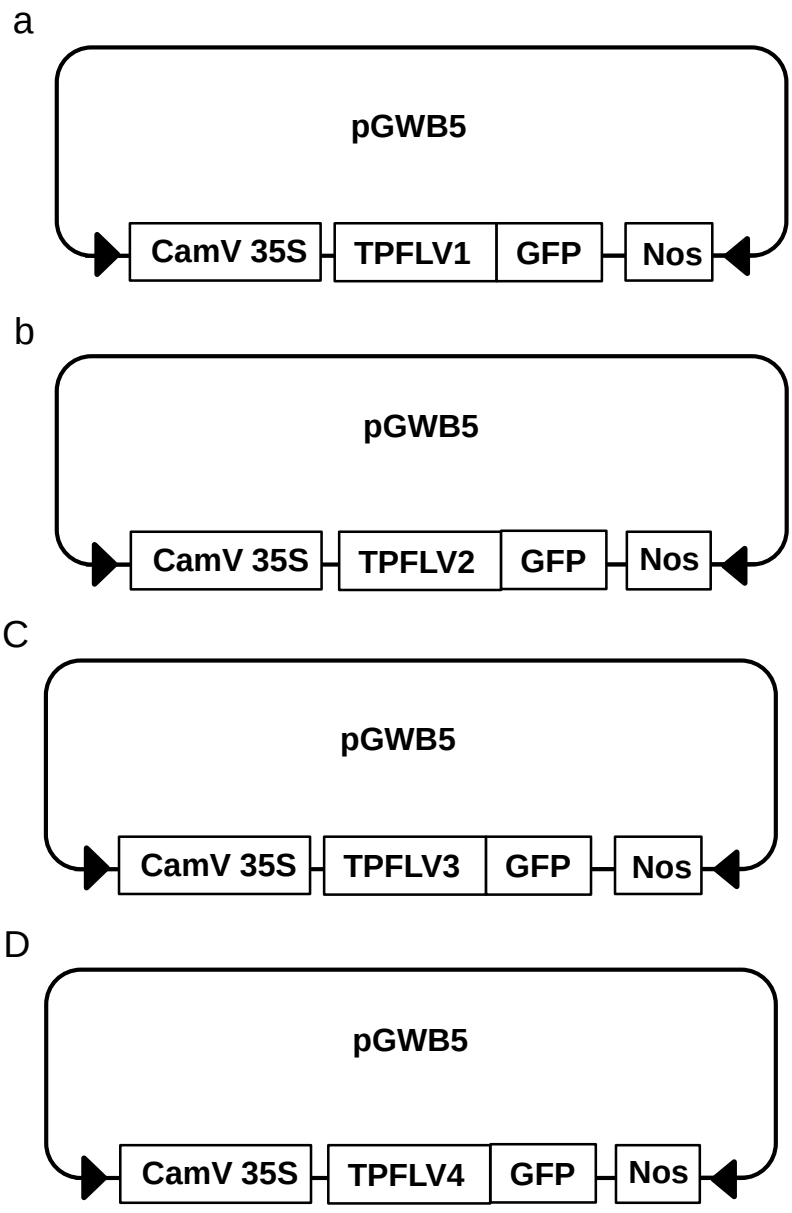

Appendix Figure 1. Schematic representation of binary vector for Flv localization studies

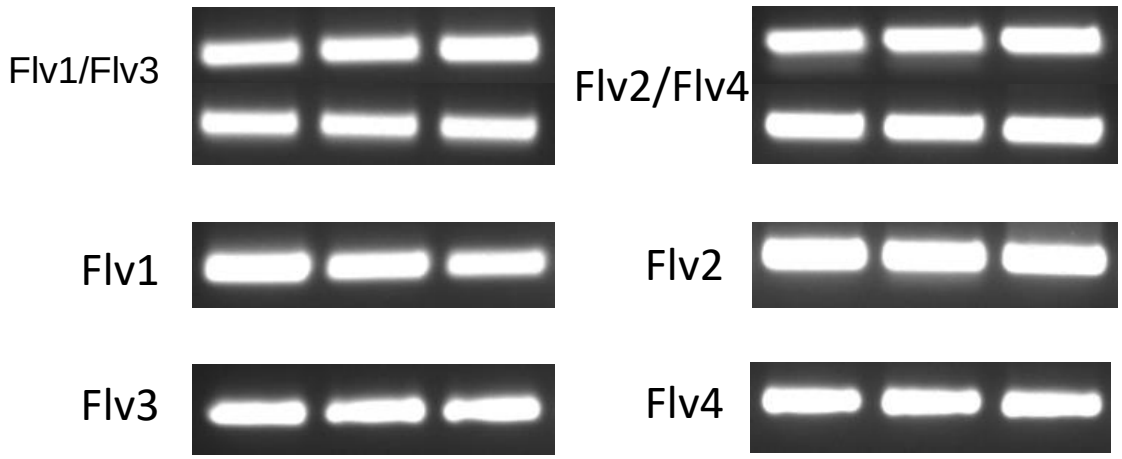

Appendix Figure 2. Expression analysis of Flv genes in tobacco plants

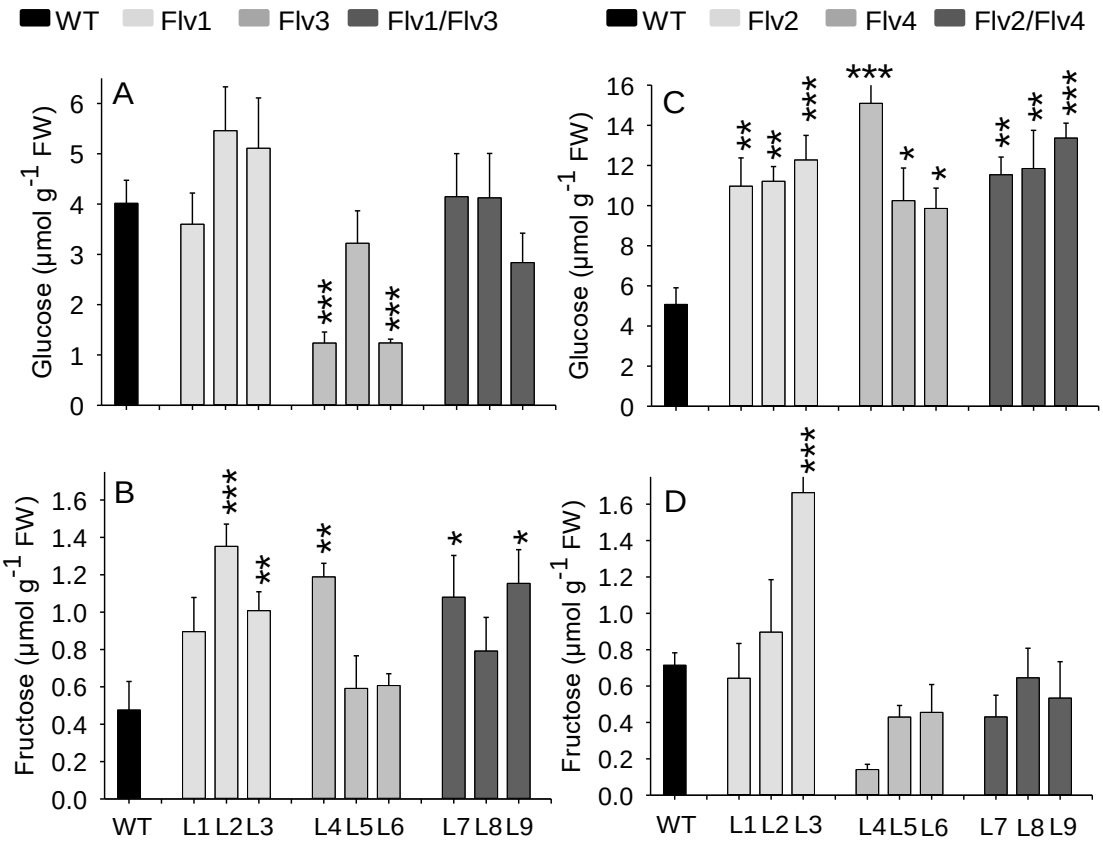

Appendix Figure 3. Determination of soluble sugars in Flv overexpression lines under drought stress conditions. (A, B) Glucose and fructose in Flv1, Flv3 Flv1/Flv3 lines and (C, D) Glucose and fructose in Flv2, Flv4 Flv2/Flv4 lines were measured in three independent lines. Bars represent means of 7 biological replicates±SE. Significant differences between wild type and Flv-expressing lines are indicated by asterisks according to student's t test (*p≤0.05, **p≤0.01 and ***p≤0.001).

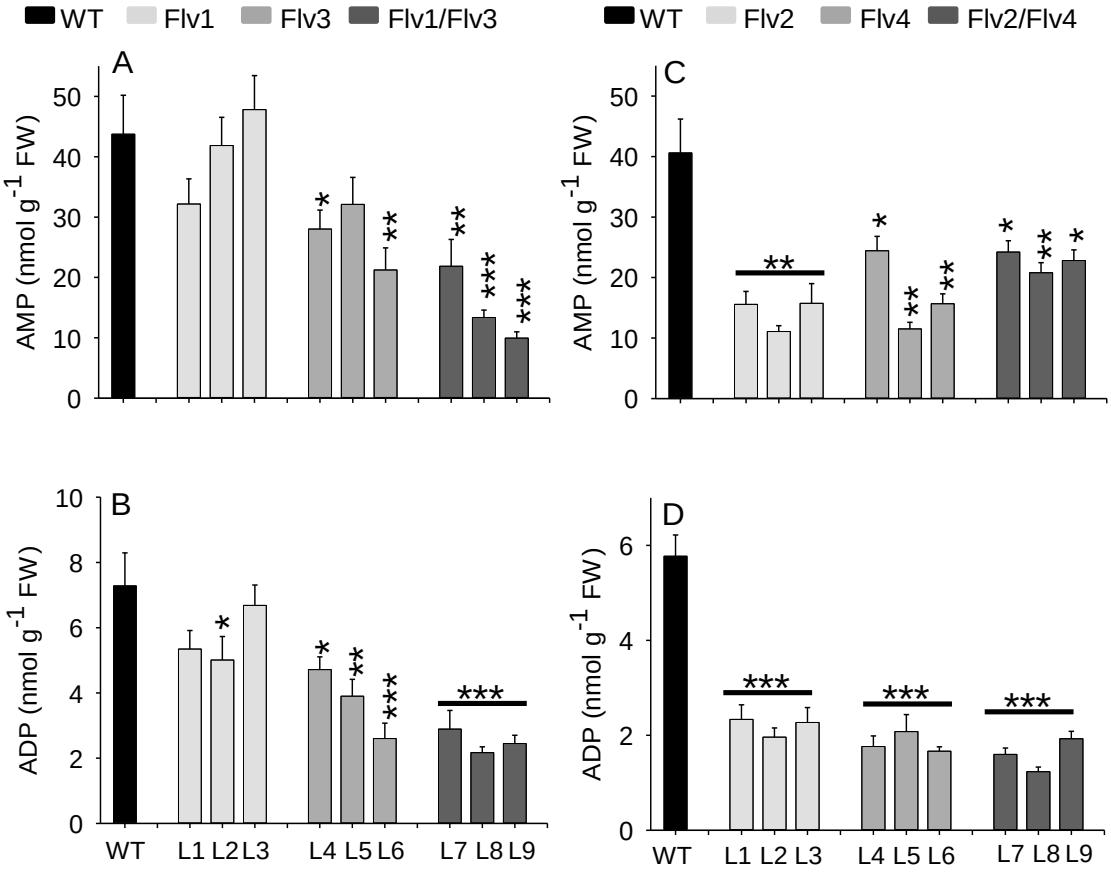

Appendix Figure 4. The concentration of ADP and AMP levels in Flv-expression lines under drought stress conditions. (A, B) AMP and ADP in Flv1, Flv3 Flv1/Flv3 lines and (C, D) AMP and ADP in Flv2, Flv4 Flv2/Flv4 lines were measured in three independent lines. Bars represent means of 7 biological replicates±SE. Significant differences between WT and Flv-expressing lines are indicated by asterisks according to student's t test (*p≤0.05, **p≤0.01 and ***p≤0.001).

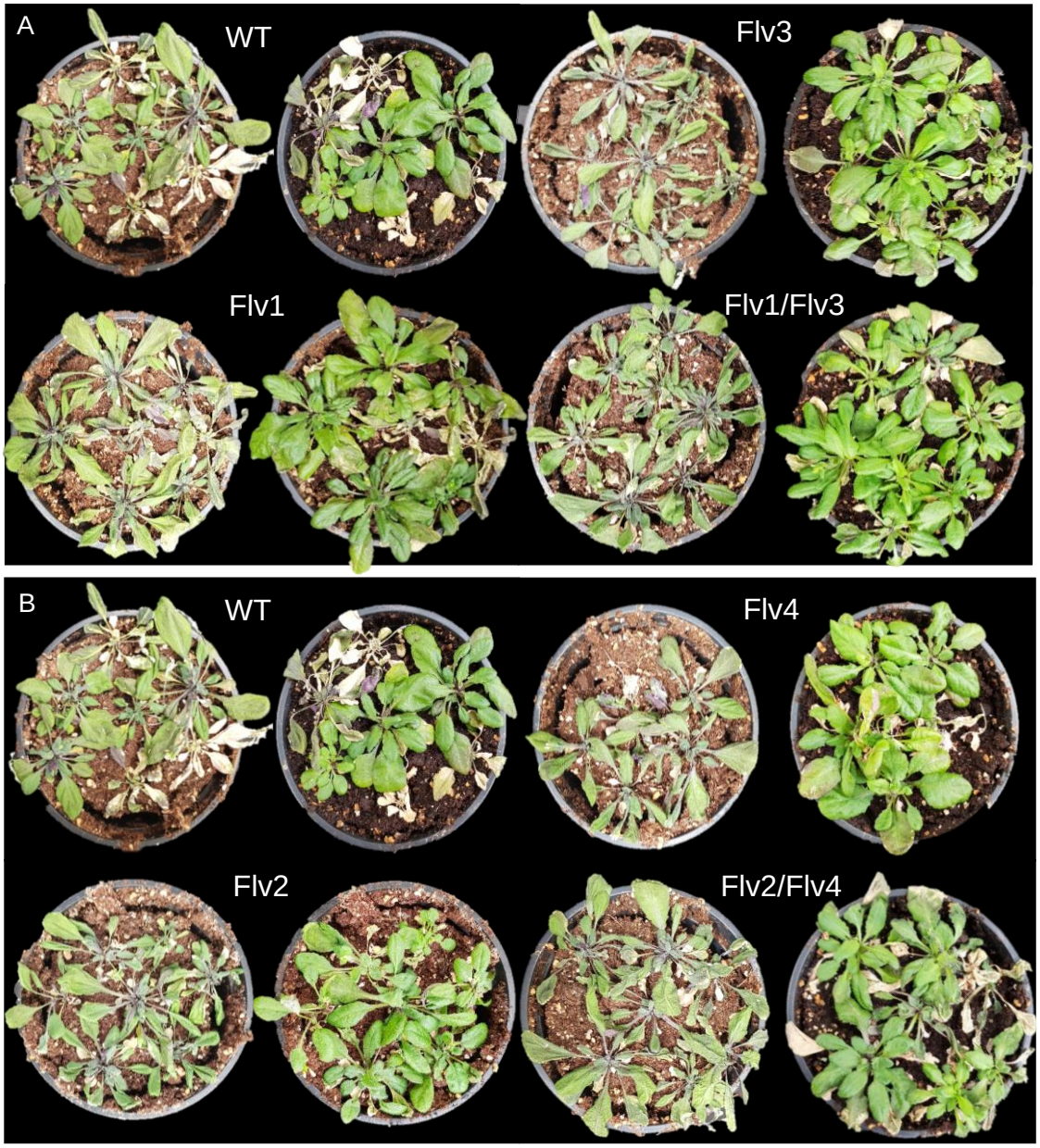

Appendix Figure 5. Faster recovery from drought stress in Flv expression lines after re-watering. Soil grown WT plants and Flv expressing lines exposed to natural drought stress. Stress experiments were repeated thrice with 7 plants per pot. Photograph of one of the representative lines is shown here.

11. Publications and proceedings related to the submitted thesis

Gómez R, Carrillo N, Morelli MP, **Tula S,** Shahinnia F, Hajirezaei MR, Lodeyro AR (2017). Faster photosynthetic induction in tobacco by expressing cyanobacterial flavodiiron proteins in chloroplasts. Photosynth Res, DOI 10.1007/s11120-017-0449-9

Tula S, Shahinnia F, Melzer M, Rutten T, Gómez R, Lodeyro AF, von Wirén N, Carrillo N, Hajirezaei MR. 2018. Integration of an electron sink through cyanobacterial flavodiiron proteins enhances plant growth in *Arabidopsis thaliana* (Submitted)

Tula S, Shahinnia F, von Wirén N, Gómez R, Carrillo N, Hajirezaei MR. 2018. Improvement of plant development using cyanobacterial proteins. 31st Conference "Molekularbiologie der Pflanzen"Dabringhausen, Germany. February 20th - 23rd, 2017.

Tula S, Shahinnia F, von Wirén N, Gómez R, Carrillo N, Hajirezaei MR. 2018. Improvement of plant development using cyanobacterial proteins. Minisymposium: Role of ROS in plant stress signaling. Bonn, Germany. December 07th - 08th December 2017.

12. Declaration

I hereby to declare that the thesis was written by me using the following references and resources as mentioned. This thesis is submitted for the purpose of academic examination in its original form.

Date

Signature of the applicant